ANKARA YILDIRIM BEYAZIT UNIVERSITY

GRADUATE SCHOOL OF NATURAL AND APPLIED SCIENCES

TOPOLOGY OPTIMIZATION AND STRESS ANALYSIS OF FUSELAGE BRACKETS

M.Sc. Thesis by

Yasin AKBAŞ

Department of Mechanical Engineering

July, 2023

ANKARA

TOPOLOGY OPTIMIZATION AND STRESS ANALYSIS OF FUSELAGE BRACKETS

A Thesis Submitted to

The Graduate School of Natural and Applied Sciences of

Ankara Yıldırım Beyazıt University

In Partial Fulfillment of the Requirements for the Degree of Master of Science

in Mechanical Engineering, Department of Mechanical Engineering

by

Yasin AKBAŞ

July, 2023

ANKARA

M.Sc. THESIS EXAMINATION RESULT FORM

We have read the thesis entitled, "**TOPOLOGY OPTIMIZATION AND STRESS ANALYSIS OF FUSELAGE BRACKETS"** completed by **YASİN AKBAŞ** under the supervision of **ASSIST. PROF. DR. YASİN SARIKAVAK** and we certify that in our opinion it is fully adequate, in scope and in quality, as a thesis for the degree of Master of Science.

Assist. Prof. Dr. Yasin SARIKAVAK

Supervisor

Prof. Dr. Adem ÇİÇEK

Jury Member

Assoc. Prof. Dr. Tunç APATAY

Jury Member

Prof. Dr. Sadettin ORHAN

Director

Graduate School of Natural and Applied Sciences

ETHICAL DECLARATION

I hereby declare that, in this thesis which has been prepared in accordance with the Thesis Writing Manual of Graduate School of Natural and Applied Sciences,

- All data, information and documents are obtained in the framework of academic and ethical rules,
- All information, documents and assessments are presented in accordance with scientific ethics and morals,
- All the materials that have been utilized are fully cited and referenced,
- No change has been made on the utilized materials,
- All the works presented are original,

and in any contrary case of above statements, I accept to renounce all my legal rights.

Date: 2023,28 July

Signature:…..……..

Name & Surname:…….…….

ACKNOWLEDGMENTS

I would like to express my heartfelt gratitude to my esteemed advisor, Assistant Professor Dr. Yasin SARIKAVAK, for his invaluable contributions, guidance, and unwavering enthusiasm throughout my graduation project. Working with him has been an absolute honor and a delightful experience.

I am also profoundly grateful to the respected faculty members at the Graduate School of Natural and Applied Sciences of Ankara Yıldırım Beyazıt University, as well as my dear friends, for their scholarly insights and unwavering support during my studies.

Lastly, I would like to extend my sincerest appreciation to my beloved parents, whose endless encouragement has been a constant source of strength and motivation throughout my life.

I am genuinely grateful for the unwavering support and companionship I have received on this journey. Thank you from the bottom of my heart.

July, 2023 **Yasin AKBAŞ**

TOPOLOGY OPTIMIZATION AND STRESS ANALYSIS OF FUSELAGE BRACKETS

ABSTRACT

Topology optimization (TO) has acquired significant matter in aerospace engineering according to its capacity to get the optimum material distribution and decreasing masses. There are still not many implementations of topology optimization, which may be considered a relatively new branch in the aerospace field. This thesis focuses on structural analysis, topology optimization, and the optimization's capability to decrease the aerospace bracket's mass under predetermined boundary conditions. The crack implementation on the bracket was also studied, where semi-elliptical cracks, which are mode I dominant, were applied to the structure by using finite element methods (FEM) against the material fracture toughness. The primary goal of this study is to develop a redesigned wing-fuselage bracket for a middle-sized aircraft by utilizing a topology optimization tool under predetermined boundary conditions while considering stress and stress intensity factors. Analyses, density-based topology optimization methods, and SMART (Separating Morphing and Adaptive Remeshing Technology) crack growth analysis were performed on the structure. According to the results, two types of new wing-fuselage brackets have been designed, resulting in a total mass decrease under predetermined boundary conditions, while ensuring it can withstand the existing stress and stress intensity factors. The thesis demonstrates that a mass reduction exceeding 20% has been achieved under specific boundary conditions, highlighting the potential for substantial weight savings. The correct permanent attachment of the bracket can be determined by comparing these results with established criteria and requirements.

Keywords: Topology optimization, Structural design, Finite element analysis (FEA), Structural analysis, Fracture toughness, Semi-elliptical crack, Wing-fuselage bracket, Aerospace.

GÖVDE BRAKETLERİNİN TOPOLOJİ OPTİMİZASYONU VE GERİLİM ANALİZİ

ÖZ

Topology optimizasyonu (TO), optimum malzeme dağılımını elde etme ve kütlenin azaltılması kapasitesi nedeniyle havacılık mühendisliğinde büyük önem kazanmıştır. Havacılık alanında topoloji optimizasyonuyla ilgili henüz çok fazla uygulama bulunmamaktadır ve bu, yeni bir dal olarak kabul edilebilir. Bu tez, yapısal analiz, topoloji optimizasyonu ve önceden belirlenmiş sınırlayıcı koşullar altında havacılık braketinin kütlesini azaltabilme yeteneği üzerine odaklanmaktadır. Aynı zamanda, çalışma brakete çatlak uygulamasını da araştırmaktadır. Mode I dominant yarı eliptik çatlaklar, malzeme kırılma dayanımına karşı sonlu eleman yöntemi (FEM) kullanılarak yapıya uygulanmıştır. Çalışmanın temel amacı, yapılanma ve gerilim ve gerilim yoğunluk faktörlerini hesaplarken, önceden belirlenmiş sınırlayıcı koşullar altında bir orta büyüklükteki uçak braketinin topoloji optimizasyon aracıyla yenilenmiş bir tasarımını oluşturmaktır. Kanat-gövde bağlantı parçası tahmini bir optimizasyon problemi olarak formüle edilir ve sonlu eleman yöntemi (FEM) kullanılarak çözülür. Yapı üzerinde analizler, yoğunluk tabanlı topoloji optimizasyon yöntemleri ve SMART çatlak büyümesi analizi gerçekleştirilir. Sonuçlara göre, iki farklı yeni kanat-gövde bağlantı parçası tasarlanmıştır, bunlar birbirleriyle karşılaştırılmış ve önceden belirlenmiş sınırlayıcı koşullar altında toplam kütlesinde azalma sağlanmıştır. Bu koşullarda parça mevcut düzeydeki gerilim ve gerilim yoğunluk faktörüne dayanabilecek durumdadır. Bu tez, belirtilen sınırlayıcı koşullar altında %20'den fazla kütlenin azaltıldığını ve parçanın doğru kalıcı bağlantısının karşılaştırılarak bulunduğunu göstermektedir.

Anahtar Kelimeler: Topoloji optimizasyonu, Yapısal tasarım, Sonlu elemanlar analizi (FEA), Yapısal analiz, Kırılma tokluğu, Yarı eliptik çatlak, Kanat gövde braketi, Havacılık.

CONTENTS

NOMENCLATURE

Acronyms

AISI	American Iron and Steel Institute
TO	Topology Optimization
AM	Additive Manufacturing
FE	Finite Elements
DOF	Degree of Freedom
SIMP	Single Isotropic Material with Penalization
CAD	Computer-Aided Drawing
LEFM	Linear Elastic Fracture Mechanics
SIF	Stress Intensity Factor
MSD	Multiple Site Damage
FEM	Finite Element Method
FEA	Finite Element Analysis
APDL	Ansys Parametric Design Language
SMART	Separating Morphing and Adaptive Remeshing Technology
DEM	Displacement Extrapolation Method
IIM	Interaction Integral Method
MPa	Megapascal
GPa	Gigapascal
ISE	Isotropic Solid Empty
SIMP	Solid Isotropic Material with Penalization
VCCT	Virtual Crack Closure Technique
ERR	Energy Release Rate
2D	Two Dimensional
3D	Three Dimensional
Lcr	Largest Contour Radius
g	Load Factor

Symbols

F_x	Force along the X direction (N)
F_y	Force along the Y direction (N)
Fz	Force along the Z direction (N)
E	Young Modulus (N/m^2)

N	Newton (N)
W	Work done per unit area (J/m^2)
ΔE	Change in energy (J or Nm)
v	Poisson's Ratio (-)
ε	Strain (-)
θ	Angle (rad)
r	Radial distance (m)
u,v,w	Displacement field (m)
σ	Normal Stress (Pa)
$б_y$	Yield Strength (Pa)
τ	Shear Stress (Pa)
Γ	The path or contour along which the integration is performed
δ	Displacement of the material in the direction (m)
n	Normal vector
G	Shear Modulus (Pa)
Φ	Airy Stress Function
K	Stress Intensity Factor (MPa.$m^{1/2}$)
K_I	Stress Intensity Factor for Mode I (MPa.$m^{1/2}$)
K_{II}	Stress Intensity Factor for Mode II (MPa.$m^{1/2}$)
K_{III}	Stress Intensity Factor for Mode III (MPa.$m^{1/2}$)
G	Modes energy release rate (J/m^2)
K_c	Fracture Toughness (MPa.$m^{1/2}$)
J	J Integral (J/m^2)
c	Half Length of Crack length (mm)
a	Crack depth (mm)

LIST OF TABLES

LIST OF FIGURES

CHAPTER 1

INTRODUCTION

1.1 Background

Aircraft have revolutionized transportation, opening new frontiers and facilitating global connectivity while playing a vital role in national security and economic development. Their continued advancements and contributions ensure their ongoing significance in shaping the world we live in. These sophisticated and complex mechanical structures, created by human ingenuity, have been flying in the sky since the early 20th century. They serve various purposes, from enabling swift and efficient travel for cargo and passengers to fulfilling critical military requirements during times of war or peace. Civil transportation aircraft carry people across vast distances, connecting people and cultures in ways never before possible, while fighter jets ensure the security and sovereignty of nations. Aircraft have consistently delivered exceptional performance and reliability throughout history, showcasing their immense importance to nations and societies worldwide. Their impact on global trade and diplomacy is undeniable, and they continue to be at the forefront of technological innovation and progress, driving advancements in aeronautical engineering and pushing the boundaries of what is possible in flight.

There can be any other classification according to engine system (turbojets, turbofans, etc. [1]), their size, or air speeds. The design of these advanced mechanical structures is a challenging task for humans because they should withstand different loads while they are flying and maneuver movements in the sky. According to this information, it is evident that these structures will experience varied and significant loads.

Although aircraft differ based on their duties, there are common structural elements found inside the structure. The primary structural elements, known as lugs, are widely used in the airframe structure of planes. They are commonly used in the airframe of planes [2]. Except for their duties, all of them have various brackets inside their wings. They are used for attaching the wing fuselage. Wing fuselage brackets convey all

forces from the wings to the fuselages, shown in Figure 1.1. The wing fuselage bracket is a structural component that is used to connect the wing of an aircraft to its fuselage. It is designed to transmit and distribute the various forces and loads experienced during flight, such as lift, drag, and bending moments, from the wings to the fuselage. The wing fuselage bracket plays a critical role in ensuring the structural integrity and stability of the aircraft by providing a secure attachment point between these two major components. It is typically made of strong and durable materials, such as aluminum alloys or composites, to withstand the forces and loads encountered during flight. According to this, the wing fuselage bracket is a critical structure in aerospace applications and carries significant loads on it.

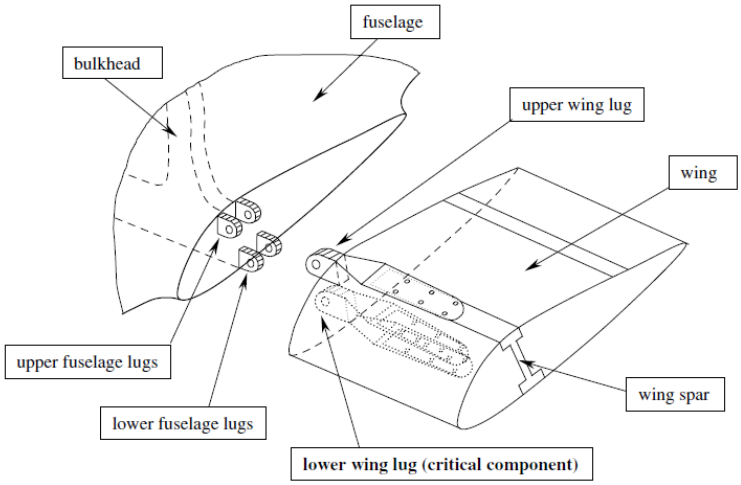

Figure 1.1 Typical example of wing fuselage connector of aircraft [2].

In today's aviation industry, there is a strong emphasis on lightweight structures for critical components. The weight of an aircraft is a crucial factor, as reducing it leads to lower fuel consumption and increased useful load capacity. In response to this demand, engineers are employing new approaches. They utilize advanced CAD and FEA software for materials and optimization work and explore innovative production methods such as additive manufacturing. Topology optimization is one of the design methods employed by engineers, enabling mass optimization through the use of engineering software. It enhances existing designs and empowers designers to pursue new approaches to creating lighter structures.

By leveraging this advanced software, production methods, and techniques, it becomes possible to create and manufacture new designs that are even more lightweight than their predecessors. This allows for the development of more innovative designs and the ability to analyze results effectively. Lightweight designs that meet static and dynamic requirements will continuously gain traction among producers and manufacturers.

1.2 Aims and Objectives

As illustrated in Section 1.1, aerospace designers focus on creating lighter structures. Thanks to additive manufacturing, creating new designs without restrictions in manufacturing methods is now possible. Using these additive manufacturing methods, the layer-by-layer building offers a real opportunity to quickly produce complex shapes, including ribs or honeycomb structures. At this moment, topology optimization has become a valuable tool. Topology optimization is a useful tool in aerospace design due to its ability to reduce weight, improve performance, explore design options, save time, cost, and integrate with advanced manufacturing technologies. It helps create efficient, lightweight, and optimized aerospace structures. Reducing mass while considering the load circumstances and without compromising performance makes it possible to decrease fuel consumption by increasing the valuable load area. Moreover, this approach aligns with environmental considerations.

This thesis aims to improve existing designs by reducing their mass. It aims to significantly focus on mass reduction and develop new designs that can efficiently and effectively withstand the current load by utilizing topology optimization applications in combination with the finite element analysis (FEA) method. Simultaneously, the thesis will analyze the new model from various perspectives, including structural behavior, performance, and durability, both static and transient analyses. In addition to examining stress levels, it will evaluate the structural integrity by calculating stress intensity factors (SIF) and investigate the behavior and propagation of cracks in an optimized typical wing fuselage bracket. The analysis results will not only determine whether the wing fuselage bracket is capable of withstanding small cracks in the structure but also provide valuable insights into potential design improvements and

failure prevention strategies. The workflow during the study is summarized in Figure 1.2, illustrating the systematic approach employed to achieve the research objectives.

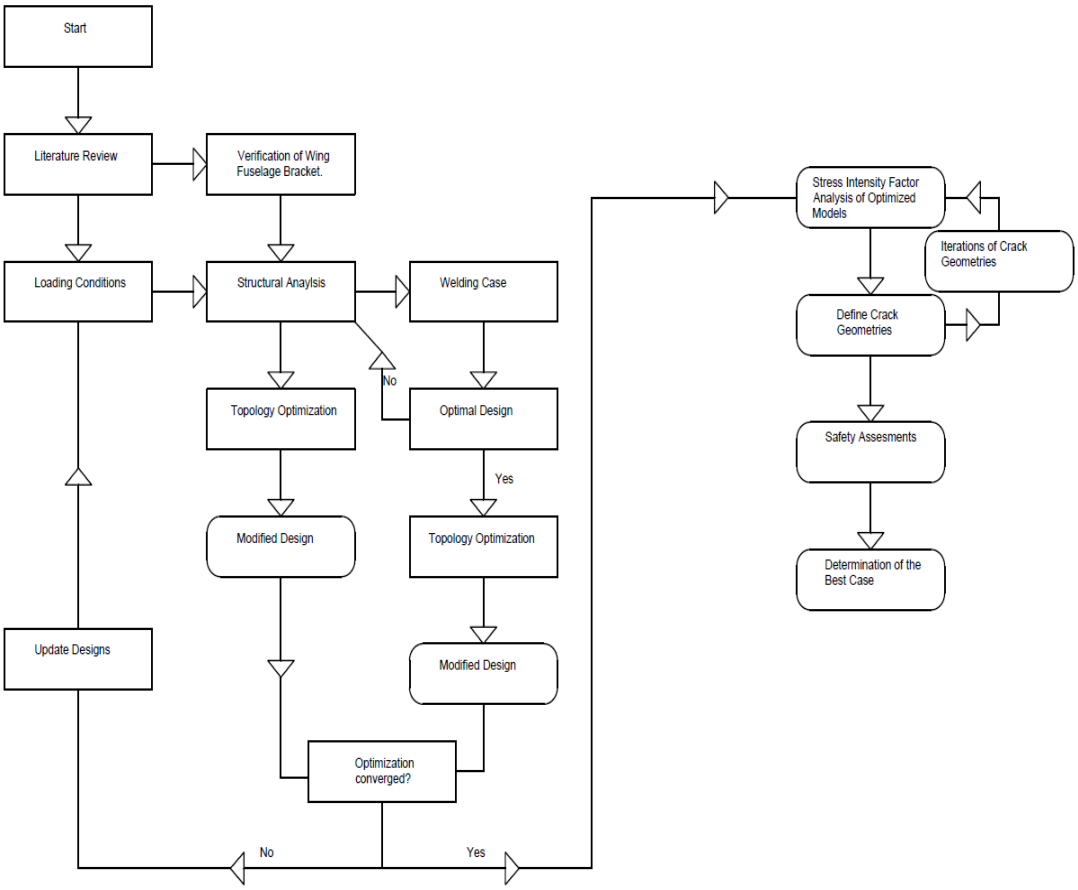

Figure 1.2 Workflow chart.

CHAPTER 2

LITERATURE REVIEW

2.1 Overview

The wing fuselage bracket plays a vital role in aerospace applications, serving as a crucial component. Typically, these brackets encounter various atmospheric conditions, including moisture, warm air, and cold air, which can have an impact on their performance. Corrosion can affect the inside of the structure, and fatigue failure or crack propagation can be progressed according to this problem after 5000-6000 hours of usage [2]. These brackets are used not only for wings but also for pylon supports or landing gears, even if engines [3]. It is well understood that wing fuselage brackets hold significant importance as structural elements in aerospace applications, finding extensive usage and occupying considerable space within the structures. These brackets contribute to a substantial mass of the overall structure. Therefore, it is essential to emphasize that one of the key challenges in aerospace applications is the need for mass reduction. Generally, applications of mass reduction activities should be held with their structural functionalities. At this moment, topology optimization is an excellent key point for reducing mass because it is an effective tool for mass reduction without using any performance capacities [4]. The benefits of topology optimization extend beyond mass reduction. By employing this approach, engineers can also enhance the bracket's resistance to fatigue and crack propagation, improving its durability and longevity. The ability to withstand the demanding operational conditions of aerospace applications is crucial for ensuring the safety and reliability of the aircraft. Topology optimization plays a vital role in minimizing material waste during the manufacturing process, making a valuable contribution to sustainability and cost-effectiveness in the aerospace industry. The industry can achieve lightweight and high-performance aerospace structures by utilizing topology optimization, resulting in notable benefits such as mass reduction, enhanced structural integrity, and improved overall efficiency. This approach proves to be advantageous in terms of optimizing resources and achieving optimal performance in aerospace applications. Figure 2.1 shows the optimized version of a simple structure.

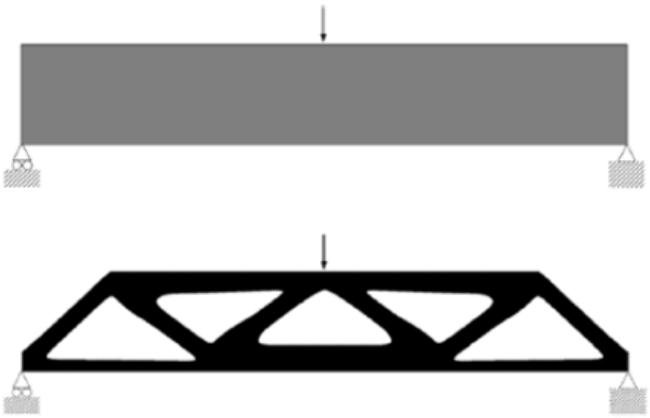

Figure 2.1 Typical example of topology optimization [5].

This chapter informs the applications of topology optimization, additive manufacturing, and failure problems in aerospace applications. Such research endeavors contribute significantly to understanding various aspects, including the materials employed, attachment types utilized, and the methodologies applied in the studies. These investigations seek to address pertinent questions in these domains. In general, the research findings demonstrate that topology optimization holds the capability to address the concerns in this field. Additionally, new designs should undergo thorough analysis by subjecting them to static and transient load conditions, ensuring that durability is maintained in optimized lightweight designs. Furthermore, stress intensity factor analysis becomes crucial in critical stress points, as it helps identify potential failure modes. By considering static and transient analyses alongside stress intensity factors, comprehensive evaluations can be conducted to enhance the design and durability of these critical components.

Harish et al. [3] conducted a stress analysis of the wing fuselage attachment bracket. The study aimed to investigate the structural behavior and performance of the bracket under various loading conditions. The design was developed for a six-seater transport airframe structure. Geometry was similar to other published works in literature. AISI 4340 was used according to its high material properties, for instance, yield and ultimate tensile strength. Rivets joints were simulated by using FEA methods, which gives valuable information about the attachment of lug and fuselage brackets in the system. The authors analyzed stress distribution, deformation, and load-carrying capacity

factors by applying analytical and computational methods to assess the bracket's integrity and stability.

Zhu et al. [4] studied a comprehensive work on topology optimization. Different models were studied in the paper. Manufacturability is one of the significant problems for similar components successfully solved by applying additive manufacturing methods. This paper generally focuses on density-based topology optimization methods and shows their efficiency via weight reduction. According to the study, topology optimization is classified as one of the most efficient ways to implement in aerospace applications with additive manufacturing.

Bendsoe et al. [5] investigates several aspects of topology optimization including theory, methods, and applications where topology optimization solves fundamental engineering problems about the masses while covering structure rigidity

Seabra et al. [6] focus on the pros of additive manufacturing (AM) as the most promising method. The primary objective was to demonstrate how AM techniques enable the creation of designs not constrained by traditional machining methods. To achieve this, the researchers selected an aluminum aerospace bracket as their subject. Paper employed topology optimization to determine the optimal mass distribution for the bracket, followed by conducting finite element verifications. The authors successfully produced the bracket using additive manufacturing methods, resulting in a remarkable 28% reduction in mass. Moreover, this paper sheds light on the correlation between aerospace applications and topology optimization, offering valuable insights into the relationship between the two. Additionally, the study provides detailed information on powder bed fusion methods, which represent a prominent approach for producing metal components using additive manufacturing techniques.

Tomlin et al. [7] conducted topology optimization by using a component of the Airbus A320. Airbus A320’s hinge bracket was optimized which was made of steel. Results show a 64% reduction in mass. This study shows that the topology optimization's power might be higher as mass reduction. The study yielded a remarkable achievement of achieving mass reductions exceeding fifty percent.

Berrocal et al. [8] conducted an extensive study on the synergy between topology optimization and additive manufacturing techniques for aerospace components. The study employed three models for their optimization efforts, with two of them being manufactured using laser beam melting technology. The research demonstrated the effectiveness of topology optimization in creating lightweight structures, proving its potential in designing and producing optimized aerospace parts. This study underscores the significance of integrating advanced optimization techniques with additive manufacturing processes, highlighting their role in developing efficient, high-performance aerospace components.

Bhasha et al. [9] focused on the fuselage bracket of an airplane. The researchers aimed to calculate the stress intensity factor of the bracket using various methods. The paper highlighted the criticality of fuselage brackets, emphasizing the potential for catastrophic failure. Stress intensity factor calculations were employed as a valuable tool for predicting such failures in brackets. The researchers conducted their analysis by modeling the brackets using different materials. Stress intensity factors and additional criteria, such as deformation, were calculated and compared from a material perspective. Essentially, the stress intensity factor provides insight into the stress states near the crack tip, allowing for a better understanding of potential failure modes in fuselage brackets.

Ferro et al. [10] conducted a comparative analysis of 3D printing methods and milling processes for a spar cap fitting in a wing fuselage. The research's primary objective was to compare additive manufacturing methods with conventional machining techniques, particularly on the wing bracket. The geometry of the bracket was similar to that in the study conducted by Bhasha et al. [9], but it incorporated a lug portion within it. The bracket was designed for a UAV aircraft. This research indicates that the wing fuselage bracket has a wide range of applications, and optimizing its structure can offer an economically viable approach for the aerospace industry.

Rao et al. [11] conducted a dynamic and fatigue analysis of an airframe structure. They were focusing on the utilization of steel 4340 and aluminum 2024 materials. The research was performed considering the specific scenario based on the g factors experienced by an airplane. The researchers investigated the structural behavior of the

bracket under dynamic loading conditions and evaluated its fatigue life. Notably, Steel 4340 and aluminum 2024 were prominent materials in this analysis. The findings revealed that under 3g conditions, the bracket exhibited an infinite life, suggesting its structural integrity and suitability for prolonged use in such operational scenarios. This research contributes valuable insights into the performance and durability assessment of airframe structures, aiding in selecting and optimizing materials for aerospace applications.

Reddy et al. [12] conducted a comprehensive study on static and fracture analysis, building upon previous work similar to that undertaken by Bhasha et al. [9]. However, the study incorporated additional information regarding CAD data, providing a more detailed analysis. Different materials were once again employed to compare the results. The study excluded I beams from the structural analysis and focused on the attachment bracket. As a result of the investigation, stress intensity factors and J integrals were calculated, enabling a comprehensive comparison of these results across different materials. The findings of this study demonstrate the relationship between stress intensity factors and J integrals, highlighting their relevance in assessing fracture behavior. This research expands our understanding of static and fracture analysis, particularly regarding attachment brackets, and contributes to the field of structural integrity assessment in engineering applications.

Sriranga et al. [13] focused on wing fuselage brackets. Materials were chosen as aluminum and AISI 4340 steel. The overall structure of the fuselage bracket was like other brackets, apart from specific regions. Rivets were once again utilized as the means of fastening the lug and fuselage bracket together. By applying finite element methods, the researchers determined the maximum stresses experienced by the bracket. The study revealed that these attachment brackets operate under high-stress levels, underscoring their critical role in the overall structural integrity of the aircraft. Moreover, the study identified rivets as the optimal attachment method for this type of bracket. Rivets, being non-separable, single-piece connectors, effectively join the bracket and lug, ensuring a secure and reliable attachment. This research contributes valuable insights into the design and attachment methods of wing fuselage brackets, aiding in the advancement of aerospace engineering practices.

Ganesh et al. [14] conducted a design and analysis of a wing fuselage bracket for a medium-sized fighter jet. The materials selected for the I spar, and lug portion were Aluminum 2024 and AISI 4340 steel, respectively. The researchers provided a comprehensive technical drawing that serves as a valuable resource for further study. The paper performed stress level calculations and assessed the fatigue life of the design, concluding that it met safety requirements for usage. The use of Aluminum 2024, a two-series alloy, was advantageous due to its low density, contributing to the reduction of the I beam mass. This research contributes to understanding wing fuselage bracket design and offers insights into the material selection for optimal performance in aerospace applications. In this paper, a stress analysis of the wing-fuselage attachment bracket is conducted. The study focuses on identifying the maximum tensile stress, which occurs at one of the lug holes. A Finite Element Method (FEM) approach is adopted for stress analysis. This computational technique allows for accurately modeling and analyzing the bracket's structural behavior under different loading conditions. The findings from this study provide valuable insights into the stress distribution and critical areas of the bracket, facilitating the optimization and enhancement of its structural design.

Rigby and Aliabadai [15] focused on the calculation of the stress intensity factor in attachment brackets. The study revisited the use of semi-elliptical cracks as a representation of these types of brackets. The paper primarily emphasized the significance of J integrals and discussed the role of fasteners in bracket attachment. It highlighted that the stress distribution near this region tends to be high, and the presence of cracks can lead to sudden propagation, ultimately resulting in bracket failure. The study also explored various analytical formulations in three-dimensional strength mechanics. Additionally, the researchers examined various ratios of crack depth to length, including ratios such as 1 to 1.6, within the study. This paper contributes valuable insights into stress analysis and crack propagation behavior in attachment brackets, providing a foundation for further research and understanding in the field.

Venkatesha et al. [16] focused on transport aircraft and their frame structure. It confirms using rivets as the preferred method for joining these brackets. The

attachment of frames and stringers was achieved through the application of rivets. Similar to previous research, aluminum materials from the 2000 series were utilized for this purpose. The static analysis conducted in the study revealed significant stress distribution near the holes and attachment points. The article employs the MVCCI (Modified Virtual Crack Closure Integral) method to calculate the stress intensity factor. Various crack lengths were applied to the structure, enabling the calculation of strain energy release rate and stress intensity factor during the analysis. This research provides valuable insights into the structural behavior of attachment brackets, shedding light on the stress distribution and the importance of rivet application in the context of transport aircraft frame structures.

Mikheevskiy et al. [17] focused on fatigue crack growth in the aluminum model, which is the 7000 series. Stress intensity factors were calculated for this purpose. The paper discusses the wide range of applications for lugs in engineering structures, explicitly focusing on circular cracks. The geometry of the lugs was intentionally kept simple to facilitate analysis. The study analyzed the effects of different sizes and shapes of cracks on the lug. By varying the crack size and shape, the researchers could evaluate the impact on the structural behavior and performance of the lug. This research contributes to understanding crack propagation and its influence on the reliability and durability of lugs in various engineering applications.

Yang and Chahande [18] conducted topology optimization of automotive products. This article shows that topology optimization is a vast area that may apply to different industries. The study conducted a topology optimization analysis of a truck frame and highlighted the potential benefits of topology optimization as a valuable tool in automotive applications.

Sigmund and Maute [19] provide a comprehensive and comparative analysis of topology optimization methods. The review serves as a valuable guideline for researchers interested in topology optimization. It covers various aspects of structural optimization, including the principles and methodologies of topology optimization. The authors discuss different methods used in topology optimization and provide insights into their strengths and weaknesses.

Shi et al. [20] focused on the aerospace bracket. This study prepared the aerospace bracket through additive manufacturing. The selective laser melting method was used to produce the bracket. According to research, 18% mass reduction was obtained on the aerospace structure. It was a process from the original design to the final product. Some tensile tests were done on the structure. Size optimization was applied to the structure in conjunction with topology optimization.

Munk et al. [21] focused on showing the benefits of topology optimization works on aerospace applications. Landing gear for an aircraft was designed in this study. The topology optimization tool achieved a 40% mass reduction on this structure. Moreover, an engine mount was designed by using topology optimization. The studies conducted yielded significant mass savings, resulting in more lightweight structures.

Munk and Miller [22] concentrated on aircraft components utilizing topology optimization to develop new designs to reduce stress levels and weight while increasing the structural lifespan. The researchers aimed to enhance the performance of the components by distributing stress more effectively throughout the structure. The study demonstrates the effectiveness of topology optimization as a superior tool for achieving these objectives in aircraft component design.

J.C. Newman Jr et al. [23] emphasize that the stress intensity factor is determined by the crack depth and crack length, with additional factors considered in modern approaches and practical applications. Three-dimensional finite element analyses are essential for accurately assessing stress intensity factors. Major and minor radii are commonly used terminologies concerning crack length and crack depth. As mentioned in the referenced article [24] and the book, the crack depth ratio to length typically falls within the range of 0.2 to 2. These sources note that fatigue failures often originate from cracks at surfaces or corners, with elliptical cracks being the specified crack type. It is worth noting that earlier studies relied on approximate analytical methods due to the absence of finite element software. Additionally, numerous configuration parameters were considered. The investigations primarily focused on bending load cases, which align with the loading conditions discussed in this paper.

Meneghetti G et al. [25] focus on welding joints and examine different types of cracks, particularly V-notch cracks commonly observed in welding joints. These cracks differ from semi-elliptical cracks, and the study provides figures displaying pre-crack length and range. The analysis involves crack lengths varying from 1 mm to 50 mm, emphasizing the significant influence of figure configuration on crack length during the study. Additionally, the size of the crack is constrained by the region in which it occurs. This investigation provides valuable insights into the behavior and characteristics of V-notch cracks, significantly contributing to the understanding of crack propagation in welding joints.

J. Qian and A. Fatemi [26] provide insights into mixed-mode crack studies, which may fall beyond the scope of our research but offer valuable ideas regarding analytical analyses of structures. The study presents information on the obtained normalized stress factor, where the theoretical value is divided by the respective mode used, whether it is mode I or mode II. In particular, regions where the ratio of the mode's stress intensity factor to its theoretical value is below one are considered safe zones, while areas with ratios at or above 1 indicate potential crack growth.

The critical threshold of 1 serves as the criterion to determine crack propagation. Figure 2.2 depicts this graph, illustrating the relationship between crack growth and normalized SIF factors. Furthermore, these parameters are almost exclusively limited to the linear elastic fracture mechanical regime, as the stress-intensity factor often expresses them in applications. No criteria include detailed considerations from the perspective of elastic-plastic fracture mechanics. Not only one parameter gives a convincing correlation in all load conditions.

Experimental results also indicate that when structures are subjected to shear loading (mode II), the opening mode (mode I) dominates. This observation also holds for mode III, where mode I remains predominant. Consequently, most literature and experimental studies focus on mode I. This dominance can be attributed to several factors in aerospace applications. This also explains why all the literature works or other experimental studies take mode I as the main study instead of mode II and mode III.

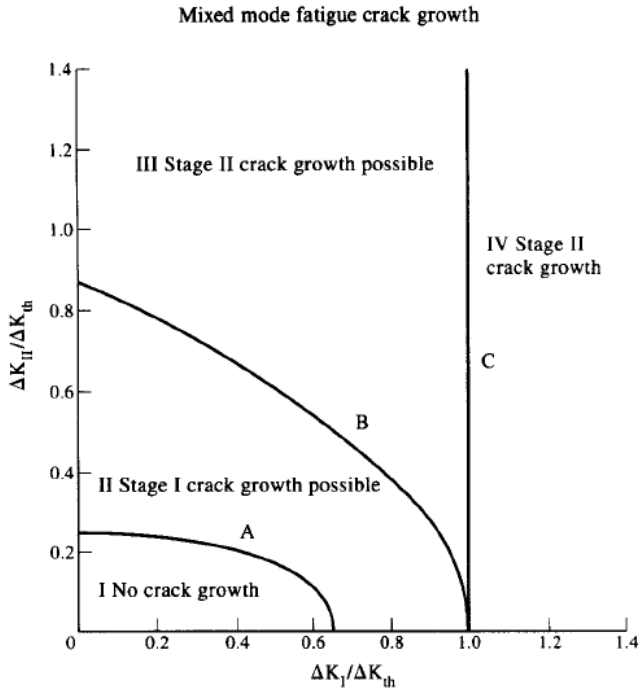

Figure 2.2 Relationship between crack growth and normalized SIF factors [26].

Mode I, also known as the opening or tensile mode, represents the most prevalent type of crack in aerospace. It involves the separation or opening of material and is associated with tensile stresses commonly encountered in aerospace applications. Various factors, such as aerodynamic forces, thermal expansion, and mechanical loading, contribute to the presence of these tensile stresses, which can initiate and propagate cracks within the structure.

The significance of mode I cracks in aerospace lies in their direct impact on structural integrity. If addressed, mode I crack can lead to catastrophic failure, posing significant risks to the safety and performance of aircraft. Therefore, aerospace engineers and designers prioritize preventing and managing mode I cracks during the design phase. Structural components are carefully designed to withstand and minimize the effects of tensile stresses, reducing the risk of mode I crack initiation and propagation. Safety regulations imposed by regulatory bodies and certification standards in the aerospace industry further underscore the importance of addressing mode I cracks. These regulations establish specific requirements and guidelines for inspections, maintenance procedures, and structural analysis techniques to detect and mitigate

mode I cracks. By adhering to these regulations, the aerospace industry ensures aircraft's structural integrity and airworthiness, enhancing overall safety and reliability.

Moreira et al. [27] conducted a 3D element analysis on a riveted column, investigating the influence of crack length on its behavior. The study incorporated the simulation of symmetrical and asymmetrical cracks, considering various crack lengths ranging from 0 to 8.605 mm. The analysis revealed that the selection of crack lengths was limited to a small number, typically observed in structural applications. Additionally, the study found that the stress intensity levels of K_{II} and K_{III} were comparatively minor when compared to K_I. These findings contribute to our understanding of crack behavior and stress distribution in riveted columns, providing insights into the significance of crack length and the relative stress intensity levels associated with different crack modes.

Figure 1.2 presents a workflow chart that was developed based on the literature reviews and studies conducted. A comprehensive analysis of the available research and examinations shows that topology optimization plays a crucial role in achieving mass reduction in aerospace applications. The studies also highlight the importance of stress intensity factor (SIF) calculations, which involve considering factors such as crack depth-length ratios. These insights gleaned from the literature reviews and studies served as the primary focus of the current research, guiding its direction and objectives.

CHAPTER 3

THEORY

3.1 Structural Optimization

Generally, optimization can be defined as reaching maximum efficiency under some circumstances. The essential purpose of optimization is to figure out the best possible solution under given circumstances [28]. It can be run mathematically or structurally. The essential f function of x can be classified as mathematical optimization work. While trying to optimize f(x) as minimal or maximum, optimization efforts to minimize or maximize f(x) have already been undertaken in the paper. In industry, engineers aim to produce the most efficient version of products. The critical point here is economic; decreasing the number of materials will give the most efficient version of the products. Indeed, while trying to reduce the mass of the material, we should also check the appropriation of the situation. Safe and efficient production is a goal for the engineers. Structural optimization can be examined for this purpose.

Spillers [29] defined structural optimization as the mathematical programming of a model. The goal is to find the optimum material distribution according to a given load and restriction. It can work on mass, displacement, or compliance. It is an iterative-intuitive process [28]. Iterative results should be interpreted by intuitive approaches.

To study optimization, work can be classified into three stages; In the first stage, designs should be prepared according to dimensions and conditions (loads). After this step, designs should be verified by using finite element methods. In step three, the optimization stage is finished if the needs are responded to. On the other hand, if the needs of the structure cannot be satisfied, the loop will start, and stages one and two should be repeated.

All structural problems consist of three variables mathematically:

The objective function (f): Used to classify designs, and it often measures weight, displacement in a specified direction, and critical stresses. The target function returns

a number for each possible design that indicates the health of that design. It is usually chosen to minimize the specified variable [30].

Design variable (x): A function or vector that defines the design and can be changed according to optimization. It might show geometry or material variation. Where it represents a geometry, it can be the interpolation of a complex shape, the area of a bar, or the thickness of a sheet [30].

State variable (y): A function or vector representing the response for variable x of a particular structure or design. For a mechanical structure, it can mean reaction force, displacement, and stress [30].

A structural optimization problem tends to minimize f(x, y) concerning x and y [30]. The results should be interpreted by workers (designers or analysts). Experience and intuitive approaches can be affected the results of optimization works. According to research, structural optimization can be divided into three areas named size optimization, shape optimization, and topology optimization [28].

3.1.1 Size Optimization

Size optimization, also known as sizing optimization, is a specific branch of structural optimization that focuses on optimizing the dimensions or sizes of structural components. The primary goal of size optimization is to determine the optimal distribution of material within a structure, considering various design constraints and performance requirements.

In size optimization, the dimensions of individual components or elements are adjusted to achieve desired objectives, such as minimizing weight, maximizing stiffness, or reducing stress concentrations. The optimization process involves iteratively modifying the dimensions of the components to find the most efficient configuration that meets the specified design criteria. Size optimization considers factors such as material properties, loading conditions, manufacturing constraints, and structural integrity requirements. By optimizing the sizes of the structural elements, engineers can achieve designs that are lighter, more cost-effective, and exhibit improved performance.

The process of size optimization typically involves mathematical algorithms, numerical methods, and simulation techniques. These tools help to analyze the structural behavior and evaluate the impact of different size configurations on the performance of the system. The optimization algorithms iteratively explore the design space, searching for the optimal size distribution that satisfies the specified objectives and constraints.

Size optimization can be applied to various structures and components in aerospace engineering, such as aircraft wings, fuselage sections, support structures, or mechanical systems. By optimizing the sizes of these components, designers can achieve weight reduction, improved fuel efficiency, increased payload capacity, or enhanced structural robustness. It can be considered the simplest form of structural optimization. The shape of the structure is already known, and the target is to adjust the size of the components. Sizes of the structural element should be considered as a design variable, which is x. The thickness of the sheet metal or a cross-sectional area can be examples of this optimization. It can be performed in 2D or 3D. Figure 3.1 shows an example work of size optimization.

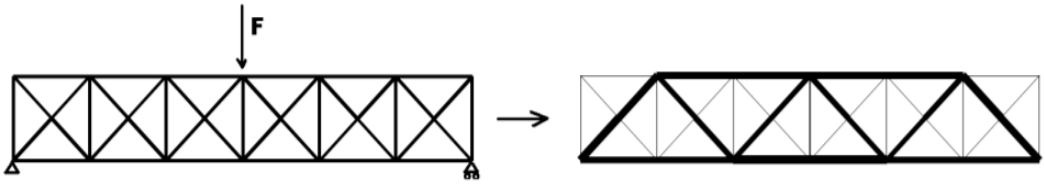

Figure 3.1 Size optimization [28].

Overall, size optimization is a powerful tool in aerospace engineering that allows engineers to find the most efficient size configurations for structural components, leading to improved performance, reduced weight, and enhanced overall design quality without any change in the structure. This is particularly critical in aerospace, where even small reductions in weight can have a significant impact on fuel efficiency, payload capacity, and maneuverability. By carefully optimizing the size of components such as wings, fuselages, and propulsion systems, aerospace engineers can achieve remarkable advancements in aircraft and spacecraft design, ultimately pushing the boundaries of what's possible in the realm of flight.

3.1.2 Shape Optimization

Shape optimization is a specialized field within structural optimization that focuses on optimizing the geometry or shape of a component or structure to achieve desired performance objectives. In shape optimization, the goal is to find the optimal shape that maximizes or minimizes a particular performance metric while satisfying specified constraints. The shape of a component plays a crucial role in determining its structural behavior, strength, aerodynamic properties, and overall performance. By modifying the geometry of the component, engineers can improve its efficiency, reduce stress concentrations, or achieve other desired outcomes. Shape optimization involves iteratively modifying the component's geometry, either by adding or removing material or adjusting its surface contours. The optimization process seeks to find the shape configuration that yields the best performance, considering factors such as weight, stiffness, drag, lift, stress distribution, or other relevant criteria. In aerospace engineering, shape optimization can be applied to various components, such as wings, airfoils, turbine blades, or structural elements. By optimizing the shape of these components, engineers can achieve improved aerodynamic efficiency, reduced drag, enhanced structural integrity, or other performance enhancements.

Some of the variables which are already known before the size optimization cannot change by using size optimization similar to radius, chamfers, or corners. In this point, shape optimization can be mentioned to change shapes. It optimizes existing holes or any other features on the structure. It will not open a new hole in the structure, but it can change the geometry of existing ones. This means that there will be no change in the topology of the structure. It may apply after topology optimization, which will be interpreted in the next section. X can be represented by the diameter of a hole, contour, or fillet. Boundary conditions will not change because of shape optimization. Figure 3.2 will clarify the idea.

The perturbation vector approach is one way to introduce shape changes to the discretized finite element model. Then, the optimization problem can find the optimum set of shape weights [28]. The Perturbation Vector Approach is a mathematical technique used in optimization and sensitivity analysis to approximate the changes in

a system's output or performance due to small perturbations in its input variables. It is beneficial when the system's response cannot be readily determined analytically or when the system is highly nonlinear.

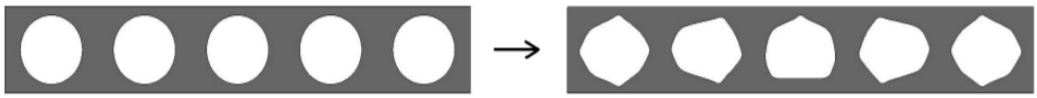

Figure 3.2 Shape optimization [28].

3.1.3 Topology Optimization

Topology optimization is a powerful technique used in the field of aerospace engineering to optimize the design of structures subjected to various loading conditions. It involves determining the optimal distribution of material within a given design space to achieve desired performance objectives while satisfying certain constraints. Topology optimization aims to find the most efficient and lightweight design that can withstand the applied loads and meet specific performance requirements.

Topology optimization is a subject that has been in our life for approximately 40 years. Topology optimization and advancement have turned into a viable apparatus for least-weight and execution plans, particularly in air transportation and aeronautic design. Topology optimization plays a crucial role in aerospace applications, where weight reduction is of utmost importance for enhancing fuel efficiency and increasing payload capacity. By systematically removing unnecessary material and redistributing it in regions experiencing higher stress or load concentrations, topology optimization can significantly reduce the weight of aerospace components while maintaining their structural integrity. One of the critical advantages of topology optimization in aerospace is its ability to generate complex and organic-shaped structures that are difficult to understand through traditional design methods [4]. Purpose of getting maximum efficiency from the existing product. For topology optimization, the purpose is to get the minimum mass for maximum performance. The main difference between topology optimization, size, and shape optimization is that topology optimization does

not deal with predefined configurations. The result of the topology optimization can be rearranged by using the intuition and knowledge of the designer or users. While doing this work, size and shape optimization can be used to make arrangements for the topology optimization results. Once the optimum distribution of material is achieved, the optimization process is considered successful. It is also possible to modify the geometry of the structure using topology optimization.

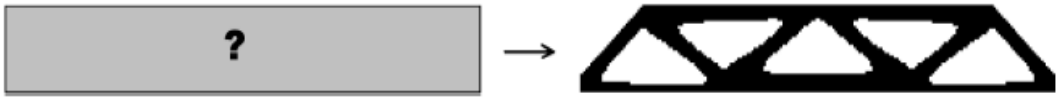

Figure 3.3 Topology optimization [28].

Topology optimization starts with defining the design space, representing the volume or region in which the optimization is performed. The design space is divided into smaller elements or voxels, each representing a potential material location. The optimization process then iteratively redistributes the material within the design space based on mathematical algorithms and objective functions. The objective functions used in topology optimization for aerospace applications typically involve minimizing structural weight, maximizing stiffness, or reducing stress levels while meeting various design and performance constraints, such as allowable displacements, stress limits, and geometric constraints. These objectives are essential for ensuring the structural integrity, reliability, and safety of aerospace components.

During the optimization process, finite element analysis (FEA) is commonly employed to evaluate the structural response and performance of the design. Thanks to this operation, it is easy to make complicated calculations. The FEA calculates stress, displacement, and other relevant parameters, allowing the optimization algorithm to adjust the material distribution iteratively until an optimal design is achieved [28]. Figure 3.4 shows the process of optimization. It is easy to see that it starts from the original design to FEA results. According to the figure, topology optimization can simplify steps; first, you need to find or design a geometry and then apply boundary conditions to this model. After these processes, you must optimize your topology and

verify your boundary condition. Until the final design, you can repeat your FEA processes.

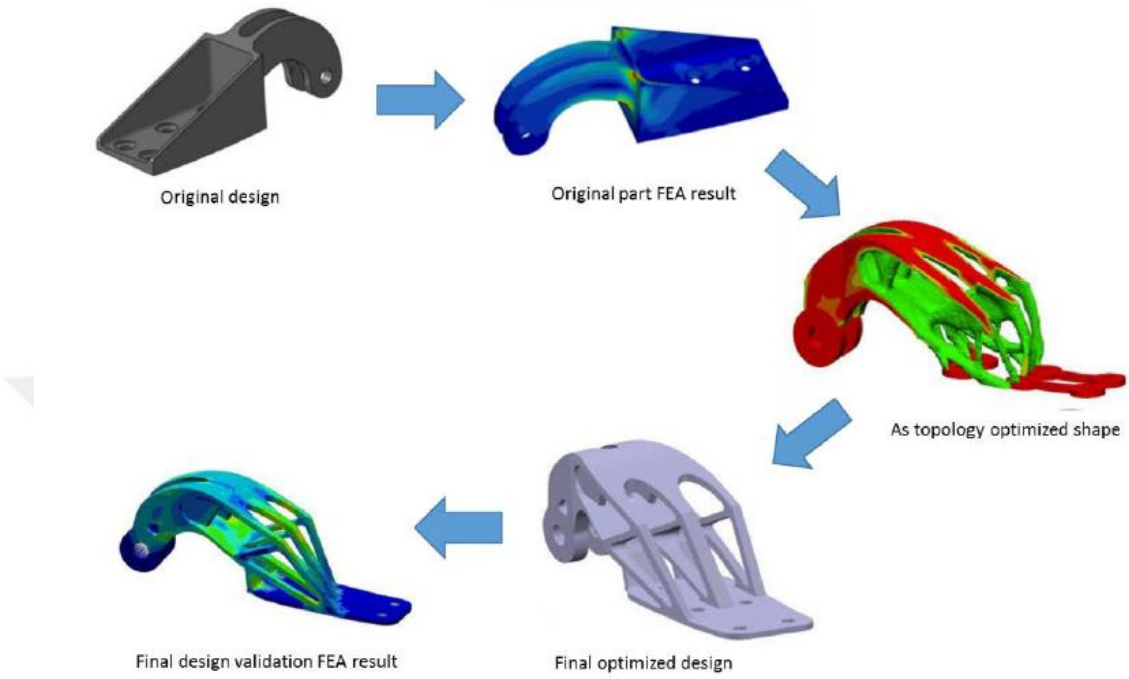

Figure 3.4 Topology optimization process [31].

By integrating topology optimization into the aerospace design workflow, engineers can explore vast design space and discover novel, high-performing solutions that were previously unattainable. The resulting designs are often lightweight, structurally efficient, and tailored to specific loading conditions, leading to improved fuel efficiency, enhanced maneuverability, and increased overall performance of aerospace systems. It is important to note that topology optimization in aerospace also considers manufacturing constraints and practical limitations. The optimized designs must be manufacturable using available production methods and materials, ensuring that the proposed solutions can be realized in practice.

In conclusion, topology optimization offers significant benefits in aerospace applications by enabling the creation of lightweight, efficient, and structurally optimized designs. By leveraging advanced mathematical algorithms, engineering intuition, and FEA, aerospace engineers can push the boundaries of design

possibilities, ultimately leading to more advanced and high-performance aerospace systems.

Topology optimization can be formulated as a zero or one problem, depending on the specific formulation and approach used. In its binary form, the optimization algorithm determines whether each element or voxel in the design domain should be present (assigned a value of 1) or absent (assigned a value of 0). This binary representation indicates whether a particular region should be filled with material or left empty. However, it is essential to note that gradient-based approaches also allow for intermediate values between 0 and 1, representing partial material densities. These approaches provide more flexibility in the optimization process and can lead to smoother and more realistic designs. The choice between binary and gradient-based approaches depends on various factors, including the specific objectives, constraints, and available computational resources. Both approaches have advantages and limitations, and the selection should be based on the specific requirements of the problem. This means that there are two choices for the elements in the region. They may exist or not [32]. Figure 3.5 illustrates the sensible of zero one approach.

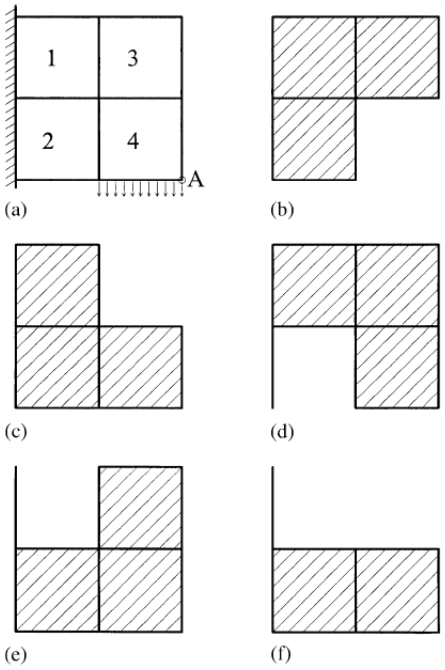

Figure 3.5 Topology optimization zero-one situation for the ISE [32].

Figure 3.5 depicts the boundary condition and loading area of the structure. In Figure 3.5 (b), a solution is shown that is deemed invalid for optimization. Area 4 represents the loading region and is attached to the boundary condition as a loading state. It is essential to retain this section, and it cannot be removed from the optimization process. On the other hand, Figure 3.5 (c) represents an example of a valid solution, while other possibilities also exist, some of which may not be suitable for optimization. This scenario exemplifies a classic 0-1 problem, where the decision of whether the regions or elements labeled as 1, 2, 3, and 4 should be included in the topology optimization or not arises. The 0-1 approach is employed to tackle this challenge, determining the optimal inclusion or exclusion of these regions in the topology optimization process.

When employing the 0-1, or black and white, approach in this process, we can consider two possibilities for the elements or regions: they can either exist or not exist within the optimization. This binary approach allows for a transparent decision-making process where each element or region is evaluated independently and included or excluded based on its potential contribution to the optimization objectives. Utilizing this 0-1 approach, the optimization algorithm can effectively determine the optimal configuration by selecting the elements or regions that provide the most favorable outcome while disregarding those that may not contribute significantly to the desired objectives. The optimization can be numbered as 2^N (for one material) of combinations; here, N shows the number of elements more than thousands during the optimization. This makes problems that cannot be solved by using standard analytical solutions [28, 32]. Finite elements analyzing programs can help to find a solution for these kinds of problems. Isotropic materials can be solved by using two main strategies, which are called the density and homogenization methods [28].

Density Method

It is a gradient base method to find the optimum solution for the topology. It targets finding the minimum value of the objective function. Density is considered the black and white approach in this method. 0% or 100% density should be taken for the material. Figure 3.6 will show this idea more clearly; the most famous one is named solid isotropic material with penalization (SIMP). SIMP focuses on the element densities and optimizes them according to the 0-1, making the formulation more

confusing. ANSYS also used this density-based method to finish the operations. It gives density to each finite element unit through design variables [28, 32-34].

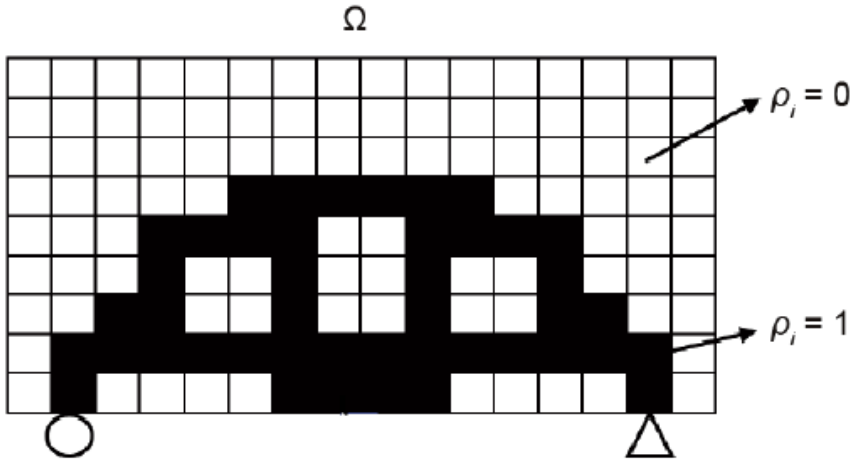

Figure 3.6 Density-based approach [33].

$$\rho_{\mathrm{I}} = \begin{cases} 1\ \Omega_i \subset \Omega^{mat} \\ 0\ \Omega_i \subset \Omega \backslash \Omega^{mat} \end{cases} \quad \textbf{(3.1)}$$

Figure 3.6 and Eq. 3.1 show the topology of the structure where (ρ_i= 1) represents the black elements which are material, and (ρ_i= 0) shows the white region, which is space. Ω_i is the domain of the ith element, Ω represents the design domain, and Ω^{mat} represents the structural topology [33].

This method uses a density field to represent the material distribution within the design domain. The density field is updated iteratively based on the structural response and optimization criteria. Elements with low densities are considered void or removed, while elements with high densities are considered solid materials.

Homogenization Method

In this method, optimization works like the density method. Still, the difference between the two methods can be called as this method interprets the density of a material as a microstructure. The homogenization method in topology optimization is a mathematical approach used to model and optimize the behavior of heterogeneous materials or structures. It is based on the concept of homogenizing the material

properties at a macroscopic level, considering the microscopic variations within the material. In the context of topology optimization, the homogenization method aims to find the optimal distribution of material phases or constituents within a given design space. It involves dividing the design domain into smaller sub-domains or elements and assigning different material properties to each element. These material properties can represent different phases, such as solid and void regions or materials with varying mechanical properties. This method was offered by Bendsoe and his friend. These methods change the microstructure as a composite material. It generally produces porous structures and then tries to the optimum distribution of the structure. By using this method orientation of the materials gain importance. When we compare it with the density method, it is easy to find that there will be more design variables during the optimization process [35, 36]. Figure 3.7 shows an example of a microstructure with rectangular holes(a) and layered ones(b).

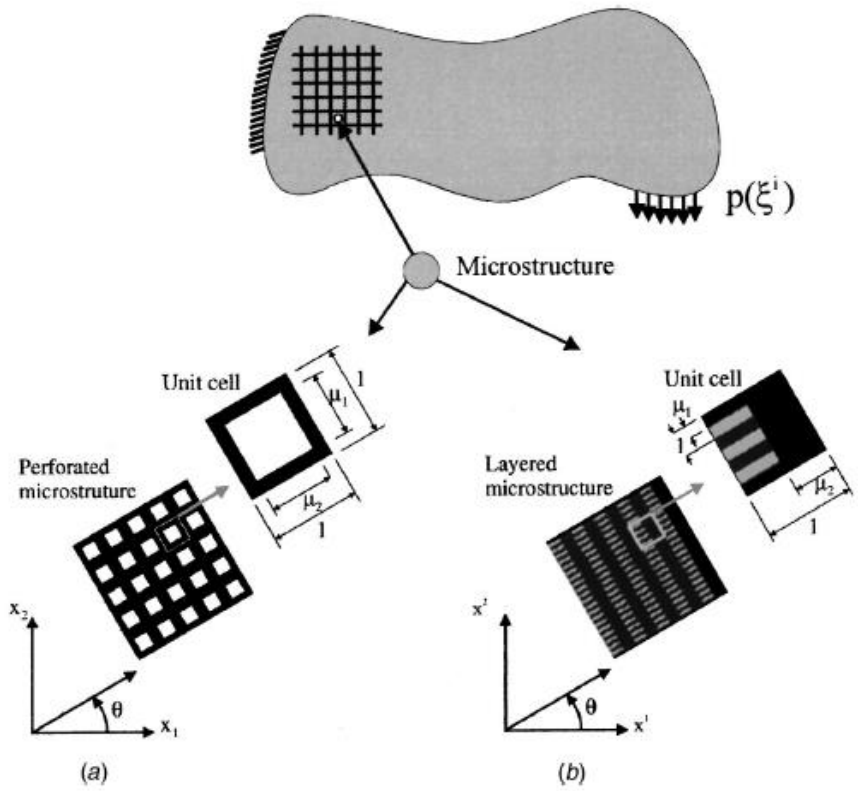

Figure 3.7 Homogenization method's unit cells in the structure with rotation [28].

3.1.4 Topology Optimization and Additive Manufacturing

Topology optimization and additive manufacturing are two groundbreaking technologies that have revolutionized the field of advanced design and manufacturing. Both methodologies offer unique advantages, and when combined, they unleash tremendous potential for creating highly efficient and innovative structures. The manufacturing industry is improving every single day. According to this, additive manufacturing can be considered a new area when we compare it to other methods, such as conventional or non-conventional machining methods. Thanks to the rapid development of additive manufacturing, topology optimization is also developed. The most crucial problem of topology optimization is that it is impossible to produce some geometry using conventional machining methods or conventional machining tools like endmills, drills, or inserts. It is difficult to ensure the results of topology optimization studies, which might be produced using traditional machining methods. Rib, cage structure, or geometries, which are harsh to make tooling to create them, cannot be machined easily by using conventional or non-conventional machining methods. These limitations can be passed by using additive manufacturing methods. Thanks to their flexibility, additive manufacturing (AM) methods enlighten or encourage topology optimization studies. Nowadays, there are many methods to produce new products using additive manufacturing as a metal structure. 3D printing methods create a flexible area for the metal structure and topology optimization operation. Thanks to the design flexibility of AM, topologically optimized designs can be readily manufactured without extra geometric constraints or tooling problems. It is a rapidly developing technology, and due to this situation, topology optimization works can be more important than now in the future [37, 38].

In conclusion, the combination of topology optimization and additive manufacturing represents a significant leap forward in advanced design and manufacturing. This powerful synergy offers engineers unprecedented opportunities to create optimized, lightweight, and highly complex structures. As these technologies evolve and mature, their integration will pave the way for even more innovative and sustainable solutions in various industries, revolutionizing how we design, produce, and use products.

3.2 Linear Elastic Fracture Mechanics (LEFM)

Linear Elastic Fracture Mechanics (LEFM) is a branch of fracture mechanics that deals with the behavior of cracks in materials under conditions of linear elasticity. It provides a theoretical framework for analyzing the growth and propagation of cracks in structures subjected to mechanical loading. LEFM assumes that the material in which the crack is present behaves linearly elastic, meaning that it deforms elastically under applied loads and returns to its original shape when the load is removed. The theory focuses on the stress and strain fields around the crack tip and the concept of stress intensity factor (K), which quantifies the level of stress concentration at the crack tip. Linear Elastic Fracture Mechanics (LEFM) is based on several fundamental principles. First, it recognizes that the crack tip acts as a stress concentrator, causing an increase in stress levels compared to the surrounding material. The stress intensity factor (K) is a key parameter in LEFM, as it quantifies the magnitude of stress concentration at the crack tip. The value of K depends on factors such as the applied load, crack geometry, and material properties [39].

Fracture toughness (Kc) is another crucial concept in LEFM. It represents a material's resistance to crack propagation and indicates its ability to withstand the growth of a crack under applied stresses. Fracture toughness is a material property that influences the critical stress intensity factor (Kc), which is used to assess the fracture resistance of a material. Crack propagation can occur if the stress intensity factor at the crack tip exceeds the critical value.

In LEFM, crack growth is assumed to occur when the stress intensity factor reaches a critical value known as fracture toughness. This critical value determines the rate at which the crack will propagate through the material. By understanding and analyzing the stress distribution, stress intensity factors, fracture toughness, and critical values, engineers can evaluate the structural integrity of components, predict crack growth behavior, and make informed decisions regarding the design and maintenance of structures to prevent catastrophic failures. LEFM provides a basis for designing and analyzing structures to prevent catastrophic failure caused by crack propagation. It is commonly used in engineering applications to assess the structural integrity of

components, determine safe operating limits, and predict the fatigue life of materials under cyclic loading conditions. Basically, isotropic and homogenous material stresses around the crack tip are generally examined by using linear elastic fracture mechanics [40]. It simply analyses of cracks in the linear elastic materials [41]. This theory was developed by using the stress intensity factor (SIF). The stress area, which is close to the crack tip, is computed using the elasticity theory. If the SIF is bigger than the material's fracture toughness, the crack will be advanced because of the high-stress values and accumulation. Firstly, stresses near the crack tip should be calculated before the stress intensity factor is examined. To do this calculation, materials are accepted as elastic, isotropic, and homogeneous. Figure 3.8 shows the coordinate system (r and θ) for the stress components.

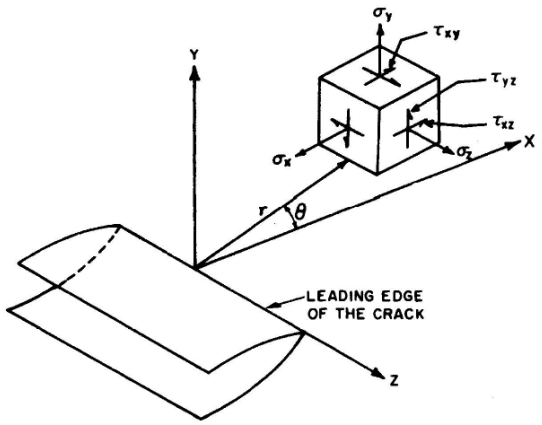

Figure 3.8 The coordinates (r,θ) for the stress components [40].

There are some governing equations for linear elastic analysis in 2D. The strain-displacement relations can be represented by Eq. 3.2 to 3.4, where ε denotes strain and u denotes displacement according to axis [42],

$$\varepsilon_{xx} = \frac{\partial u_x}{\partial x} \quad \textbf{(3.2)}$$

$$\varepsilon_{yy} = \frac{\partial u_y}{\partial y} \quad \textbf{(3.3)}$$

$$\varepsilon_{xy} = \frac{1}{2}\left[\frac{\partial u_x}{\partial y} + \frac{\partial u_y}{\partial x}\right] \quad \textbf{(3.4)}$$

To associate them with stress, consider the condition $\varepsilon_{zz} = \varepsilon_{xz} = \varepsilon_{yz} = \tau_{xz} = \tau_{yz} = 0$ for plane stress, where σ represents normal stresses and τ denotes shear stress. E represents the

Young's modulus, and *G* stands for the shear modulus.

$$\sigma_{xx} = \frac{E}{(1+v)(1-2v)}\left[(1-v)\varepsilon_{xx} + v\varepsilon_{yy}\right] \quad \textbf{(3.5)}$$

$$\sigma_{yy} = \frac{E}{(1+v)(1-2v)}\left[(1-v)\varepsilon_{yy} + v\varepsilon_{xx}\right] \quad \textbf{(3.6)}$$

$$\tau_{xy} = 2G\varepsilon_{xy} = \frac{E}{1+v}\varepsilon_{xy} \quad \textbf{(3.7)}$$

$$\sigma_{zz} = v\left(\sigma_{xx} + \sigma_{yy}\right) \quad \textbf{(3.8)}$$

For plane stress, where $\sigma_{xx} = \varepsilon_{xz} = \varepsilon_{yz} = \tau_{xz} = \tau_{yz} = 0$ and v is poisson's ratio; the Equations 3.5 to 3.8 can be formed as 3.9 to 3.12,

$$\sigma_{xx} = \frac{E}{1-v^2}\left[\varepsilon_{xx} + v\varepsilon_{yy}\right] \quad \textbf{(3.9)}$$

$$\sigma_{yy} = \frac{E}{1-v^2}\left[\varepsilon_{yy} + v\varepsilon_{xx}\right] \quad \textbf{(3.10)}$$

$$\tau_{xy} = 2G\varepsilon_{xy} = \frac{E}{1+v}\varepsilon_{xy} \quad \textbf{(3.11)}$$

$$\varepsilon_{zz} = \frac{-v}{1-v}\left(\varepsilon_{xx} + \varepsilon_{yy}\right) \quad \textbf{(3.12)}$$

Eq. 3.13 and 3.14 represent the equilibrium equations for a two-dimensional stress field in a material [42],

$$\frac{\partial \sigma_{xx}}{\partial x} + \frac{\partial \tau_{xy}}{\partial y} = 0 \quad \textbf{(3.13)}$$

$$\frac{\partial \sigma_{yy}}{\partial y} + \frac{\partial \tau_{xy}}{\partial x} = 0 \quad \textbf{(3.14)}$$

And the compatibility equation can be evaluated as Eq. 3.15 [42],

$$\left[\frac{\partial^2}{\partial x^2} + \frac{\partial^2}{\partial y^2}\right]\left(\sigma_{xx} + \sigma_{yy}\right) = 0 \quad \textbf{(3.15)}$$

3.2.1 Stress Intensity Factor (SIF)

The stress intensity factor (SIF) is a parameter used in fracture mechanics to assess the severity of a crack or flaw in a material. It quantifies the stress field near the tip of the

crack and provides a measure of the stress concentration at the crack tip. According to usage and other circumstances, cracks can be formed in the structure. They are the most common defects in the engineering structure [43]. The stress intensity factor (SIF) can be used to define the structural strength of this crack. It is known as “the stress field ahead of a sharp crack in a test specimen or a structural member” [40]. This knowledge helps to calculate the crack growth rate in the structure. When a crack exists in a material under applied stress, the stress intensity factor represents the ratio of the applied stress to the square root of the crack size. It is denoted by the symbol K and has units of stress times the square root of length (such as MPa√m or ksi√in). The stress intensity factor is a critical parameter in fracture mechanics because it influences the behavior of cracks and determines their tendency to propagate. As the stress intensity factor increases, the crack becomes more prone to growth and eventual failure. Therefore, the stress intensity factor is often used to predict the fracture strength and fatigue life of materials. The stress intensity factor calculation depends on factors such as crack geometry, applied loading conditions, and material properties. Different analytical and numerical methods, such as the stress analysis around the crack tip and finite element analysis, are employed to determine the stress intensity factor in specific cases. Understanding the stress intensity factor is essential for assessing the structural integrity of components with cracks or flaws, as it helps engineers and researchers predict the behavior and failure of materials under different loading conditions [24, 44].

Multiple side damage (MSD) refers to the simultaneous growth of cracks in structures. This phenomenon commonly occurs near holes and rivet connections in the wings, where stress concentration points are present. MSD is a critical concern in aerospace applications as it can lead to accelerated crack propagation and structural failure. As a precaution for these kinds of cracks, stress intensity factors gain extra importance. Stress concentration loaded near to crack tip and stress concentration points for multiple cracks, formulas, and details will be more complicated [43, 45].

According to finite element methods, first, we need to identify the stress concentration point. Stress concentration refers to the localized increase in stress that occurs at a geometric feature, such as a notch, hole, or sharp corner, in a structural component.

When a member is subjected to an applied load, the stress distribution is not uniform. The presence of a stress concentrator causes stress to be amplified at that particular location, resulting in higher stress levels than the surrounding material. For the aerospace structure, it can be a connection point or any other place according to geometry. In these fields, cracks can be formed in three different modes. They can be named as mode I, II, and III. Mode I illustrate the opening mode, which is given in Figure 3.9. Mode II and III are also shown in Figure 3.9 and named sliding and tearing modes.

1. Mode I (Opening Mode or Tensile Mode): In Mode I, the crack surfaces are subjected to tensile or opening stresses perpendicular to the crack propagation direction. This mode is characterized by crack growth due to the separation of crack surfaces.

2. Mode II (Shearing Mode or Sliding Mode): In Mode II, the crack surfaces experience shearing or sliding stresses parallel to the crack propagation direction. This mode involves crack growth due to the relative sliding or shearing of the crack surfaces.

3. Mode III (Tearing Mode or Anti-Plane Shear Mode): In Mode III, the crack surfaces are subjected to tearing or anti-plane shear stresses perpendicular to the crack propagation direction. This mode is associated with crack growth caused by the tearing or shearing of the material.

4. Mixed Mode: Mixed mode crack growth refers to situations where multiple modes of crack growth co-occur or where the mode of loading changes during crack propagation. It can involve a combination of Mode I, Mode II, and Mode III stresses.

The K value, or stress intensity factor, is commonly chosen for calculating stress intensity factors (SIF) in fracture mechanics for several reasons. Mode I crack propagation dominates many engineering applications, representing crack opening or tensile stress. The K value specifically quantifies the stress field near the crack tip under Mode I loading conditions, making it suitable for assessing crack growth in these

scenarios. It is primarily used in linear elastic fracture mechanics (LEFM), which assumes elastic behavior and linear stress-strain response. The K value has undergone extensive research and validation, and it has a well-established theoretical foundation and wide application across various materials and structures. Additionally, it is supported by standardized testing and design codes, making it a widely accepted parameter for fracture analysis and design purposes. For simple geometries, stress intensity factors can be formalized as seen in Eq. 3.16, where *K* represents the stress intensity factor, σ is the nominal stress value in this point, and *a* is related to the crack size. Here *P* is a variable parameter that can vary according to geometry which is unitless [46-48].

$$K = \sigma\sqrt{\pi a}P \tag{3.16}$$

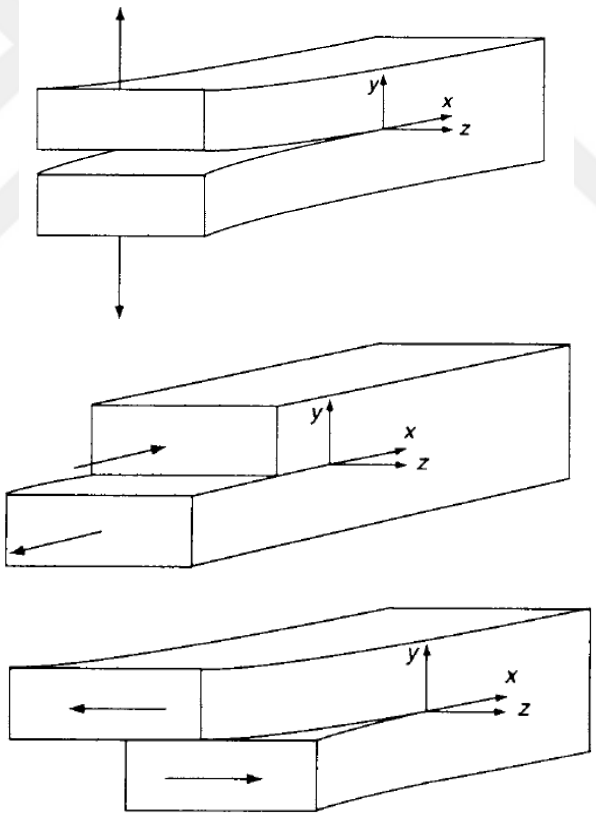

Figure 3.9 Mode shapes I, II, and III [49].

To talk about mode shapes, these arrows show the loading condition for mode I (opening mode), which is the most common [26]. One, it is easy to see the

perpendicularity of the crack when we compare it with the load. Mode I crack growth is prevalent in aerospace applications and other fields for several reasons. Aerospace structures often experience tensile loading conditions, where the applied stresses act perpendicular to the crack surfaces. This leads to Mode I crack growth, as the crack surfaces are subjected to opening or tensile stresses. Additionally, many aerospace materials have higher fracture toughness in Mode I compared to other modes, making them better suited for applications where safety and structural integrity are paramount. Aerospace structures are carefully designed to minimize stress concentrations and avoid geometric features that could promote Mode II or Mode III crack growth. Non-destructive inspection techniques used in aerospace, such as visual inspection and ultrasonic testing, are particularly effective at detecting Mode I cracks. It generally happens symmetrically. Opening mode (Mode I) crack growth is the most common type of crack observed in aerospace applications for several reasons. Aerospace structures are subjected to various types of loads, including aerodynamic forces, thermal expansion, and mechanical loading, which often result in tensile stresses. These tensile stresses can cause crack initiation and propagation along the plane perpendicular to the applied load, making Mode I cracks the dominant mode of crack growth. The structural integrity of aerospace components is heavily influenced by Mode I cracks, which can lead to catastrophic failure if left unchecked. Therefore, preventing and managing the mode I crack is a crucial consideration during the design phase. Aerospace engineers prioritize measures such as material selection, geometry optimization, and the incorporation of crack arrest features to minimize the effects of tensile stresses and mitigate the risk of crack growth. Safety regulations in the aerospace industry also emphasize detecting and mitigating Mode I cracks through inspections, maintenance procedures, and structural analysis techniques. Extensive research and experience support the prevalence of Mode I crack growth in aerospace, further highlighting its significance in ensuring the structural integrity and safety of aircraft. Shearing and tearing modes do not occur frequently. According to Figure 3.9, it is easy to catch those shearing modes when the crack faces slide on each other in the x direction. Similarly, as said before, tearing mode, which is mode III, happens by sliding faces along the z-direction. They are rare ones, like mode I [50]. This thesis also focuses on mode I cracks.

The airy function, which is Φ, can also be used to identify stresses on the crack tip. Φ can be used to govern equations near to stress field by using K_I as seen in Eq 3.17, where r represents a distance or radial coordinate, and θ is the angle.

$$\phi = \frac{K_I}{3\sqrt{2\pi}} r^{3/2} \left(\cos\frac{3\theta}{2} + 3\cos\frac{\theta}{2}\right) \quad \textbf{(3.17)}$$

Adding into Eq. 3.15 results in Eq. 3.18 [42],

$$\frac{\partial^4\phi}{\partial x^4} + 2\frac{\partial^4\phi}{\partial x^2\,\partial y^2} + \frac{\partial^4\phi}{\partial y^4} = 0 \quad \textbf{(3.18)}$$

Stresses in this crack field can be specified as Eq. 3.19 to 3.23 [51],

$$\sigma_x = \frac{K_I}{\sqrt{2\pi r}}\cos\frac{\theta}{2}\left(1 - \sin\frac{\theta}{2}\sin\frac{3\theta}{2}\right) \quad \textbf{(3.19)}$$

$$\sigma_y = \frac{K_I}{\sqrt{2\pi r}}\cos\frac{\theta}{2}\left(1 + \sin\frac{\theta}{2}\sin\frac{3\theta}{2}\right) \quad \textbf{(3.20)}$$

$$\tau_{xy} = \frac{K_I}{\sqrt{2\pi r}}\cos\frac{\theta}{2}\cos\frac{3\theta}{2}\sin\frac{3\theta}{2} \quad \textbf{(3.21)}$$

$$\sigma_z = v\left(\sigma_x + \sigma_y\right) \quad \textbf{(3.22)}$$

$$\tau_{xz} = \tau_{yz} = 0 \quad \textbf{(3.23)}$$

Displacement on the nodes u, v and w can be specified as seen in Eq. 3.24 to 3.26, and they can also be used for Displacement Extrapolation Method (DEM) [52],

$$u = \frac{K_I}{G}\sqrt{\frac{r}{2\pi}}\cos\frac{\theta}{2}\left(1 - 2v + \sin^2\frac{\theta}{2}\right) \quad \textbf{(3.24)}$$

$$v = \frac{K_I}{G}\sqrt{\frac{r}{2\pi}}\sin\frac{\theta}{2}\left(2 - 2v - \cos^2\frac{\theta}{2}\right) \quad \textbf{(3.25)}$$

$$\mathrm{w} = 0 \quad \textbf{(3.26)}$$

In 2D perspectives, formulas can be simplified according to the mode I crack. But in real cases, which are 3D, they are not easy to calculate by using analytical methods.

As mentioned in future sections, many different methods exist to calculate the SIF factor [50].

Generally, the stress intensity factor can show different results according to geometry; we can compare circular crack or corner crack formulations which can be found in the handbooks manuals. We will get two different formulas when we check K_I values. As mentioned before, when geometry becomes more complicated, we must use the finite elements method according to boundary conditions or other dominants. There are some essential criteria for the FEA methods applications around the crack region, such as mesh sizes [48].

3.3 Finite Element Method (FEM)

Finite element method (FEM) is a computational technique used to solve partial differential equations (PDEs) and simulate the behavior of complex systems in engineering and scientific applications. FEM divides a complex domain into smaller, simpler subdomains called finite elements. By approximating the governing equations within these elements and assembling them into a global system, engineers can numerically solve the equations and obtain solutions for unknown variables. The main idea of FEM is to represent the behavior of a continuous system by discretizing it into finite elements. Each element is described by a set of mathematical equations, typically based on variational principles such as the principle of minimum potential energy. The behavior within an element is approximated using interpolation functions that relate the unknown variables to their values at specific locations within the element. The discretized equations are then assembled into a global system of algebraic equations by connecting the nodes or shared points between adjacent elements. This system represents the overall behavior of the entire system. Various numerical techniques, such as matrix inversion or iterative methods, are used to solve this system and obtain the values of the unknown variables. FEM is a versatile and robust method that can handle a wide range of engineering problems, including structural analysis, fluid dynamics, heat transfer, electromagnetics, and more. It allows engineers to analyze the response of structures and systems under different loading and environmental conditions, evaluate their performance, and optimize their design. FEM provides

insights into stress distribution, deformation, fluid flow patterns, temperature distribution, and other important system behavior factors. One of the key advantages of FEM is its ability to handle complex geometries and irregular boundaries by using flexible meshing techniques. Additionally, it offers good accuracy in capturing local phenomena and provides a cost-effective alternative to physical prototyping and testing. However, implementing FEM requires expertise in areas such as mesh generation, selection of appropriate element types, and interpretation of results [53].

In summary, finite element methods are a widely used numerical technique in engineering and science that enable the analysis and simulation of complex systems by discretizing them into smaller elements. They have revolutionized the field of computational engineering analysis and have become an essential tool for understanding and optimizing the behavior of diverse systems and structures. Finite elements methods are widely driven to predict some strength properties of the materials. It is easy to foresee stress values of structure or any other strength properties of it. It makes complex engineering calculations with software such as ANSYS. To do that, they generally use meshing methods. Meshes are built by using nodes. Node's location might be changed according to their coordinates too. Irregular shapes become sensible by using meshes which are volumes or elements. There are some different meshing methods, like quad-dominant, triangles, or multizone elements. The newer version of the program generally looks at the meshing methods from two main points of view. Hexagonal and tetrahedron elements can be said for them. Tetrahedron (tet) elements, called tets, offer a better solution when we compare them with hexagonal elements (hex) for complex geometry and complex analyses. There are some methods to measure the quality of these meshes. Skewness, element quality, or orthogonal quality count as some of them. Good quality meshes offer precise results for your analysis independently. For the skewness, it might be said that lower than .4-.5 is an excellent quality. From the element quality perspective, this value should be higher than .7. There are some graphs inside the program to make comments about the quality of meshes [54-58].

Selective or hybrid meshing is another vital point for analyses. It helps to individual meshing for individual elements. Some figure or element does not have to carry on a

complicated meshing element inside of it. They are a transition element to make analysis more straightforward and more professional than other ones. It is an important point to pay attention to. Besides these, the program also offers solutions about different perspectives like fluent, dynamic, heat transfer, or topology. Stress intensity factors. It means that it also studies fracture mechanics. According to literature research, the most efficient way to predict SIF is finite element methods because of the complexity of the equations and geometries. In ANSYS, there are two methods to evaluate stress intensity factors. These methods are named as Displacement Extrapolation Method (DEM) and Interaction Integral Method (IIM) [51]. DEM formulas were mentioned in the previous section, but they can be more complicated according to mixed modes or any other situation.

3.3.1 Interaction Integral Method (IIM)

The Interaction Integral Method (IIM) is a computational technique used in fracture mechanics to analyze and predict crack growth in materials. It provides a means to calculate the stress intensity factor (SIF) and obtain accurate estimations of crack growth rates. This method offers better results when we compare it with the traditional method. It needs fewer meshes, too; this situation can be considered the main advantage of this method. This method is related to energy release too. The interaction integral method only needs J-integral to study on crack. J integral can be calculated by using Eq. 3.27 below [52, 59].

$$J(s) = \lim_{\Gamma \to 0} \int_{\Gamma} \left(W\delta_{1i} - \sigma_{ij} u_{j1} \right) n_i d\Gamma \qquad \textbf{(3.27)}$$

According to Figure 3.10, this formula is valid in a region that can be named a stress concentration field. In the provided context, Γ(s) represents an integral contour surrounding the crack tip. The variable σ_{ij} denotes the Cauchy stress, while W represents the strain energy density. The components of the displacement gradient tensor are represented by u_{jl}, and δ_{ij} refers to the Kronecker delta [52]. According to these fields, which are named actual and auxiliary fields, the total J integral should be calculated by using the finite elements method. After these steps, displacement vector stresses around these regions, strains, and K values can also be evaluated using complex formulas. It is a powerful method, but ANSYS workbench does not explicitly

incorporate the Interaction Integral Method (IIM) as a built-in feature because it is powerful for 2D approaches. On the other hand, the IIM's numerical integration along the crack front can be computationally demanding, especially for complex geometries, and ANSYS workbench may have prioritized computational efficiency by utilizing other techniques that provide accurate results within reasonable computational resources. But it is possible to use it by using Mechanical Ansys Parametric Design Language (APDL) mechanical [51].

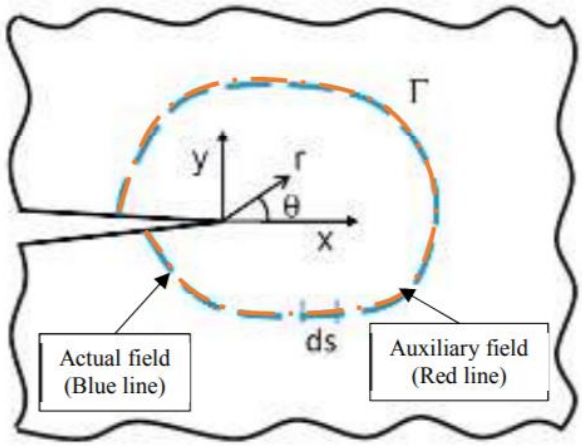

Figure 3.10 Crack tip region and its outline [52].

3.3.2 Virtual Crack Closure Technique (VCCT)

The Virtual Crack Closure Technique (VCCT) is a widely used method in fracture mechanics for calculating the stress intensity factor (SIF) and analyzing crack propagation in materials. It is a numerical approach that is commonly applied in conjunction with finite element analysis (FEA) to simulate and study crack behavior. The VCCT is based on the principle of energy release rate and conservation. It assumes that a crack grows by the release of stored elastic energy in the material. By analyzing the energy release rate, one can determine the driving force for crack propagation and evaluate the stability of a crack. The Virtual Crack Closure Technique is used to calculate the energy release rate (ERR). After the calculation, generally, it helps to calculate stress intensity factors too. The VCCT involves simulating the crack propagation process by incrementally extending the crack and calculating the change in energy release rate. The method assumes that crack growth occurs through the

opening and closing of the crack faces, and it estimates the difference in energy associated with this process. In delamination problems, total strain energy release rates can be useful. The virtual crack closure technique (VCCT) is generally used to evaluate energy release rates according to continuum mechanics [60].

The basic steps of the VCCT can be summarized as follows. It Generates a finite element model. Using finite element analysis, a numerical model of the structure or component containing the crack is created. The model should accurately represent the material properties, geometry, and loading conditions. Then it applies displacement or traction boundary conditions. Simulates the applied loads and boundary conditions on the model to represent the actual loading conditions experienced by the structure. After these applications, it is time to compute the stress field and solve the finite element model to obtain the stress distribution within the material. Finally, it calculates the energy release rate by using the stress field. This involves evaluating the work done on the crack faces as the crack extends or closes. Thanks to this, it assesses crack stability and propagation. By comparing the energy release rate with the critical energy release rate (fracture toughness) of the material. If the energy release rate exceeds the critical value, the crack is expected to propagate. The VCCT provides a practical and efficient method for analyzing crack growth in structures. It is particularly useful for studying cases where linear elastic fracture mechanics assumptions are applicable, and the crack tip behavior can be accurately captured using finite element analysis. The direction and rate of crack growth can also be estimated based on the stress field. Many finite element methods programs are used virtual crack closure techniques such as ANSYS [51, 61].

The two-step crack closure method can be contemplated as the elder of the virtual crack closure technique. This method is based on Irwin's crack closure integral. It examines two steps, which are crack started and extended ones. According to Figure 3.11, it can be formulated as seen in Eq 3.28 and 3.29 [61].

$$\Delta E = \frac{1}{2}[X_{1\ell}\Delta u_{2\ell} + Z_{1\ell}\Delta w_{2\ell}] \quad \textbf{(3.28)}$$

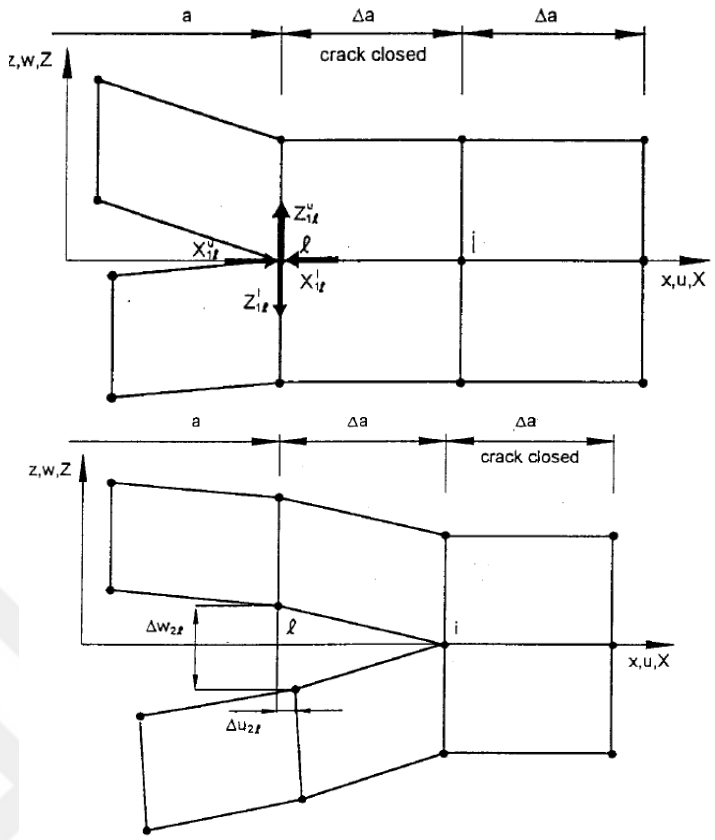

Figure 3.11 Two-step crack [61].

Modified crack closure method, which is also named as virtual crack closure technique, generally uses the same assumption as the two-step ones. Except for this, the virtual crack closure technique assumes that crack extension does not change on the crack tip region. It decreases the equation according to Figure 3.12 *where* $Z_i = Z_i^l = Z_i^u$ and $X_i = X_i^l = X_i^u$ from equilibrium, and more specified information about calculation and 2D-3D version can be found in [61],

$$\Delta E = \frac{1}{2}[X_i \Delta u_\ell + Z_i \Delta w_\ell] \quad \textbf{(3.29)}$$

Indeed, with in-depth studies and further analysis, it is possible to calculate the strain energy release rate, G, of the structure, which can calculate per mode. By dividing the

change in strain energy by the change in crack opening displacement, you obtain the stress intensity factor, K.

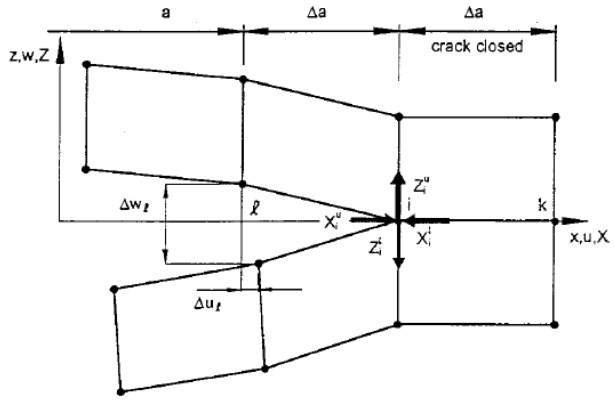

Figure 3.12 VCCT one step [61].

3.3.3 J Integral

The J-integral method is a widely used technique in fracture mechanics for analyzing crack behavior and predicting failure in materials. It provides a measure of the strain energy release rate along the crack front, which is a critical parameter for assessing crack stability and determining the conditions under which crack propagation may occur. In fracture mechanics, the J-integral represents the work done per unit crack length required to extend the crack. It is particularly useful for cases involving large plastic deformation, non-linear material behavior, or mixed-mode loading conditions, where the stress intensity factor (SIF) approach may not be applicable. The J-integral is determined by constructing a closed contour or path around the crack tip. The contour should enclose the region of interest and capture the stress and strain fields associated with the crack. The J-integral is calculated by performing a domain integral along this contour, integrating the product of stress and displacement gradients. Also, there is a relationship between the J value and the K value in fracture mechanics. The *J* value and the *K* value are both stress intensity factors that provide information about the crack driving force and the potential for crack growth. In certain cases, they can be related to each other through Eq. 3.30 [51].

$$J = \int_A \left[\sigma_{ij} \frac{\partial u_j}{\partial x_1} - w\delta_{1i}\right] \frac{\partial q}{\partial x_i} dA \qquad \textbf{(3.30)}$$

ANSYS provides capabilities for performing J-integral calculations. The ANSYS software offers various tools and commands to define the contour, perform the domain integration, and evaluate the J-integral for a given model and loading conditions. In ANSYS Mechanical APDL, the J-integral calculation is typically performed using the "CINT" command, which allows users to specify the contour or path for integration. The software computes the J-integral by numerically evaluating the domain integral along the specified contour using the stress and displacement fields obtained from finite element analysis [51].

While the J-integral also plays a significant role in fracture mechanics and offers advantages in certain situations, such as when dealing with plastic deformation or mixed-mode crack propagation, the K value remains the primary choice for SIF calculations in many engineering applications due to its simplicity, historical usage, and well-established framework within linear elastic fracture mechanics.

CHAPTER 4

MATERIALS and METHODOLOGY

4.1 Materials

As mentioned before, AISI 4340 is a common material for aerospace structures according to its extreme mechanical qualifications and manufacturing quality. It is a material that is easy to manufacture when we compare it to any other aerospace materials, similar to titanium or superalloys. AISI 4340 is a popular and widely used alloy steel known for its excellent strength, toughness, and high hardenability. It belongs to the nickel-chromium-molybdenum (Ni-Cr-Mo) alloy steel family and is often referred to as a "high-strength, low-alloy" (HSLA) steel.

Some heat treatment operations provide outstanding mechanical properties. According to literature studies, it is possible to get ultimate tensile strength values that are higher than 1900 MPa and high fracture toughness values by doing heat treatment operations [62]. It is classified as high-strength alloyed steel and offers different properties at different temperatures [63]. Table 4.1 shows the chemical properties of AISI 4340 steel, and Table 4.2 illustrates the mechanical properties of AISI 4340 steel.

Table 4.1 Chemical properties of AISI 4340 steel [63].

Elements	**C**	**Si**	**Mn**	**Ni**	**Cr**	**Mo**	**P**	**S**
wt. (%)	0.39	0.24	0.61	1.46	0.67	0.17	0.02	0.006

AISI 4340 exhibits high tensile strength and toughness, making it suitable for demanding applications where strength and impact resistance are critical. It has a good balance of strength and ductility, allowing it to withstand heavy loads and absorb energy without fracturing. This unique set of properties makes AISI 4340 particularly well-suited for use in critical industries such as aerospace, automotive, oil and gas, and machinery, where reliability under stress and the ability to withstand challenging environmental conditions are essential [63].

Table 4.2 Mechanical properties of AISI 4340 steel [14].

S.NO	PARAMETERS	Steel Alloy, AISI-4340
1	Young's Modulus(N/mm^2)	203000
2	Poison's Ratio	0.32
3	Ultimate Tensile Strength (N/mm^2)	1835
4	Yield Stress, σ_y (N/mm^2)	1600.8
5	Fracture Toughness (MPa.mm^(1/2))	1581,14

First and foremost, it exhibits excellent strength and toughness properties, making it suitable for withstanding the demanding operating conditions experienced by aerospace components. The high tensile strength of AISI 4340 allows it to withstand heavy loads and resist deformation, ensuring the structural integrity of critical parts. Additionally, its toughness helps to prevent catastrophic failures by absorbing energy and resisting crack propagation. Another reason for the popularity of AISI 4340 is its good hardenability, which enables it to be heat-treated and achieve high levels of hardness and strength. This makes it suitable for applications where increased hardness and wear resistance are required, such as gears, shafts, and structural components. AISI 4340 also offers good fatigue resistance, which is crucial in aerospace engineering, where components are subjected to cyclic loading and varying stress levels. Its fatigue properties allow it to endure repeated stress cycles without significant degradation, contributing to aerospace structures' long-term reliability and durability. Furthermore, AISI 4340 exhibits good machinability, which simplifies the manufacturing process and allows for efficient production of aerospace components. It can be readily machined into complex shapes and configurations, facilitating the fabrication of intricate parts with tight tolerances. Lastly, the availability and cost-effectiveness of AISI 4340 contribute to its widespread use in aerospace engineering. It is a commercially available alloy with a reasonable price point, making it an attractive choice for manufacturers [63].

Considering its combination of strength, toughness, hardenability, fatigue resistance, machinability, and cost-effectiveness, AISI 4340 has established itself as a common

and reliable material for various aerospace applications, including aircraft structural components, landing gear systems, engine parts, and transmission components.

Aluminum 2024 can be classified as one of the materials which are suitable for the infrastructure of wings. According to their density, they can be classified as lightweight structures. Aluminum 2024, an advanced aluminum alloy for aerospace applications, offers better fracture toughness, ductility, and damage tolerance when we compare it with ordinary aluminum. These qualifications make them suitable materials for advanced aerospace applications and make them aerospace alloys [64, 65]. Also, it is easy to process higher revolutions, and feed can be used to manufacture them. Table 4.3 shows the chemical properties of it, and Table 4.4 offers mechanical properties of it. According to its density and other extreme properties, it can be used as a wing spar in the wings to get light structures for aerospace applications [66]. Simply, it is a popular high-strength aluminum alloy known for its excellent mechanical properties and good machinability. It belongs to the 2000 series of aluminum alloys and is primarily composed of aluminum, copper, and small amounts of other elements.

Table 4.3 Chemical properties of Aluminum Alloy-2024-T351 [67].

Elements	**Zn**	**Mg**	**Cu**	**Cr**	**Mn**	**Si**	**Fe**	**Ti**
wt. (%)	0.25	1.2-1.8	3.8-4.9	0.10	0.3-0.9	0.50	0.50	0.15

Table 4.4 Mechanical properties of Aluminum Alloy-2024-T351 [14].

S.NO	**PARAMETERS**	**Aluminum Alloy-2024-T351**
1	Young's Modulus(N/mm^2)	72400
2	Poison's Ratio	0.33
3	Ultimate Tensile Strength (N/mm^2)	503.7
4	Yield Stress, $б_y$ (N/mm^2)	472.6

Different heat treatment operations can be named T3 (T351) or with different numbers; it offers different mechanical properties according to different levels of heat treatment operations.

Figure 4.1 shows the fuselage bracket which is used for this study and its material specification. The wing fuselage bracket uses 4340 steel, and the I beam uses aluminum alloy. Figure 4.2 shows the welding case model too. There are many studies about welding aluminum 2024 alloy [68], which can be subject to the study as a welding case.

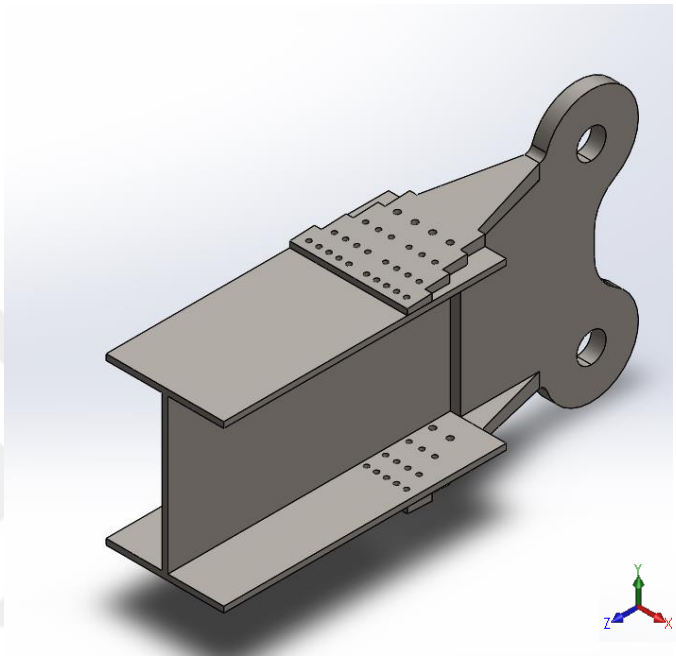

Figure 4.1 Wing fuselage bracket for case 1 (riveted case).

This model was taken from literature works. There are lots of models which were mentioned in the literature review section. It is designed as a wing fuselage bracket for a fighter jet which is a medium size fighter aircraft. Necessary dimensions were taken from [14] and designed by using Solidworks software. SolidWorks is a popular computer-aided design (CAD) software application used for creating and modeling 3D designs of mechanical and industrial components and assemblies.

It is simple to understand that there are two parts to this structure. This thesis only focuses on wing fuselage attachment brackets. I spar beam is used for the load application. Also, the reference paper says that rivet connections were used to attach the I spar and lug attachment bracket. In the Finite Element Analysis (FEA) modeling

of the structure, the chosen boundary conditions align with those described in the literature.

In constructing the structure, specific materials were chosen to fulfill the required mechanical properties and achieve the desired performance characteristics. The attachment bracket, serving as a crucial component, was fabricated using AISI 4340 heat-treated steel. This steel alloy is renowned for its exceptional strength, toughness, and resistance to wear and fatigue, making it suitable for applications where high rigidity and mechanical properties are essential. An aluminum alloy known as 2024-T3 was employed for the I spar beam. Aluminum alloys are favored in aerospace applications due to their excellent strength-to-weight ratio and corrosion resistance. The 2024-T3 alloy exhibits high tensile strength and good fatigue resistance, making it ideal for the lightweight requirements of the medium-sized fighter jet. The selection of steel alloy for the attachment bracket and aluminum alloy for the I spar beam reflects a balanced approach, capitalizing on the rigidity and extreme mechanical properties of steel while taking advantage of aluminum's lightness and favorable characteristics. This combination creates a medium-sized fighter jet with optimal strength, durability, and efficiency in its design and performance.

During the study, two cases were conducted to analyze the attachment bracket. In Case 1, represented by Figure 4.1, the objective was to perform topology optimization on the attachment bracket made of steel alloy. This involved optimizing the design to reduce mass while maintaining structural integrity. In Case 2, depicted in Figure 4.2, a different approach was taken, focusing on welding as the attachment method. Topology optimization operations were applied to both cases to improve the design and achieve desired objectives. After the topology optimization, static-transient verification analyses were conducted to evaluate the performance and structural integrity of the optimized brackets. These analyses assessed factors such as stress distribution and load-bearing capacity to ensure the brackets could withstand operational conditions. Additionally, stress intensity factors were examined, providing insights into crack initiation and propagation potential. It is important to note that Figure 4.2 illustrates a design devoid of elements like rivets, suggesting the utilization of an alternative attachment method, such as welding. This variation highlights the

exploration of alternative joining techniques and the potential benefits they can offer regarding structural performance and weight reduction.

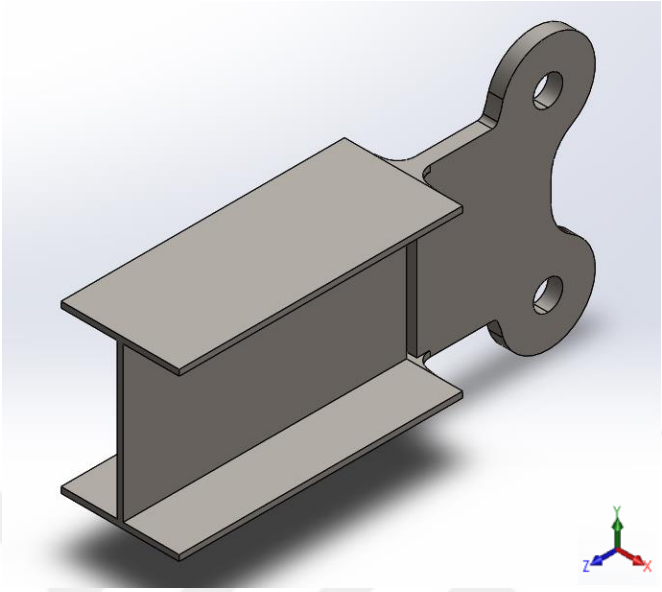

Figure 4.2 Wing fuselage bracket for case 2 (welded case).

4.2 Methodology

The models for the structural analysis were created using CAD software, specifically Solidworks 2018. Finite Element Analysis (FEA) methods were employed for the structural analysis portion of the study. ANSYS software, specifically versions 2020 and 2022 R2, was utilized for numerical modeling and analysis. Various cases and verification studies were conducted using ANSYS software, employing finite element methods. The load calculation for the existing scenario was performed based on information obtained from a medium-sized aircraft and utilizing the G methods, which are commonly employed in aerospace engineering for load calculations [14]. The combination of CAD software, FEA methods, and ANSYS software facilitated the accurate modeling and analysis of the structure, allowing for comprehensive evaluations of its performance and behavior under different loading conditions.

The total weight of the middle-sized aircraft is 6000 kg, which is equivalent to 58800 N. Considering a load factor of 6g for the ultimate loading condition, the worst-case scenario is considered in the literature. Consequently, the total load acting on the wing-

fuselage (lug) attachment bracket was determined to be P1 = 90584.62 N [14, 69]. The research examined the application of an upward load at one end of the spar beam to ensure proper structural support and accommodate the generated lift during take-off. This loading condition was crucial for generating the desired bending moment at the root of the bracket, where the wing and fuselage are connected. The study aimed to analyze and optimize the structural integrity and stability of the attachment point, thereby ensuring the safe operation of the aircraft under the calculated load conditions.

4.2.1 Wing Fuselage Bracket

Static Interpretation

After the modeling operation, which is given in Figure 4.1, the finite element methods operation started to run. The first purpose was to understand the existing situation and verify the loading conditions (see Appendix-A). Static and transient analyses were done to figure out the problem more clearly, and critical stress point points were found. Thanks to this operation, there will be an infrastructure for the topology optimization operations.

Table 4.5 Mesh details of the riveted model.

Characteristics of Mesh	General mesh
Mesh Method	Patch Conforming Method (Tetrahedron) + Face Sizing + Body Sizing
Resolution	3
Skewness	0.38013
Orthogonal Quality	0.61695
Element Quality	0.72504

Before starting the analyses, meshing operations were run according to quality assessments. All the operations and meshing methods were the same as each other, and some quality assessment methods were checked to get acceptable meshing methods. Tetrahedron elements were chosen according to their capability to mesh with high quality [70]. Tetrahedrons consist of triangular elements inside of them.

Tetrahedrons are widely regarded as one of the best meshing elements in finite element analysis (FEA) due to their versatility, simplicity, and convergence properties. They can effectively mesh complex geometries and irregular shapes, conforming well to curved surfaces and intricate features. Tetrahedral meshes are relatively easy to generate and require fewer computational resources, resulting in faster analysis setup. Their flexibility allows for local mesh refinement in areas of interest, capturing accurate results where needed. Tetrahedral elements demonstrate good convergence behavior, providing reliable and accurate solutions. Additionally, they offer uniform distribution of element sizes, contributing to accurate stress and strain calculations.

Most FEA software tools support tetrahedral meshes, making them widely accessible and supported in the industry. Ultimately, the choice of mesh element depends on specific analysis requirements, but tetrahedrons are often preferred for their versatility, ease of use, and proven effectiveness in various applications [54]. During the meshing studies, ensuring the convergence rate of the mesh was carefully monitored. It is crucial to note that while a dense mesh can provide more accurate results, the convergence of the mesh is of greater significance than its quality alone. The convergence rate determines how well the mesh approximates the actual geometry and accurately represents the structural behavior under various loading conditions. In the context of the analysis of the attachment bracket, particular attention should be given to the region around the rivets. Rivets play a critical role in joining different components, and any inaccuracies or agglomerations in this area can significantly impact the analysis results. It is essential to accurately capture the geometry and properties of the rivets in the mesh to ensure reliable and precise simulation outcomes. Element quality and skewness were important ones. When we checked the quality of the meshes, it was suitable; rough meshes and poor elements were used on the I beam, which is a transfer element. Because of this, the quality of the mesh is quite good [71]. Nevertheless, it is essential to ensure that the mesh quality and element characteristics meet the required standards in critical areas, such as near the rivets or regions experiencing high-stress concentrations. By carefully balancing the mesh quality and element characteristics based on the specific needs of the analysis, an overall satisfactory level of accuracy and reliability can be achieved in evaluating the structural behavior of the attachment bracket. Here are the criteria for using the

selective meshing method and distinguishing loading and main elements from each other. Hybrid element methods were employed in the vicinity of critical points or important regions within the structure. Sizing of elements according to their importance from a design perspective offers better meshing quality and assumption against the program standard meshing system.

According to the literature, for similar designs, rivet connection is the main joint type [3, 9, 13]. Rivets were modeled in the workbench. Fixed supports were defined on attachment points, as seen in Figure 4.3 [3, 14].

Table 4.6 shows the loading condition of the bracket. This load was calculated in the methodology section, which was taken from the literature. Loads and positions, which are given in Table 4.6, will stay the same during the thesis analysis. It will not be mentioned again if there is no change in load and application. Figure 4.3 portrays the loading conditions of the wing fuselage bracket, which is known as the riveted model (current model).

Table 4.6 Loading condition.

Force (N)	Direction (x,y,z)	Location
90584.62 N	Y direction (vectorial-up)	End of the I beam section

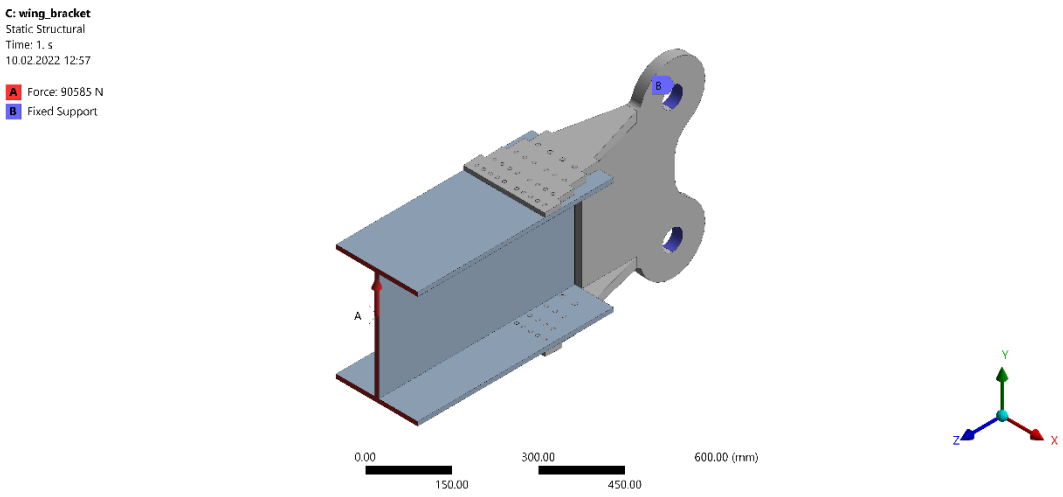

Figure 4.3 Wing fuselage bracket loading conditions (force and supports).

The model was fixed from planes located in B positions seen in and force applied to the I beam as seen in red color in Figure 4.3. The load, direction, and location are given in Table 4. The rivet connection was used to join the wing fuselage bracket, and I beam. Rivets were modeled in the ANSYS Workbench by using connection tools. As seen in Figure 4.4, different diameters exist according to the positions. In the analysis of the attachment bracket, the contact condition was defined as no separation. This contact type is suitable for simulating the behavior of rivets, nuts, or other types of connections within the structure.

No separation contact is a type of contact behavior in finite element analysis (FEA) that assumes no separation or gap formation between contacting surfaces. It is often used to model situations where the contact surfaces remain in continuous contact throughout the analysis, such as in cases where the contacting surfaces are tightly pressed or bonded together. The contact elements will enforce this behavior by applying appropriate contact forces and constraints to maintain contact throughout the analysis. In summary, no separation contact assumes no gap or separation between the connected components, providing a realistic representation of the physical connection and load transfer between them. By selecting the no separation contact condition, the analysis accurately models the behavior of fasteners, such as rivets or nuts, and their interaction with the surrounding components [72, 73].

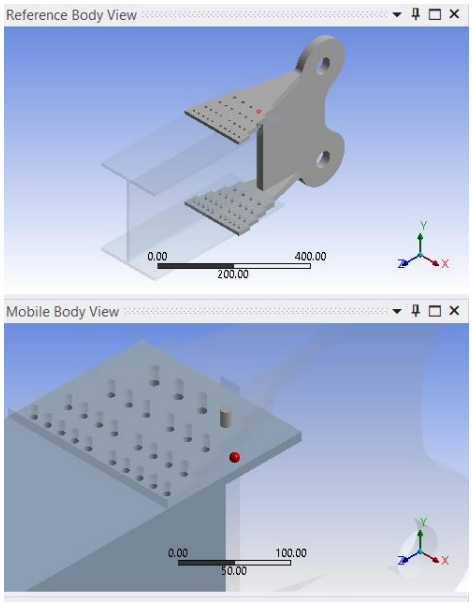

Figure 4.4 Connection elements.

This static analysis wants to make assumptions about the riveted model and foresees the topology optimization cases. Figure 4.5 shows the meshed model. This analysis also wants to obtain the structure's stress distribution and critical stress points. This will pioneer topology optimization for understanding where the critical point of the part during the loading case is. Then, it branched through a topology optimization case. It is easy to see from Figure 4.5 that I beam meshing volumes are bigger than the wing fuselage bracket because the focusing point was the wing fuselage bracket. If there are no rivets here, sweep methods are used for the I beam, where it is a constant cross-section topologically. Pipes or any constant cross-section might be examples of this. These kinds of structures are suitable for sweep mesh methods. For the welding attachment, it was correct to choose to make mesh.

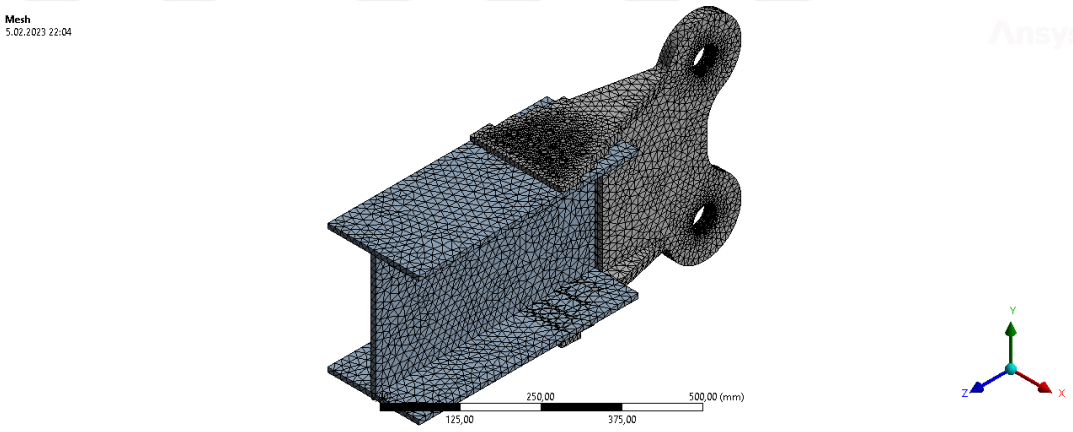

Figure 4.5 Meshed model for riveted model.

In the meshing operations, it focused on the density of the mesh should be higher close to connection points. Face sizing methods were used on the fixed supports, and tetrahedron elements were used on the general mesh, which is 9 mm elements. These triangular meshing elements give good results. Three methods were used in Figure 4.5. It is easy to catch that meshes are correctly dense around the holes. For the I beam, which is just a loading element, the body sizing methods were used, and a coarser mesh, which is 15 mm chosen for this operation. For the body sizing, 3 mm elements were chosen around the holes, which are boundary conditions of the structure. All the sizing values had a ratio between each other. Tetrahedron elements work with quite

suitable models. Primarily 3D models generally work with tetrahedron elements. For 2D applications, triangular and quadrilateral are good choices in 3D; they are converted into tetrahedral and hexahedral forms of them. They have the capacity to make mesh around complex geometries, and they give better results in complex areas [74]. The meshing operation might be classified as an art beyond science. It is not only about creating meshes but also related to the interpretation of the meshes and meshed areas. It requires one to make their own comments on the meshed picture to get better and trustable results. Also, there are some charts inside of the program to make sure about the quality of the mesh.

Transient Interpretation

Transient interpretation aims to verify static structural analysis by performing transient analysis on the structure. The loading conditions in the transient analysis slightly differed from those specified in Table 4.6. A 70-second transient loading was applied to the structure, with the loads between 60-70 seconds matching the values specified in Table 4.6. The remaining timing steps were calculated similarly based on the load calculation. The load factor is a measure of the additional load or force experienced by a structure or system compared to its static or nominal load. In the aerospace engineering context, the load factor is typically expressed as a multiple of the g-force. This analysis aimed to simulate the increased g-forces encountered by a medium-sized fighter aircraft during takeoff over a 70-second period, ranging from the most straightforward scenario to the most severe, and the results were compared with static analyses.

For instance, a load factor of 6g indicates that the aircraft or structure experiences a load six times greater than its weight due to external forces like maneuvering, turbulence, or aerodynamic forces. This load factor is crucial in designing and analyzing aircraft structures to ensure they can withstand the additional stresses and loads encountered during flight conditions. To simulate the takeoff conditions, various load factors were applied to the structure during the 70-second duration, including g to 6g. The specific values and timing steps are clearly presented in Table 4.7. Additionally, Table 4.8 provides information about the meshing conditions of the model, including mesh density and element characteristics.

Before applying these loads, modal analysis, which is a prominent type of linear transient analysis, was performed on the model. Modal analysis, also known as mode shape analysis or eigenvalue analysis, is a technique used in structural and mechanical engineering to study the dynamic behavior of a system. In ANSYS, a widely used finite element analysis software, modal analysis is conducted to determine the natural frequencies, mode shapes, and modal damping factors of a structure. This involves creating a finite element model, defining material properties, boundary conditions, and loading conditions. The software then solves the equations of motion to calculate the natural frequencies and mode shapes. Mode shapes represent the spatial distribution of displacements and deformations of the structure at each natural frequency, providing insights into its vibration characteristics. They help identify potential resonance issues, areas of high stress or strain, and structural weaknesses. Identifying the correct support types and loading information is essential to obtain accurate frequencies and mode shapes. Total deformation information cannot be obtained from modal analysis alone, as it primarily focuses on mode shapes and natural frequencies. However, total deformation contours can indicate regions of potential deformation based on frequency. Solution information is crucial for modal analysis, allowing the visualization of frequencies in different directions. The selection of mode numbers is often an iterative process guided by analysis objectives and considerations of engineering standards and guidelines. The cumulative mass fraction can be helpful for this purpose, and it must be gone through or close to 1 [75, 76]. If the desired value is not captured during modal analysis, it is necessary to increase the maximum number of modes in the program.

Table 4.7 Loads of transient state.

Time(s)	**Load(N)**
0	0
10	15097
20	30195
30	45292
40	60390
50	75487
60 to 70	90585

Other properties were the same. The loading condition was the same as in Figure 4.3, and connection methods were chosen as same as in Figure 4.4. Identical analysis setup was done for the models.

Table 4.8 Mesh properties of the transient state.

Characteristics of Mesh	General mesh
Mesh Method	Patch Conforming Method (Tetrahedron) + Face Sizing + Body Sizing
Resolution	3
Skewness	0,38013
Orthogonal Quality	0.61695
Element Quality	0,72504

According to the table, it is easy to catch that all meshing properties and quality were the same as in Table 4.5. Figure 4.6 shows the loading situation of Table 4.7. These loads were calculated from the safe situation to the most dangerous one, which is calculated according to the 6g calculation. The objective here was to simulate the most hazardous case from a motionless condition to the condition under the highest load.

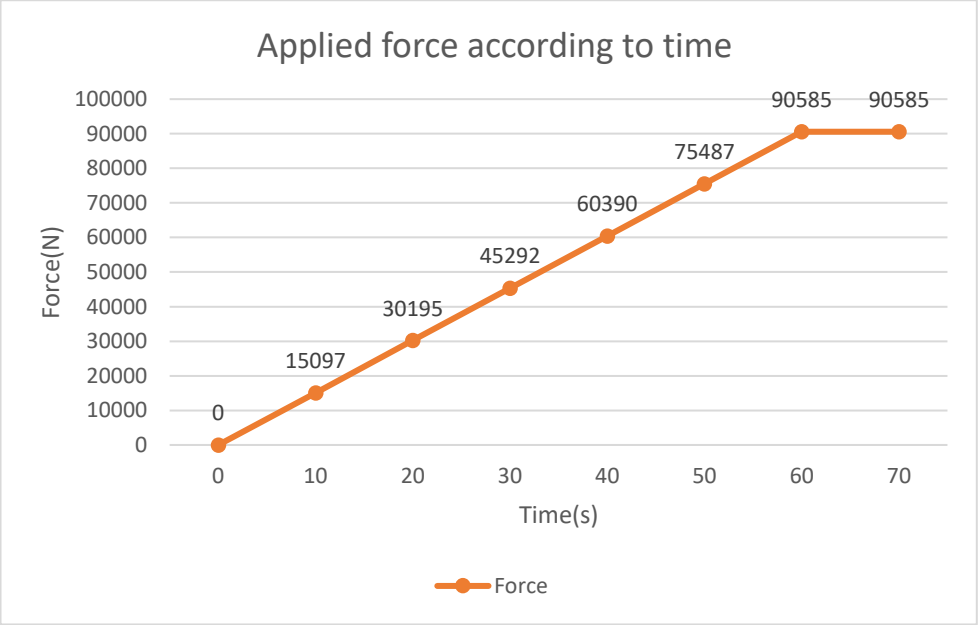

Figure 4.6 The applied force according to time in the model.

4.2.2 Welding Approach of Wing Fuselage Bracket

There are some studies on 4340 steel for welding operations. According to these studies [77, 78], welding can be one of the attachment operations for this model. To maintain this purpose, there were five or six new models were designed according to get optimum stress levels. The first one basically focuses on attaching directly to the I beam and fuselage bracket. This analysis failed according to a higher level of stress. A new model was designed in response to the identified situation, as depicted in Figure 4.2. This model aimed to address the specific requirements and considerations outlined in the study. Furthermore, Figure 4.7 illustrates the loading conditions that were applied to the newly designed model. The loading conditions depicted in the figure provide an overview of the external forces and moments acting on the structure, allowing for a comprehensive analysis of its structural response and behavior. By incorporating these design modifications and applying the specified loading conditions, the study sought to optimize the performance and reliability of the structure under the given operational scenarios (see Appendix-B).

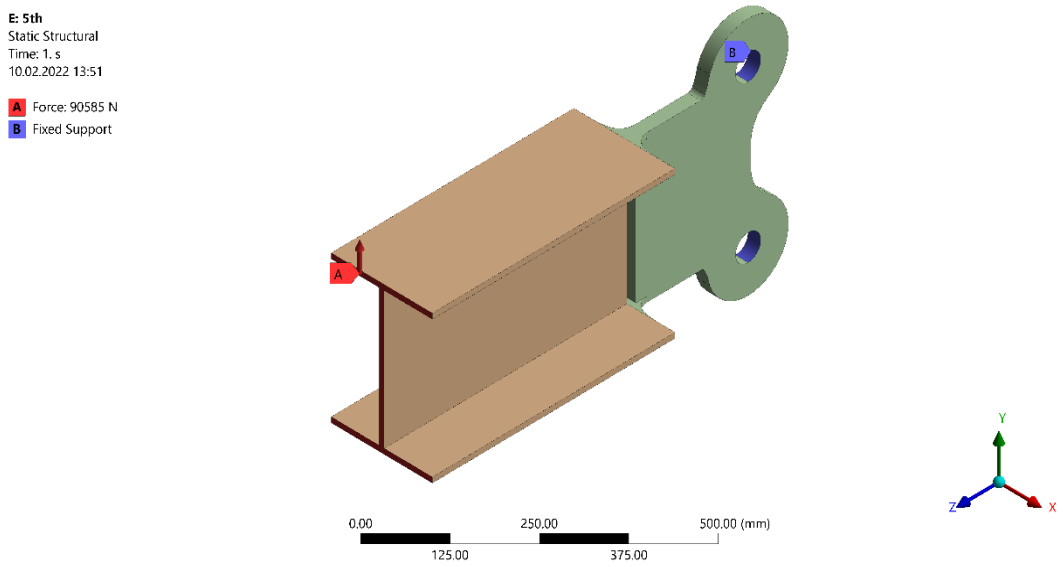

Figure 4.7 Welding model boundary condition.

Force was the same as 90584.62N, and fixed supports (loading conditions) were chosen as same as normal situation.

Table 4.9 Mesh properties of welding case.

Characteristics of Mesh	General mesh
Mesh Method	Patch Conforming Method (Tetrahedron) + Edge Sizing
Resolution	6
Skewness	0.25937
Orthogonal Quality	0.74788
Element Quality	0.8178

Table 4.9 gives information about meshing conditions, as seen in Figure 4.8. Tetrahedron elements were used, and edge sizing was applied to regions that are close to fixed support. As seen, the program chooses face meshes (sweep methods) for the I-beam region, which is more sensitive.

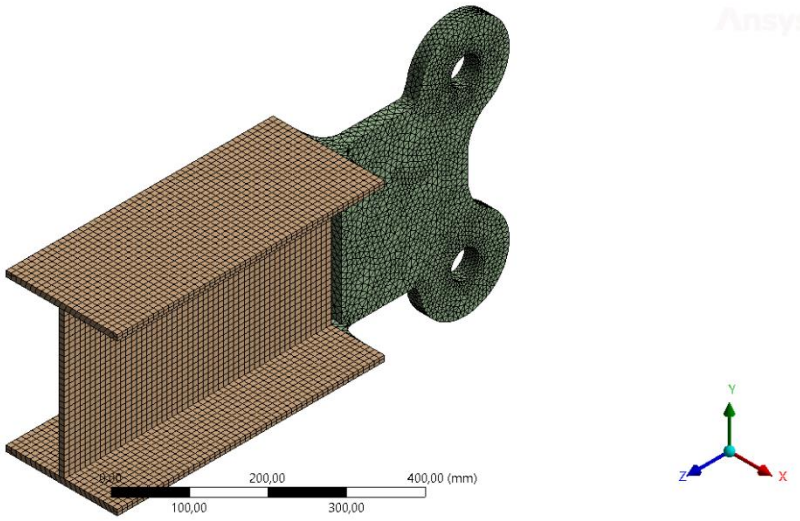

Figure 4.8 Meshing operations of welding model.

4.2.3 Topology Optimization of the Two Cases

Based on the structural analysis results, topology optimization studies were conducted to optimize the design further. These topology optimization analyses were performed based on structural analysis results, allowing for the creation of a similar static structure with consistent analysis settings. The topology optimization process utilized

the stress results obtained from the structural analysis as the response parameter. Other parameters, such as density, mass, and volume reduction, were also considered in the topology optimization setup. The study aims to create a lighter version of the models (see Appendix-C).

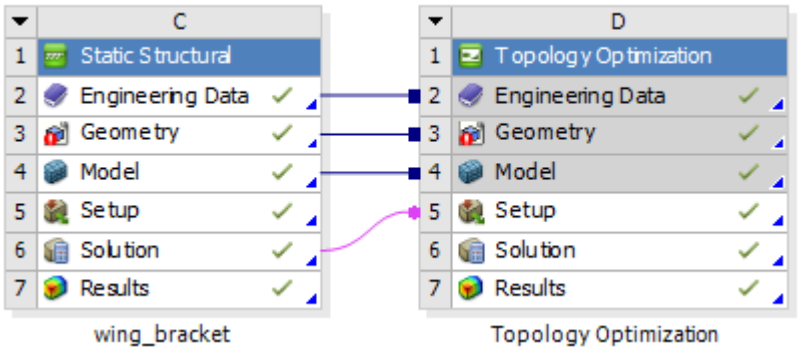

Figure 4.9 Analysis type.

As seen in Figure 4.9, the topology optimization operation uses the results of the static structural tool. The program needs to see a meshed model and stress distribution on it. According to the results of static structural analysis, topology optimization operations have started. Some points should be extracted from topology optimization analysis to accomplish this purpose. First, the program extracts boundary conditions directly from the analysis. Other parameters should be defined. Figure 4.10 shows the extracted regions of the body.

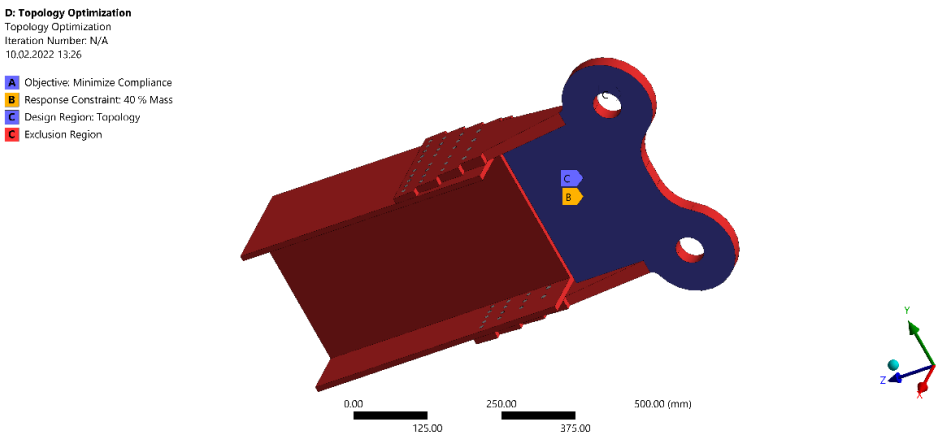

Figure 4.10 Topology optimization boundary conditions.

In the presented model, the topology was not subjected to optimization analysis because red regions were removed. The red regions may indicate specific features or areas of interest in the model but are not part of the topology optimization process. It is important to note that topology optimization typically involves analyzing the entire model or selected regions to optimize the distribution of material rather than specifically extracting or removing certain areas. The paper focused on fuselage brackets to optimize. I beam just a loading area for this analysis, and because of this reason that they were excluded from the topology optimization work. In the real case, there should be different sizes of I beam, which is not a suitable structure to optimize. Here is the point that we are focusing on the wing fuselage bracket to study. Some points on the bracket should be extracted too, which are colored red by the program. The optimization type was chosen as the density base method, which was mentioned before this section. It is a powerful approach to apply while doing mass-decreasing applications.

In the program controls, the objective is to minimize compliance, which involves reducing stress and other strength-related results while simultaneously decreasing the mass of the structure. The chosen allowable iteration number for the optimization process is 500. It is expected that an optimal result can be achieved within this number of iterations. Suppose the case is not solved within this large number of iterations. In that case, it indicates there may be an issue with the general structure of the analysis or other factors chosen for the analysis. Observing a response within the 500 iterations is crucial to ensure efficient optimization. The program may have certain restrictions or limitations that need to be considered. Additionally, program restrictions can also influence the analysis. Linear contacts are used in this study, which affects the setup of the static analysis. Therefore, it is important to reconfigure the case according to the program's restrictions and requirements. Paying attention to these critical points ensures accurate and meaningful results in the analysis process.

In this analysis, approximately 69 faces were excluded from the topology optimization study by using a software interface. These faces might be packaged to extract from the model by redefining CAD data for this study. They were chosen one by one. After making some arrangements on the response constraints, the analysis started to run

because the structural analysis was already done and branched through topology optimization analysis.

An identical approach was also employed for the welding model. Once more, the application of topology optimization results in a reduction in mass. According to this purpose, static analysis results were used and branched into the topology optimization region. Figure 4.11 shows the topology optimization study of the models, which is like Figure 4.10.

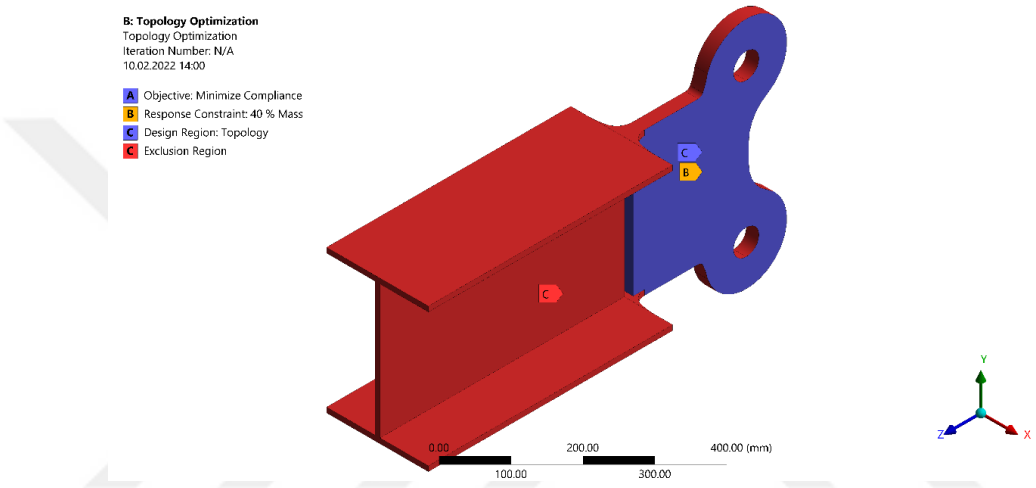

Figure 4.11 Boundary conditions in topology optimization for the welded joint.

The objective of the study is to exclude the external region of the wing-fuselage attachment bracket from the analysis conducted through topology optimization. This is why these regions are marked as red again. The responses to the analysis are arranged based on the boundary conditions. It is expected that as the mass decreases due to the new joint, there will be a significant reduction in the size of the lug when compared to the first case, where it was joined by a rivet. Both models show similar extracted regions, which can be clearly observed in Figure 4.10 and Figure 4.11. This indicates that the topology optimization process has consistently identified the same areas for extraction, regardless of the specific joining method employed.

According to topology optimization results, new designs are suggested where some verification studies of new models should be analyzed. Inside the program, some validation methods by branching further static analysis through topology optimization,

but here is the leading point this study does not make only topology optimization. It also makes size and shape optimization too. The paper is not using the direct solution of the software. The designer's viewpoint is incorporated into the model, resulting in the creation of a new model using CAD software.

4.2.4 Verification of Topology Optimized Models

Static Verification

The newly designed model should be utilized for supervisory studies. New designs, which were drawn by topology optimization results, should be loaded as regards to static analysis case of the main model (see Appendix-D). To do this purpose, meshing methods chose the same as static interpretation. Loading conditions and support did not change during the verification process. Figure 4.12 shows the newly designed case for riveted model.

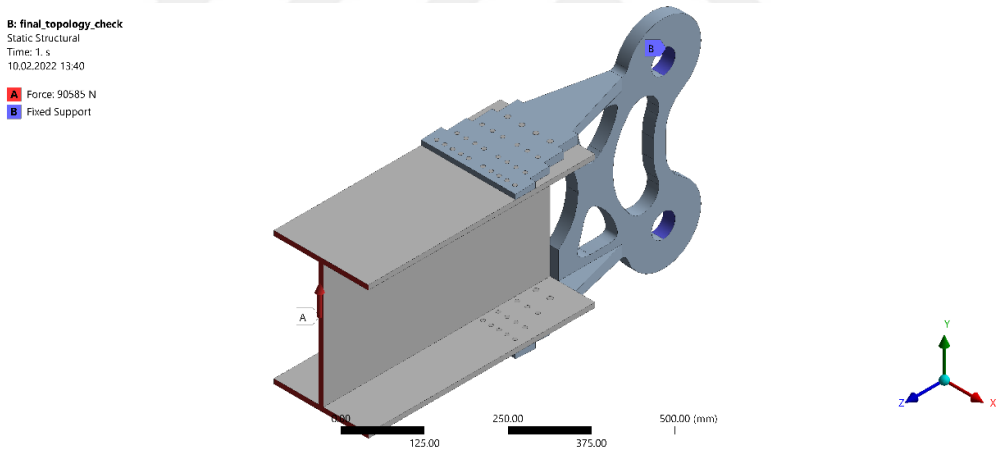

Figure 4.12 Boundary condition for optimized version of the riveted joint.

This design was prepared according to the result of the topology optimization study. STL data which will be mentioned in the reason and result section converted to a 3D model by using CAD software. Furthermore, additional data, such as topology maps referenced in the results section, were employed to inform the accurate design. Again, as shown in Figure 4.12, they were fixed from the boundary conditions, and the same load was applied on the end of the I beam. Tetrahedron elements and face sizing

method close to boundary conditions were used for the meshing operation. These properties are mentioned in Table 4.10.

Table 4.10 Mesh properties of the optimized model.

Characteristics of Mesh	General mesh
Mesh Method	Patch Conforming Method (Tetrahedron) + Face Sizing + Body Sizing
Resolution	3
Skewness	0.38119
Orthogonal Quality	0.61693
Element Quality	0.72316

Skewness, orthogonal quality, and element quality were selected within the range of acceptable values. Generally, meshing conditions of the bracket were employed as in previous models, which were not optimized. Figure 4.13 shows the meshing operation on the optimized wing fuselage bracket. As you can see in the figure, the support points' mesh density was higher than in other regions. Also, rivetted regions, which are connection points of two bodies, were chosen as mesh denser regions.

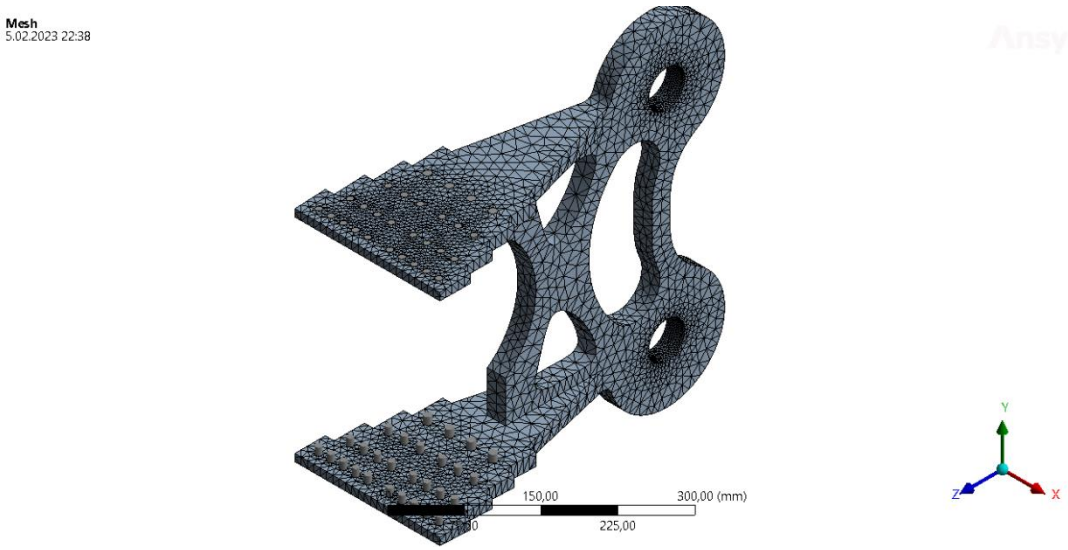

Figure 4.13 The meshed view of the optimized version of riveted joint.

It is important to understand that meshing operation, which has high density, cannot always be the best choice for operations. Acceptable ones, which are converged ones, will decrease your analysis time and give better results in future applications. Crowded mesh means tremendous analysis times. As indicated in the table, all mesh quality measurements fall within acceptable ranges, aligning with literature standards, and were validated through convergence studies conducted near critical stress points [79]. Augmenting the mesh count is unnecessary and could result in extended analysis times. Connection elements were used as same as in Figure 4.4. No separation for the movement and beam elements for the rivets were applied in the workbench on the structure, as same as not optimized model. Consider the wing-fuselage bracket as a singular entity for evaluation. In that case, it is easy to say that element quality will be better than what was written in this table because lower-quality elements were used on the I beam. Setups (loading condition, analysis settings, and load application) were similar to non-optimized (without topology optimization) models.

Welding Case

Indeed, the welding case should also be thoroughly examined in the study. While the previous analysis focused on using rivets for the joint, it is important to evaluate the structural performance and behavior of the attachment bracket when welding is employed as the joining method. The welding case introduces different considerations, such as heat-affected zones, residual stresses, and potential changes in material properties. By conducting a comprehensive analysis of the welding case, including topology optimization and verification studies, the study can provide insights into the effectiveness and feasibility of using welding technology for the attachment bracket. This examination will contribute to a more holistic understanding of the bracket's performance under different joining methods and enable the development of optimized designs for riveted and welded configurations. As mentioned, the selected boundary conditions remain consistent with those used previously. The load and loading conditions were like Figure 4.7. Again, STL data which will be mentioned in the result and discussion section, was designed by using CAD software, and the validation process was started. Figure 4.14 gives a more detailed view of it.

Welding is a permanent connection type of metal, and it has some advantages and disadvantages. It might be classified as easy to apply, strong, and durable. It is an affordable process that can be applied on any surface or performed anywhere, but it has disadvantages. Some welding types, especially gas tungsten arc welding, have low weld penetration [80].

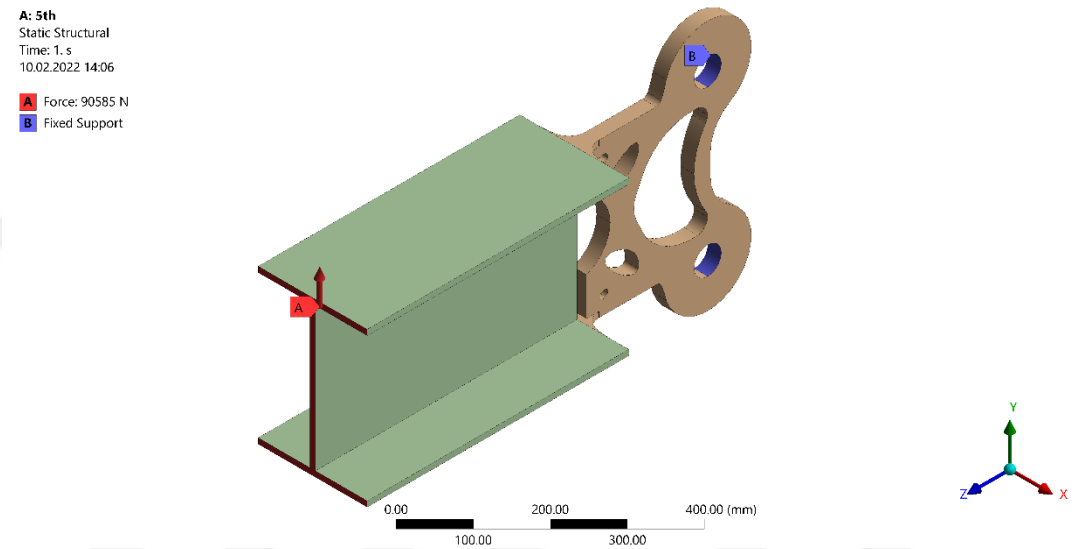

Figure 4.14 Boundary condition for optimized version of welding case.

Different meshing methods were used for the I beam and fuselage attachment bracket. A tetrahedron element was used for the I beam, and again edge sizing method was applied on fixed supports. These studies were conducted to achieve convergence in stress-dense regions as anticipated. For the I beam, the sweep method was chosen by the program as default, and by abolishing rivets and simplifying geometry, mesh quality had already increased before starting the transient analysis. I beam has a constant cross-section, then it is straightforward to create mesh volume along the cross section by using sweep meshing methods. Generally, the program offers a correct way to mesh in newer versions when we compare them with the oldest ones. A more defined mesh for this model was achieved based on a simplified version of the attachment method.

Table 4.11 Mesh properties of welding model.

Characteristics of Mesh	General mesh
Mesh Method	Patch Conforming Method (Tetrahedron) + Edge Sizing
Resolution	6
Skewness	0.2684
Orthogonal Quality	0.74382
Element Quality	0.81038

Table 4.11 gives information about meshing properties, and Figure 4.15 shows the image of the meshed model. According to the results, each model was designed with a different topology. To see the results, and discussion section should be checked.

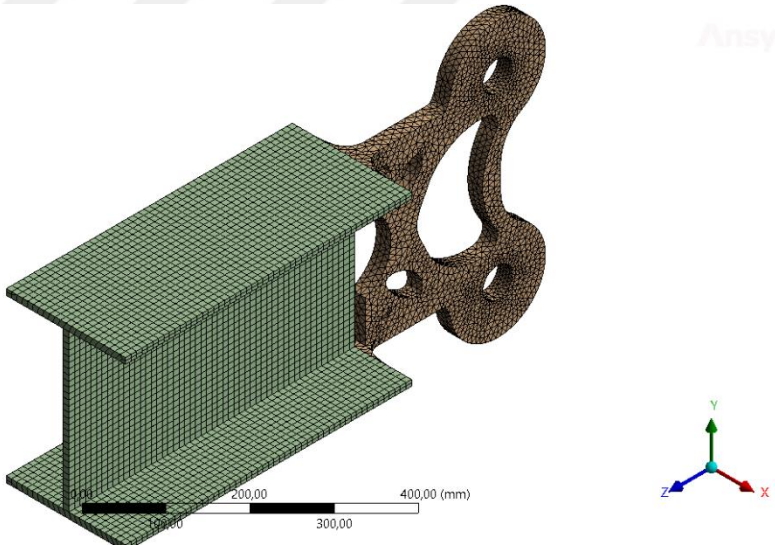

Figure 4.15 Meshing application for optimized version of welding case.

The defect and Discontinuity

Lack of penetration is a welding defect that occurs when the depth of fusion or penetration of the weld is insufficient. It means that the weld does not extend fully into the base metal, resulting in a weak joint. For welding cases, it is a common situation that lack of penetration and lack of joining can be encountered by operator errors, especially in aluminum materials. It is a dangerous situation. Generally, they happen

at very cold-welding processing. Indeed, the presence of welding defects, such as lack of penetration and inadequate joining, can be dangerous for structures like the attachment bracket in aircraft [81]. To simulate this situation, this case worked as 10% lack of bonding and 90% bonded on the welding area for a model. All mesh situations hold the same as before. 1 mm gap between the I beam, and the wing fuselage bracket was commented on due to lack of penetration, as seen in Figure 4.16. Another case was simulated as a 5% lack of bonding, and 95% bonded structural analysis was run too.

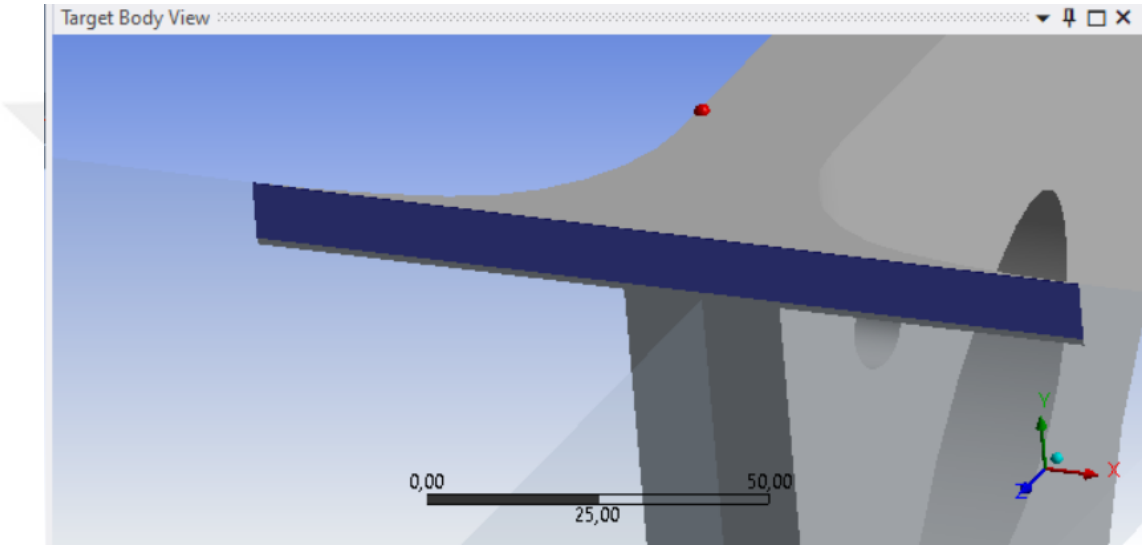

Figure 4.16 Lack of penetration image of welding state.

It shows a 1 mm unbonded region on the body, which is gray, and a 9 mm bonded body which is blue. It simulates 90% bond and 10% unbonded situation. Again, the same loading conditions were applied to the optimized body. Similar meshing methods were used for the bodies, and it prepared 78501 nodes and 34993 tetrahedron and hexahedron elements on it. Here is the purpose of finding the weakness of the welding case and potentially dangerous situation, which has been foreseen, were applied to the body. Another problem might be porosity instead of lack of penetration.

Porosity is another common welding defect when gas pockets or voids are trapped in the weld metal. These gas pockets can be in the form of small spherical or elongated cavities. Porosity can significantly weaken the weld joint and impair its integrity. A different perspective is that porosity may be problematic for these structures. Many

examination methods exist to see this type of problem in the structure. It generally causes unwanted gases in the welding area, and porosity can take shape on the floor of a weld or inside the weld bead. The same loading conditions were used for the porosity case. 5 mm and 4 mm spherical porosity were applied to the welding area and welding zone. The porosity area is expected to be a high-stress agglomeration point for the structure.

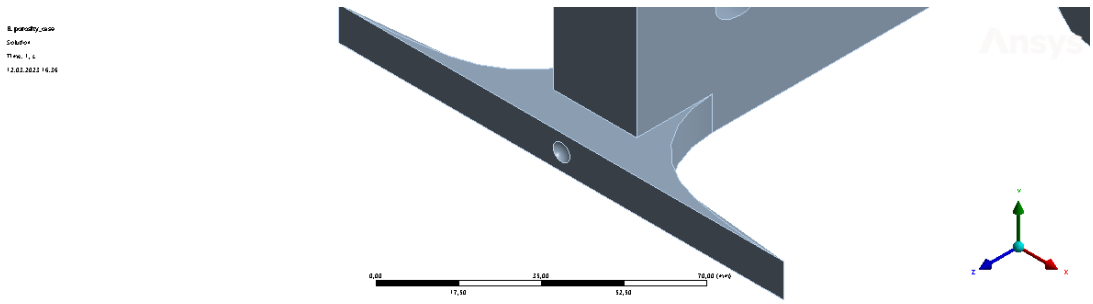

Figure 4.17 Porosity on the welding area.

Transient analysis

The optimized models undergo time-dependent analysis using the transient structural section of the ANSYS workbench. Loading information consistent with Table 4.7 is applied to the models. Modal analyses are conducted in conjunction with transient analyses to capture mode shapes and natural frequencies. These modal analyses are integral components of the overall transient analysis process. These modal analyses involve determining mode shapes and natural frequencies of the models. The outcomes obtained from the modal analysis are subsequently employed within the transient analysis to simulate structural responses under various modes of excitation. This approach ensures a comprehensive evaluation of the models' dynamic behavior and validates the results. The combination of modal analysis and transient structural analysis provides valuable insights into the dynamic behavior of the optimized models, ensuring their performance and reliability in real-world operating conditions.

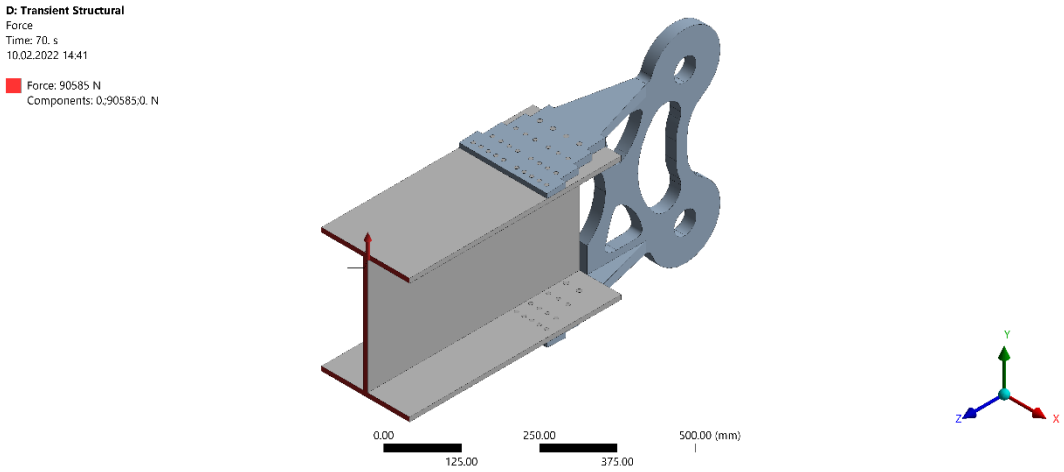

Figure 4.18 Boundary condition for transient analysis of riveted case.

In the analysis of the optimized models, a 70-second duration was considered. The meshes and force load table remained the same as previously mentioned. The loading conditions varied every 10 seconds, gradually increasing the g-factor. After 60 seconds, the loading condition stabilized at 6g. The stress levels were examined, and Figure 4.18 shows that there was no difference in load applications between the static and transient cases.

For the welded model, a similar transient analysis was performed. The boundary conditions and load information were consistent with the previous analysis. In this case, the transient structural analysis was derived from the static structural analysis, serving as a validation process for the work.

The results obtained from the transient analysis will be further discussed in the Results and Discussion section of the study. Figure 4.19 displays the boundary condition of the welding case for the transient situation, which is consistent with the boundary conditions used in other transient analysis cases. The results obtained from the analysis of mode shapes have been verified through the use of correct cumulative mass fraction values. This verification process strengthens the reliability of the results. Further discussions can be made regarding the crack types commonly observed in aerospace applications.

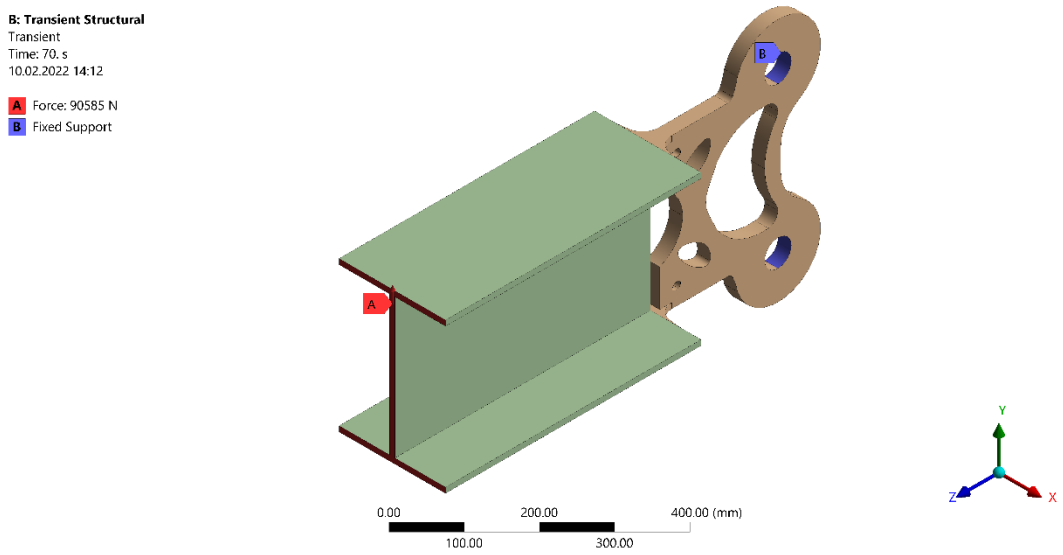

Figure 4.19 Boundary condition for transient analysis of welding case.

4.3 Stress Intensity Factors of the Optimized Wing Fuselage Brackets

After the verification process, the topology optimized models were designed. Static analyses provided valuable insights into the stress distribution within the body, particularly in identifying critical stress points. These regions are crucial for the models as they represent areas where more complex fracture problems may occur. From a fracture mechanics perspective, these areas are considered weak points, and even small defects in proximity to these regions can lead to significant failures of the models. Such failures may not have been anticipated before the analysis. Figure 4.20 illustrates the terminology used for the application of semi-elliptical cracks.

As the name suggests, a semi-elliptical crack possesses a shape resembling half an ellipse. This type of crack occurs primarily in brittle materials, such as ceramics, metals, or composites, where fracture mechanics principles are employed to assess their behavior. Semi-elliptical cracks can form due to various factors, including mechanical loading, stress concentrations, environmental effects, and material defects. 2c value is used for the major axis of the crack, and a value is used for the depth of the crack [44].

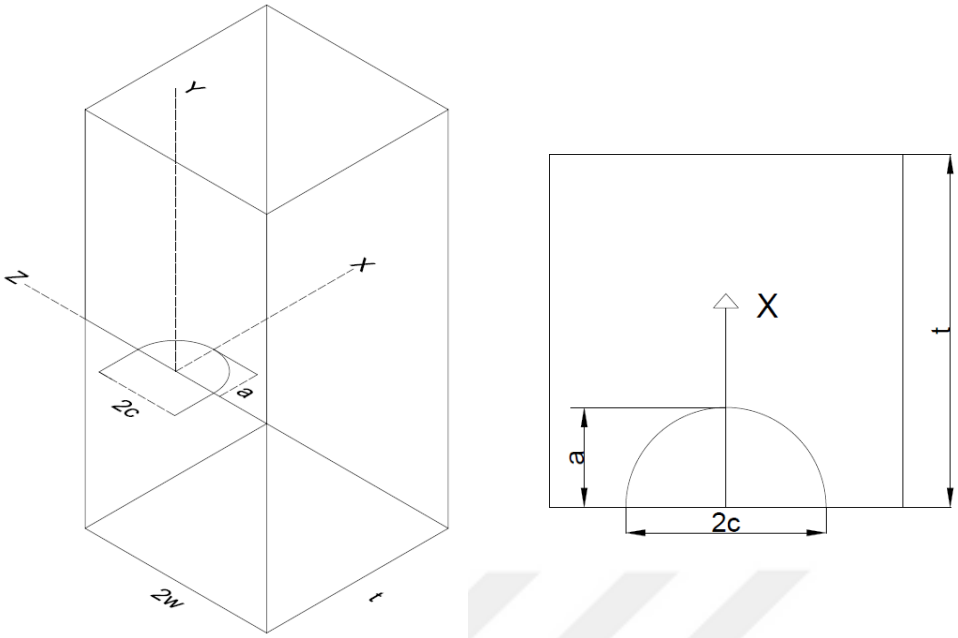

Figure 4.20 Terminology for crack applications.

The 2c value in the context of semi-elliptical cracks refers to the length of the crack front, specifically the distance between the two crack tips. In a semi-elliptical crack, the crack front follows a semi-ellipse shape, and the 2c value represents the length of the major axis of that semi-ellipse.

ANSYS Workbench can offer appointment chances about fracture mechanics. Old version, it was not possible to make these types of analyses. The fracture tool is a valuable tool for assessing these dangerous points. Based on numerical simulation of cracks close to this point, useful results can be found. The program can easily calculate the stress intensity factors of the crack tip. According to different crack sizes program can evaluate different values.

However, it is important to note that certain restrictions are associated with the methodology. These limitations will be discussed in detail in the upcoming sections. Despite these limitations, the methodology proves to be a valuable tool for determining stress intensity factor results, such as K integrals as well as J integrals. It also enables the simulation of crack growth, allowing for an analysis of the behavior of cracks as they propagate under static conditions. Additionally, the program provides G values

for 3D, mode I cracks. It is worth mentioning that the program only supports tetrahedral elements and employs a linear elastic isotropic solver method. Nonlinear geometry effects, plastic effects, and crack tip closure effects are not considered within the program's analysis capabilities [55].

It is worth noting that the methodology provides a valuable solution to avoid complex calculations and streamline the analysis process. Not all problems can be simplified in real-life scenarios to a simple beam-support relationship. Geometries can be complex and challenging to analyze accurately. Chapter 3 of the study demonstrated the calculations involved in different techniques, which can be prone to errors due to the complexity and abundance of formulas. By utilizing the finite element methods program, engineers can mitigate the risk of making mistakes and benefit from a faster situation assessment. The program is particularly useful when dealing with various sizes of cracks, as it simplifies the analysis process and provides efficient solutions.

Stress concentration and critical stress points were defined with static and transient analyses. Critical points were obtained, and these areas should be investigated by using tools. Some literature examples of elliptical cracks on the attachment lugs were seen [15]. The more simple version of this model was studied in the literature using semi-elliptical cracks with different materials close to the attachment points [9]. When we compare modes of fracture, mode I is the most dominant one instead of other modes in engineering applications [82]. Examples might be increased with references. Semi-elliptical cracks are often assumed to be in Mode I loading, which means the crack surfaces experience pure opening or tensile stress. K is particularly useful for analyzing Mode I cracks, where it directly represents the stress field at the crack tip and can be used to calculate the stress intensity factor.

The idea was to make the dominant mode I the opening mode in the fracture analysis. It means that the K_I value should be dominant in the model. Figure 5.1, which can be seen in the next chapter, was a notable example of choosing a crack point in the structure. Stress concentration points that are close to fixed support would be one of the points. The purpose was to make an overpowering K_1 mode of fracture. Once initiated, a semi-elliptical crack may propagate under the action of applied loads. Fracture mechanics principles, including stress analysis and energy release rate

calculations, help in understanding the crack growth behavior. The stress intensity factor (K) is critical in determining crack growth, which relates to the local stress distribution at the crack tip. The crack propagates further as the stress intensity factor exceeds a critical value (Kc). According to this, one of the holes was chosen, which is the stress concentration point.

To analyze the stress concentration point and simulate crack growth, a coordinate system needs to be defined in close proximity to this point. This coordinate system will serve as the reference for analyzing the crack. Based on the coordinates and the given data, such as the major and minor radii of the model, finite elements are created to form the mesh structure. During the simulation of crack growth, there are certain restrictions that need to be considered in the model analyses. One important restriction is the requirement to choose a specific method for calculating the stress intensity factors. In the analysis settings, either K or J integrals must be selected. It is necessary to specify one of these methods in order to observe and simulate crack growth. Figure 4.21 shows the meshed model of the crack. 2 different critical stress points were chosen for the models. The first coordinate (x = 0 mm, y = -174,788 mm, z = -709 mm) corresponds to the location near the fixed support points and is utilized for the topology optimized model. The second coordinate (x = -0.908 mm, y = -140.9 mm, z = -490 mm) is specifically chosen for the welding case and is close to the attachment point. (See Appendix-E).

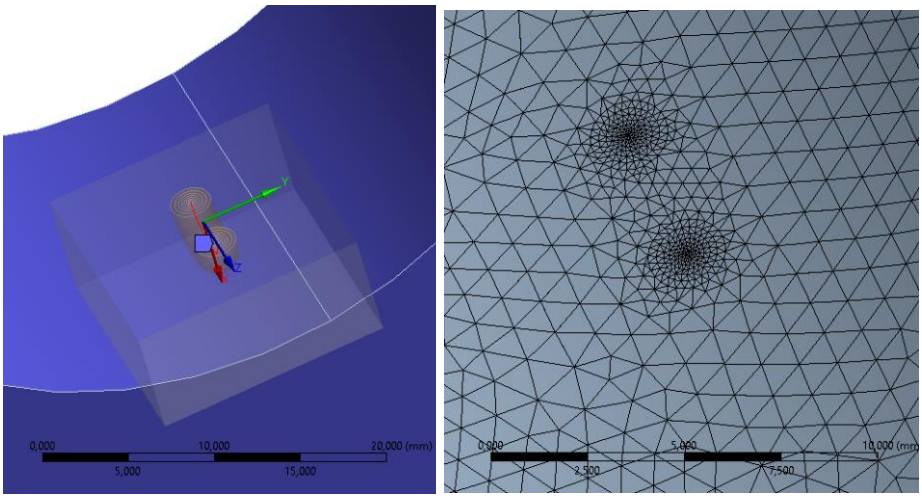

Figure 4.21 Semi elliptical crack on the wing fuselage bracket.

Figure 4.21 illustrates the meshed model near the crack tip, where a crack with a 2 mm major and minor radius are simulated. The figure shows the three axes used to simulate the crack. The X axis is represented in red, the Y axis in green, and the Z axis in blue. The X axis is directed towards the geometry and indicates the location where the crack grows towards the structure. It helps stimulate the front of the crack. The Y axis is used to determine the crack mode by orientation, with the crack being perpendicular to the Y axis and extending along the Z axis. Nodes were generally close to the number 260267. For the old studies, it was around 2600 [15]. Over the past years, meshing element quality and methods have also thrived.

To ensure that Mode I is dominant, the orientation of the coordinate system in Figure 4.21 was adjusted. A secondary coordinate system located close to the stress concentration point was used to achieve this objective. In order to initiate SMART crack growth, the crack face nodes needed to be opened, and the cracks regenerated. Opening mode is the most dominant type of crack, where tensile stresses overpower the material, causing out-of-plane cracks to open in Mode I [61].

The analysis settings were modified in detail, resulting in longer analysis times. Instead of using a time-based approach, the program was set to work step by step. It was set to study in 100 millisecond increments and write the results at each step. This modification allowed for more accurate and reliable results as the crack growth progressed. However, this also increased the analysis time and placed a heavier load on the computer. Workstations or high-performance computing systems would be beneficial for such detailed analyses. The increased time and computational requirements were considered limitations of the study. A more detailed analysis was conducted in the verification steps to compare the results with the simpler analyses. The analysis was divided into two steps per sub-time, allowing for a finer time resolution of 0.5 millisecond.

The selection of the initial flaw size for the study involved several considerations. Firstly, the size of the flaw must be appropriate for the geometry of the structure. For example, if the thickness of the structure is less than 5 mm, it would not be suitable to choose a 6 mm crack for the study. ASTM standards for fracture mechanics were consulted to determine the specific crack size. ASTM has established standards for

conducting K and J experiments, which provide guidelines for determining crack information. These standards help ensure consistency and accuracy in fracture mechanics analyses. The initial crack size was searched for and determined regardless of the specific standard. In many cases, a crack length of 0.25 inches (approximately 6.3 mm) was commonly used as the initial length. This corresponds to a semi-elliptical arc crack length of thereabout 6.3 mm. The minor and major radii of the crack were chosen accordingly based on this initial length [27,83-85]. The major diameter(length=2c) indicates the z-axis of the crack. Minor radius(depth=a) shows the x-axis of the crack, which is shown in Figure 4.20. The arc length of the semi-elliptical crack determines the length of the crack's arc feature. In the literature, this also varies for the welding models [26]. It is important to note that the specific values for the major radius, minor radius, and arc length of the semi-elliptical crack can vary depending on the specific application and the literature.

Table 4.12 Sizes of semi-elliptical crack for Figure 4.21 (a/c=1).

Major radius(c)-Half crack length	**Minor radius(a)-Depth**
2 mm	2 mm
3 mm	3 mm
4 mm	4 mm
5 mm	5 mm
6 mm	6 mm
7 mm	7 mm
8 mm	8 mm
9 mm	9 mm
10 mm	10 mm
11 mm	11 mm
12 mm	12 mm

It was sufficient to make one analysis to assess the results. Other points can be chosen as parameters and run them. To make parameter evaluation, input, and outputs should

be chosen. Figure 4.22 shows these inputs and outputs. Some parameters were set while the analysis was stopped.

	A	B
1	ID	Parameter Name
2	Input Parameters	
3	Copy of 2-6 mm (A1)	
4	P7	Semi-Elliptical Crack --Major Radius
5	P8	Semi-Elliptical Crack --Minor Radius
*	New input parameter	New name
7	Output Parameters	
8	Copy of 2-6 mm (A1)	
9	P9	Crack Extension Probe Crack Extension
10	P10	SIFS (K1) Maximum
*	New output parameter	
12	Charts	
13	Parameter Parallel Chart 0	
14	Parameter Chart 0	

Figure 4.22 Input and output parameters for the analyses.

Another substantial point might be about the crack extension. Crack extension analysis was studied from a static perspective. Here the fracture toughness of the material is going to be necessary for the analysis. K_{IC} value must be written in the program. If dominant mode K, which will be K_I for this study, exceeds the K_{IC} value, the crack will propagate. This subject is mentioned in Chapter 3. The addition of some materials might increase the strength and toughness of the material. Fracture toughness K_{IC} was chosen as 50.0 MPa.m$^{1/2}$ [86]. It is not possible to write as an MPa unit in the program. It was written as a Pa unit in software. If crack growth is observed in the program, it means that the K_I value must exceed the fracture toughness of the material. When it grows, analysis becomes more complicated than before. Every step of the crack growth meshed must be regenerated according to the new crack extension and crack size. Numerous sets of approaches for the solution could be applicable in situations where there is no occurrence of crack growth within the material, but when the crack extension starts, it can become unsolvable without a robust workstation. The program will begin to solve and use the time version of the analysis. Set solutions might need to be revised.

Another restriction is that the crack extension does not work with the contact boundary. Fracture parameter calculations based on domain integrations such as stress-intensity factors, J-integral, or material force are not based when contact elements endure inside the domain. The calculations may become path-dependent unless the contact pressure is insignificant. Because of this situation, it was not added to the parameter set. It is possible to calculate the stress intensity factor by using linear contact application, but it is not possible to obtain crack extension with contacts of the body. In literature, most of the research is done on one body as a plate or rectangular beams. There are no complex geometry works in the literature too. Generally, stiffened panels and simple types of bodies are studied. Probably due to the restriction the paper mentioned before, types of studies were chosen as simple bodies. This model consists of two bodies inside it. The model must be revised to see the crack extension clearly due to programs restriction, as seen in Figure 5.22.

Another approach was the different ratios of major and minor radii. It tries to indicate that short or long crack impacts the body [15]. The major radius shows the z-axis of the crack, where it is the crack length, and the minor radius depicts the x-axis of the crack, where it is the crack depth. Due to a/c values, which mean the aspect ratio of the crack (depth over surface half length) [87], different cases were studied, as seen in Figure 4.23. While performing long and short simulations, the depth also changed according to the a/c ratio.

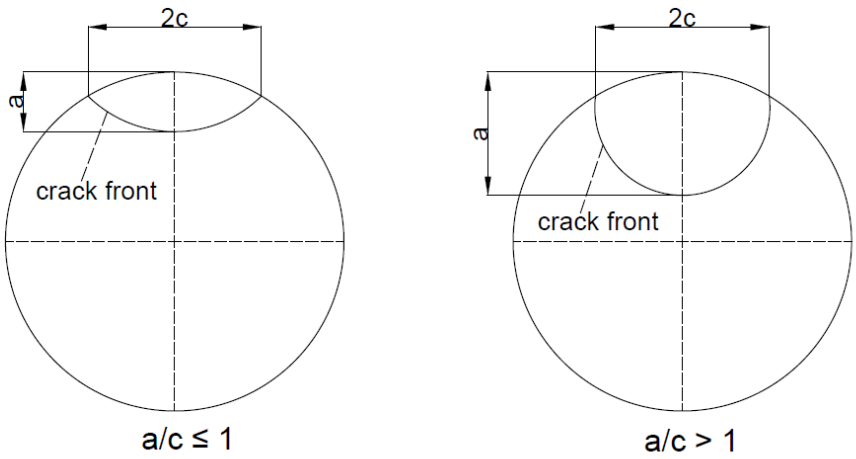

Figure 4.23 Short and long crack application's aspect ratio.

For the a/c=0.5, which is a long crack; the table was like this,

Table 4.13 a/c=0.5 crack simulation.

Major radius(c)	**Minor radius(a)**
4 mm	2 mm
6 mm	3 mm
8 mm	4 mm
10 mm	5 mm
12 mm	6 mm

The a/c=2 [23] chart was the reverse of Table 4.13, where major and minor radius values changed their positions. It simulates short cracks. These analyses aim to answer how the crack forms affect the body as long or short cracks and which ones are the most dangerous ones for fracture.

In the upcoming chapter, the results of the analysis will be presented. However, these results do not directly show the crack growth. To address this, the model is updated as a single body, where the stress intensity factors are compared with the results obtained from the no-separation contact analysis. The modeler tool was utilized to create the single-body design, allowing for the creation of new parts.

The model can be appraised as a single body that might be considered bonded. It will be similar loading conditions to a remote force application. I beam just used as a loading branch. It changes stresses close to connection points, but it will not change the bending idea in the application. Eliminating the presence of rivets between the I beam, and the wing fuselage bracket makes it easier to identify the critical stress points. In this analysis, it is essential to note that bending forces play a crucial role. Comparing the results of the critical stress points near the fixed supports between the two models (with and without rivets), the aim is to obtain similar stress patterns. This model, if it converges with the previous analysis, will be a model to see the crack extension on it. Here are the parameter settings that can consist of crack extension.

For welding cases, there is no such problem like this. This model directly simulated a bonded body which can assess as one single body. Here, connection points are the most critical region of the body that has the highest stress values on the body. The critical stress point must be close to the connection area for the welding case. Welding areas are generally dangerous for crack propagation. In the aerospace industry, it is common practice to perform fluorene penetrant inspection to detect cracks in the geometry after welding operations and before the final inspection of the bodies. This inspection method involves applying a fluorescent dye to the surface of the components, which penetrates any surface-breaking defects such as cracks. Subsequently, the excess dye is eliminated, and a developer is administered to render the cracks visible when subjected to ultraviolet light.

The setup was replicated similarly for the welding scenario as well. Semi elliptical cracks with major and minor radius were applied to the body. Figure 4.24 shows that crack in the welding model, which has a major and minor radius of 2 mm. The crack position was chosen on the far end of the model, where stress intensive region makes the dominant K_1 stress intensity factor which is one of the examples of opening mode cracks. From the beginning of 2-2 crack geometry, it continued to 7-7 crack geometry because of early failure. This case was a guide to understanding which of the connection method is safer than another one according to the crack perspective, and it answers the question of which is the better connection choice, the welding case or rivet case approach from crack implementation.

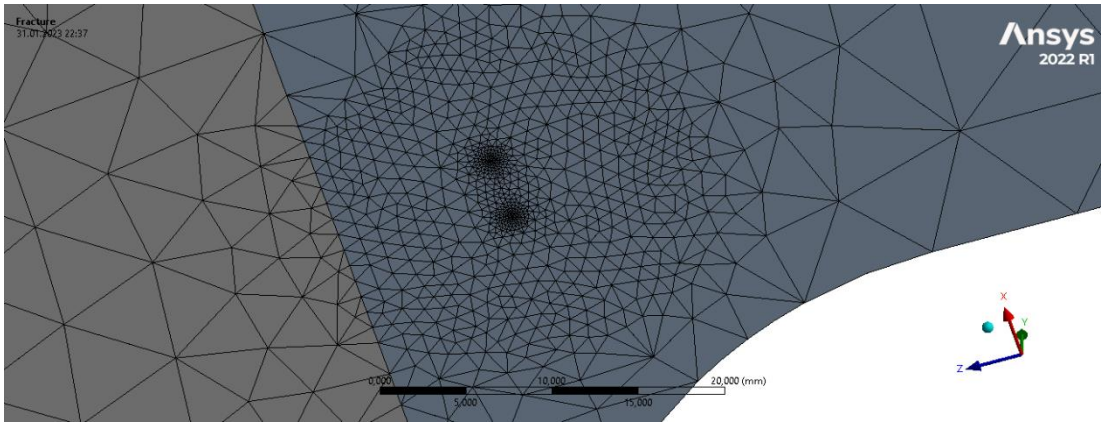

Figure 4.24 2 mm major and minor radius crack of welding model.

In general, the body must consist of tetrahedron meshing elements on it. For this purpose, previous operations were operated with tetrahedron elements. As mentioned before, tetrahedrons are good elements for solving finite element problems. As seen in Figure 4.25, there are some circular points on two crack tips. These are the contour regions. The largest contour size was chosen differently for all the crack sizes in this study. It was one of the types of assessment options for the study. It defines the circular region size for the crack's mesh. It also affects the fracture-affected zone too. When it has been checked from Figure 4.25, it is easy to catch that the grand value of the largest contour radius offers the better solution as crack growth. It is simple to observe that the crack mesh element will be denser in the crack area. Here, tetrahedron meshes offer better meshing profiles when we compare them with hexahedron meshes. That is why tetrahedron meshes support any other way for the implementation of cracks similar to arbitrary cracks or pre-meshed cracks.

The largest contour radius, which is lcr, was another perspective of the study. In the results section, some of the graphs show differences between the largest contour radius value and how it affects crack growth or stress intensity factor values. Three different largest contour radii were used during the study for ordinary state and welding state too. 1.2 mm, 1.5 mm, and 1.8 mm were applied to the topology optimized model. 1 mm, 1.5 mm and 2 mm were applied for the welding state. Figure 4.25 illustrates differences between the largest contour radius between 1.2 mm and 1.8 mm. Left one depicts 1.2 mm model mesh details, and the right one shows a 1.8 mm mesh model of the topology optimized model, which has a rivet connection.

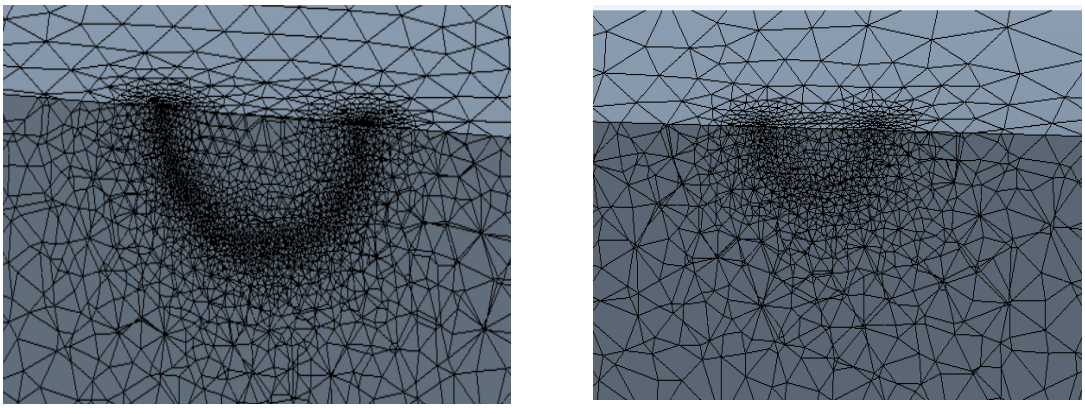

Figure 4.25 1.2 mm(left) 1.8 mm(right) largest contour radius.

When the number of increased largest contour radius values results in the mesh circles of the crack tip points being close to each other, the middle of the crack becomes more dominant due to the meshes it affects, which also influences the simulation values of crack growth. Two cracks were selected for the study, each having a 6.283 mm arc crack length. If the largest contour radius of 4 mm was chosen, there would be no crack mesh on the geometry. Therefore, it is crucial for the designer to pay attention to the correct selection of the largest contour radius value for accurate crack modeling.

In the welding model as well, various meshed models were created to facilitate the study of crack growth. Table 4.12 is also applicable to the welding model, providing an opportunity for comparison between the two models. Similar to the step analysis in the rivet case, this analysis was also performed with step solutions. Sub-steps were defined as two. The major and minor radii of the crack in the welding model were chosen as 6 mm, resulting in an arc length of 18.85 mm, which also represents the length of the arc crack. The meshing application and other analysis steps were generally like the rivet case.

However, the largest contour radius values were defined differently in comparison to the rivet case, reflecting the specific characteristics of the welding model. The arc length was calculated using Equation 4.1, where L represents the arc length, A (semi-axis) is the major radius, and h (height) is the minor radius. When the major and minor radii are equal, it results in a semicircle shape. In the case of the 18.85 mm crack, the mesh was adjusted accordingly based on the defined set parameters.

Where λ is a unitless parameter, and l depicts arc length as seen in Eq. 4.1.

$$\lambda = (A - h) / (A + h) \qquad l = a \approx \pi/2 * (A+h) * [\, 1 + 3\lambda^2 / (10+\sqrt{4-3\lambda^2}\,) \,] \qquad \textbf{(4.1)}$$

In the upcoming section, the results of the set solution analysis will be discussed and compared with the results from the ordinary model. The arc crack length can also be determined using software, although there may be slight variations due to the meshing process in the program. The program provides stress intensity factor results at various points along the crack, typically measured in millimeters.

For the initial crack, 85 points were selected to measure the stress intensity factor on the body. Although this analysis still computes stress distribution throughout the structure, variations in results were anticipated due to the presence of cracks. These points are expected to align closely with the previous stress concentration areas. As an initial observation, it can be inferred that stress concentrations will manifest around cracks situated near the prior stress concentration locations. These cracks could induce a V-shaped effect on the structure, potentially posing a critical concern in the design.

CHAPTER 5

RESULTS and DISCUSSION

5.1 Wing Fuselage Bracket

Static Interpretation

The result of the riveted model shows that stress near holes and rivets are the critical points for this structure. To interpret this result, in the real case, it cannot be as high as the analysis results for the rivets. Because of the structure of the rivet, there are some washers (or head sections of rivets) on the structure. We modeled them as a beam structure in the analysis. In a real case close to this region stress value will be less. According to the results, it was expected that there should be less stress near this region. The second point, which is the highest stress point, makes more sense and is close to fixed point regions. All the stress value was less than material yield strength. Also, these results and regions converge the references [3, 11, 14].

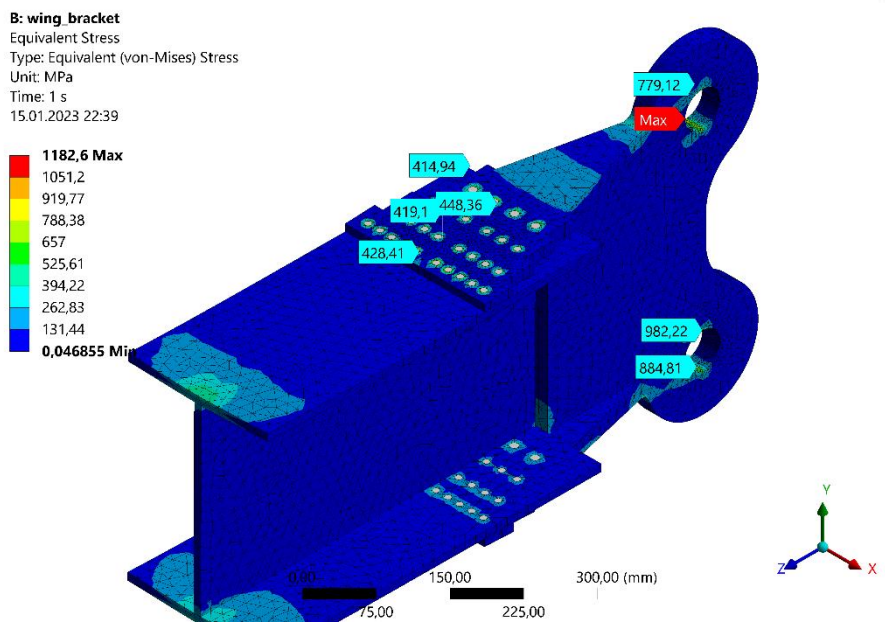

Figure 5.1 Wing fuselage bracket static analysis results.

It is certain that there is a bending load that is dominant on the wing fuselage attachment bracket. According to these loading conditions, there will be some stress points on the structure. As we expected, fixed supports and regions which are close to rivets are the most critical points for this structure. There can be a focus on the structure.

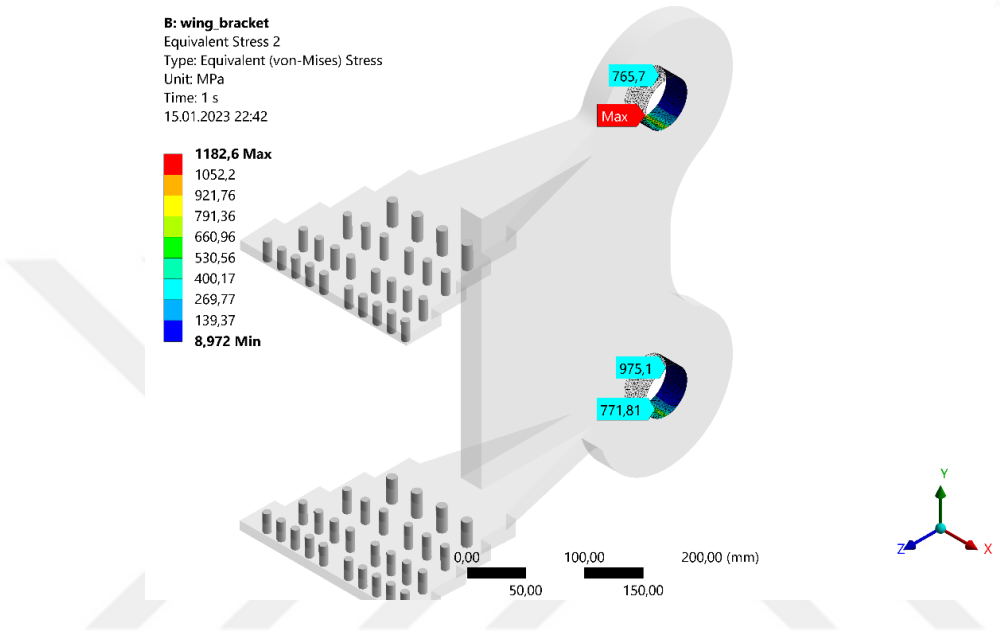

Figure 5.2 Critical stress point on the wing fuselage bracket.

According to the stress results, it is good to make a transient application on the model. It helps to see whether the results are converging or not. Figure 5.1 gives an idea of the general situation of the structure. Figure 5.2 shows the most critical regions with approximately 1190 MPa stress levels.

Transient Interpretation

Transient interpretation allows to apply a changing load over time. In line with this approach, we performed various calculations ranging from 1g to 6g. This approach facilitated the application of loads at various intervals through an incremental method. According to the literature, the load application of 6g is considered the most critical case. Transient structural analysis, on the other hand, allows for the application of different load cases and provides insights into the stress distribution on the model at different time intervals.

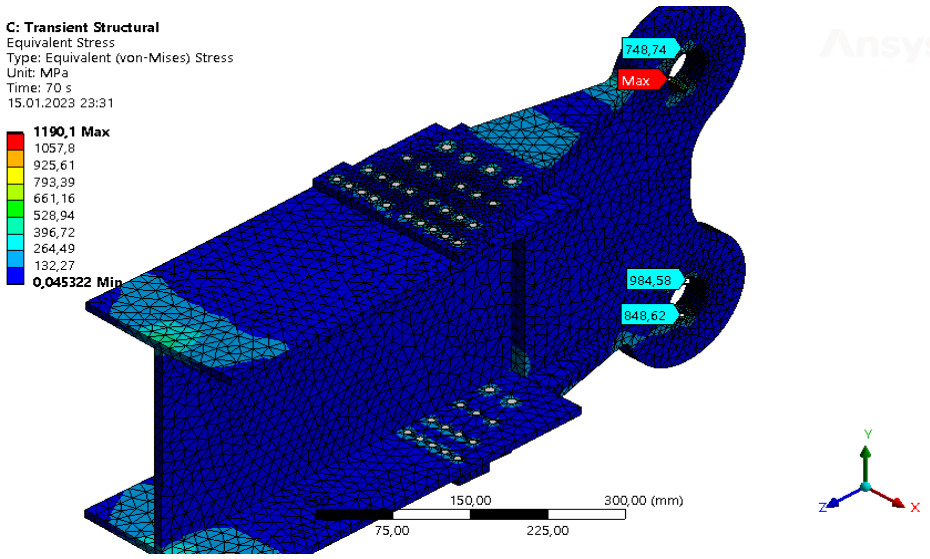

Figure 5.3 Critical stress point on the wing fuselage bracket for the transient state.

Figure 5.3 portrays the structure's most critical point, approximately 1190 MPa. It converged with static analysis results, and Figure 5.4 shows how stress changes according to time-load difference. Understandably, increasing the amount of stress during the time will increase the stress level on the structure. This loading information was given in the section before in Table 4.7. Before the transient analysis, modal analysis was employed on the structure. Different mode shapes were examined, and all the axis cumulative mass fraction goes through 1. 96 mode shapes were analyzed during the study.

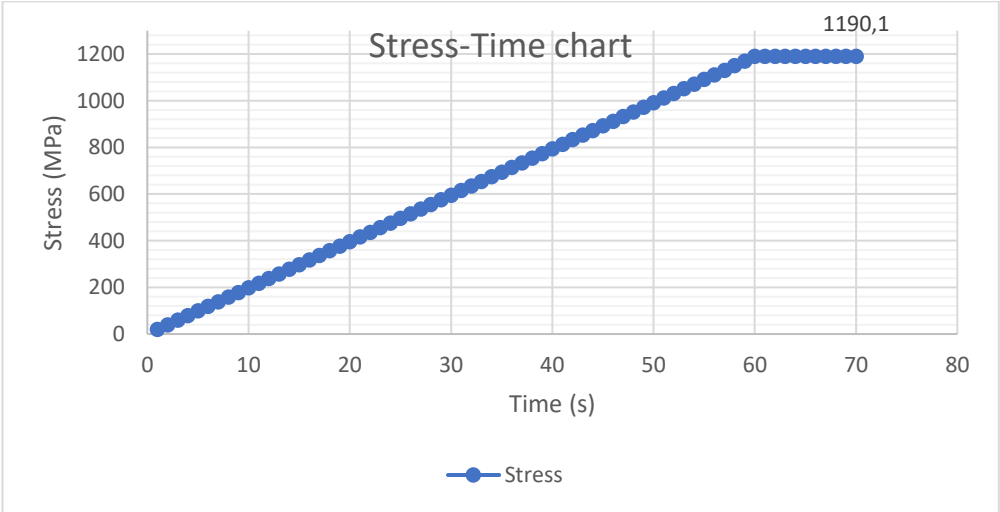

Figure 5.4 Stress-Time chart.

5.2 Welding case

As mentioned before, a welding case (case two) was used for this model. This case model is considered welded by friction stir welding or any other welding approach. In this case, contacts are applied on the body as bonded. In this case, contacts were applied to the body as bonded, assuming the model to be a single piece comprising the I beam and wing-fuselage attachment bracket. Numerous models were designed for this purpose and subjected to analysis. The objective was to ensure that the model's stress levels remained below the material's yield strength. The design process involved iterations, and the final design, as depicted in Figure 4.2, was suitable based on the analysis results.

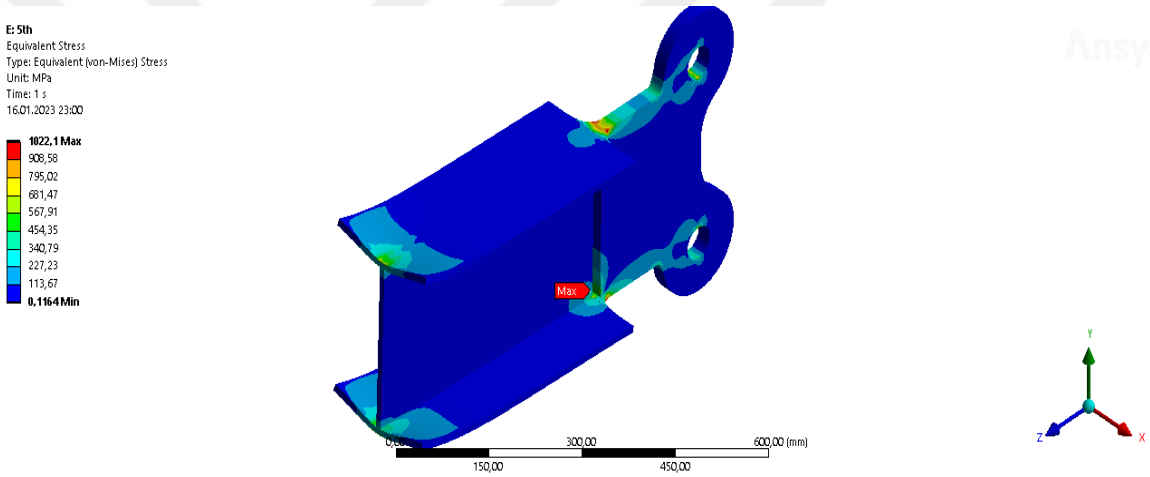

Figure 5.5 Result of welding case approach.

Several important considerations for this structure led to the selection of specific meshing properties for the model. Safety was prioritized for the welded region, and the overall material properties were considered. Meshing information was provided in Table 4.9 before the analysis, with small mesh elements utilized. The welding area played a crucial role in the study as it served as a stress concentration point for the model. The meshing details were meticulously outlined in Table 4.9, preceding the analysis. The use of small mesh elements was a deliberate choice to capture fine-scale variations in stress distribution, especially in regions of interest like the welding area. The results of this region are depicted in Figure 5.5.

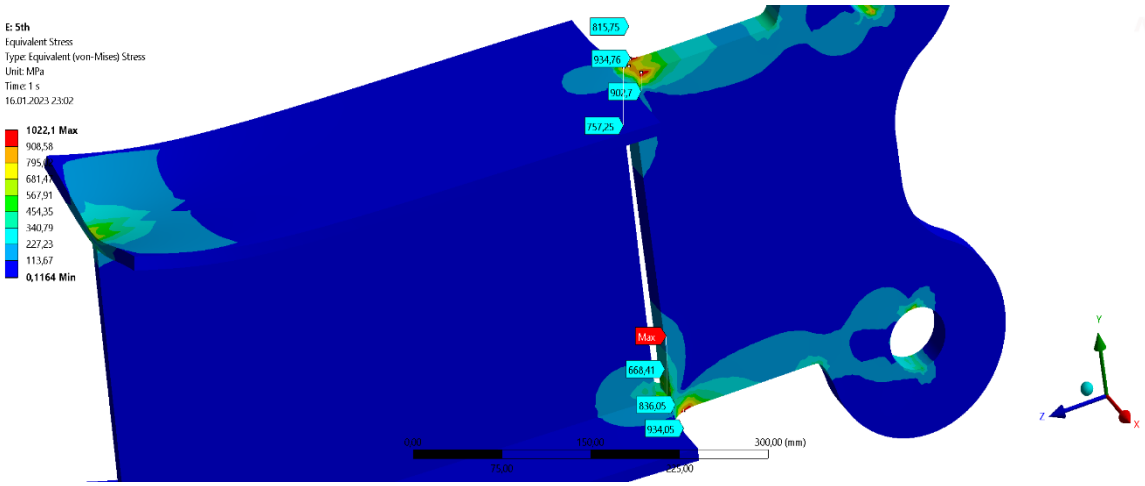

Figure 5.6 Critical stress point on the welding case.

As observed in Figure 5.6, the stress levels in the welding region were found to be within an acceptable range. It was assumed that the average yield strength of the materials in the welding area was acceptable. The mechanical properties of the materials used in the welding region can be found in Table 4.2 and Table 4.4. Based on this information, a stress level of 950-1000 MPa or slightly higher may be acceptable for the welding region. The average stress level is close to 1000 MPa. The welding region was considered a small area where the two materials mix, primarily within the I beam and bracket. Certain points on the structure were marked, and it can be stated that the observed stress levels are within an acceptable range.

The critical stress points were found to be located near the radius region of the wing-fuselage attachment bracket, which is not the welding area. These points were not welded. These areas are the critical region of these structures. Some further work which is related to crack application should be done on it. Also, this method should be verified in some experimental studies as future work. Because of the bracket, there can be needed flexibility in this structure when they are all together. According to this situation, rivets might be the best solution for these kinds of attachments. In the literature works, it was found that rivets are mainly used as attachment methods in aerospace applications. Not only rivets but also welding is used for some aerospace applications, and it is an open area. Because of this reason this method was applied to the structure.

5.3 Topology Optimization of the Cases

The use of branching cases in topology optimization, as illustrated in Figure 4.9, is a valuable strategy, particularly when the primary goal is mass reduction. Topology optimization results are generally open to interpretation. Comments for these results should be leaned on the intuition of the designer. This approach allows engineers and designers to explore various design possibilities, often resulting in innovative and efficient solutions to minimize weight while meeting structural requirements. As talked about before, Figure 4.10 and Figure 4.11 shows some restriction points of the structure, which are the red ones. First, they should be assigned. Loading areas and some important points of structure should be excluded from analyses. Some areas needed to be untouchable during the analysis. Then, analyses can be employed to make a mass reduction in the body.

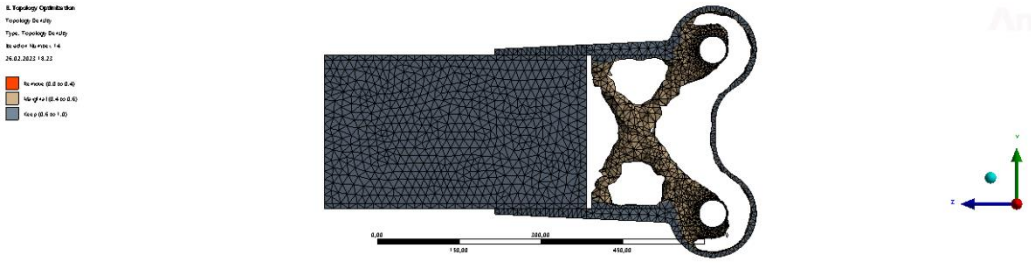

Figure 5.7 Topology optimization result of the riveted model.

The important point is that results should be examined according to dangerous areas of the structure. If there was a simple structure, according to the analysis result, it could be produced by using topology optimization directly. A plate, beam, or anything which has no connection point, rivets, or contacts might be an example of a simple structure. They have only some simple support points and loading points on them. Also, there is no contact on the body for this structure. Because of this, they might be classified as simple structures. But the wing fuselage bracket is not one of them when we compare it with simple structures due to its connection points or connection elements. However, as structures become more complex, the interaction between different parts of the structure, manufacturing constraints, stability considerations, and other non-linear effects may necessitate additional analysis and human judgment. The critical regions

of the structure, where stress concentrations or potential failure points are likely to occur, must be carefully evaluated to ensure the final design remains safe and reliable.

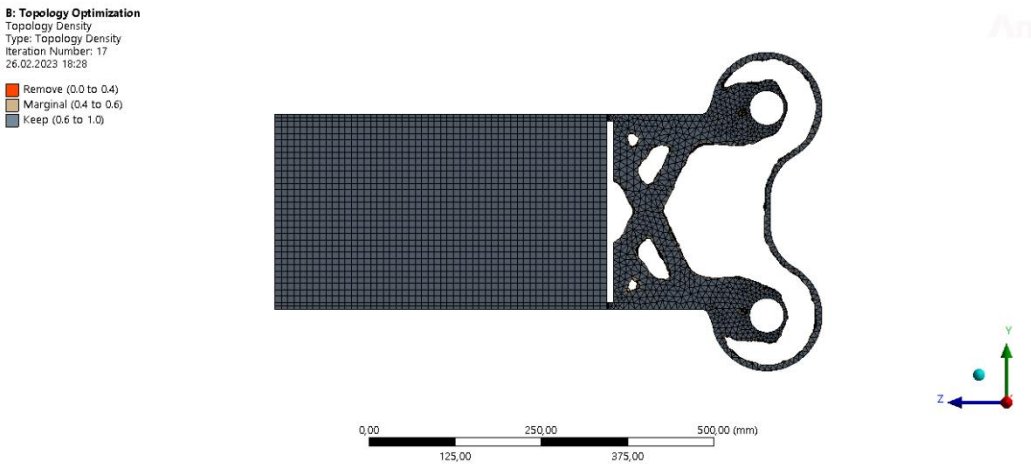

Figure 5.8 Topology optimization result of welding state.

The analyses were iterated in 14-17 steps to optimize the topology of the structure. The topology optimization results can be seen in Figure 5.7 and Figure 5.8. To organize the topographic region on the structure, CAD software was used. The resulting data, including the meshed topology, can be exported as STL files from the workbench software. These STL files can be used for additive manufacturing systems to produce simple data directly. However, in this case, the data was further designed using CAD software such as SpaceClaim and Solidworks, taking into account the existing data.

Upon examining the data, it becomes evident that extracting such large amounts of material from the boundary locations (fixed supports) is not sensible. Therefore, redesign studies should be considered to optimize the structure. Instead of relying solely on Figure 5.7 or Figure 5.8, Figure 5.11 and Figure 5.12 can provide more helpful insights for the designer to contemplate the structure. These figures can also be used for direct printing methods if the designer is confident in the topology and restrictions. It is now the time for the designer to integrate size, shape, and topology optimization for the final design.

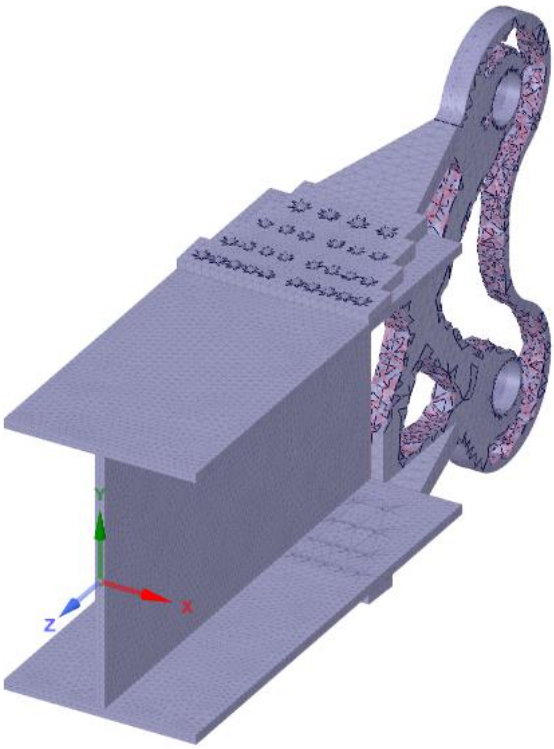

Figure 5.9 STL data and SpaceClaim environment for the riveted model.

SpaceClaim can be used for operations such as merging faces or performing other simple operations in topology optimization. It provides a convenient option for fast production by merging faces or fitting curves. However, when dealing with complex meshes, the process of merging and fast production can become more challenging. While better computers may be able to handle these complicated situations, using a combination of two programs can be the best approach.

By using SpaceClaim for dimensioning the model and Solidworks for creating the optimized geometry, it is possible to work with both 3D data and mesh surfaces. This combination allows for more efficient and accurate optimization of the model. Additionally, the capability of SpaceClaim in terms of 3D printing methods can be advantageous for producing simplified models. The integration of these two programs enables the creation of a well-optimized geometry that meets the desired specifications.

As depicted in Figures 5.9 and 5.10, the meshed models have been prepared and are ready for production and further analysis. However, in order to utilize them for subsequent analysis and make any necessary geometric modifications, it is essential to convert them into clean 3D models by clearing them from the mesh structure.

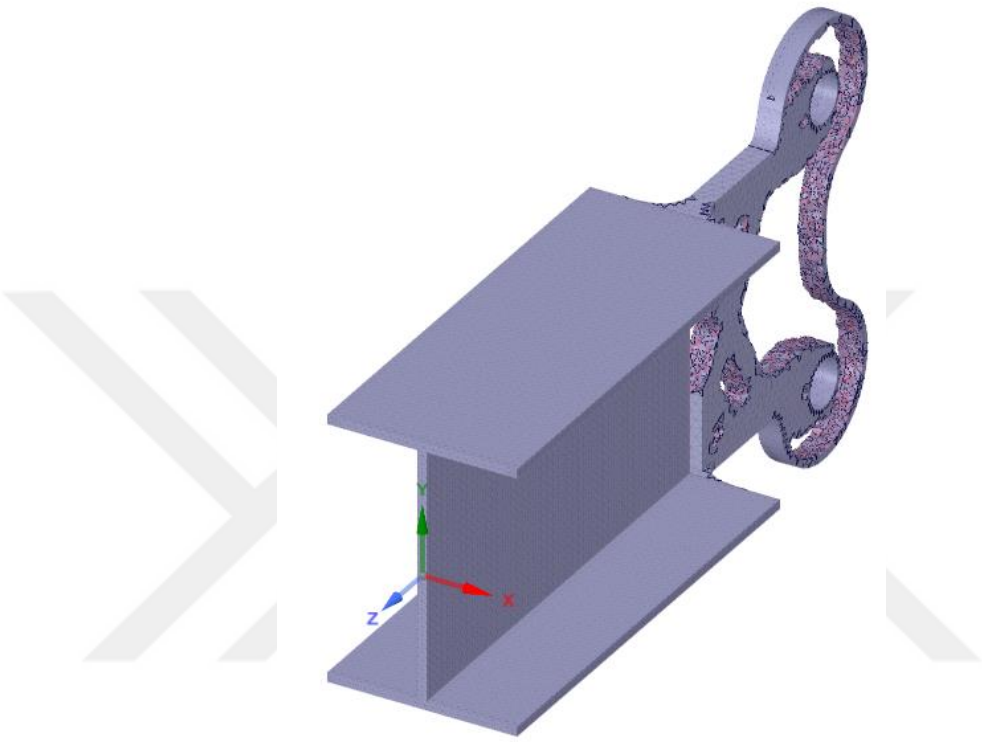

Figure 5.10 STL data and SpaceClaim environment for the welding model.

For the designing steps, some user-defined results can be helpful for the designer. These data show the critical points and removable sections of the model as a topography map. In the program, there are some opportunities to get different results that are user-defined. Some simple comments on ETOPO or TOPO show contours more clearly. Figure 5.11 and Figure 5.12 show them as more scientific data. For the designer, it is simple to make assumptions about the stress agglomeration points on the structure. These contours depict the most critical points that cannot be extracted more clearly from the model and movable points. According to scale, an interpretation of the model can be made, with boundary conditions automatically highlighted in red.

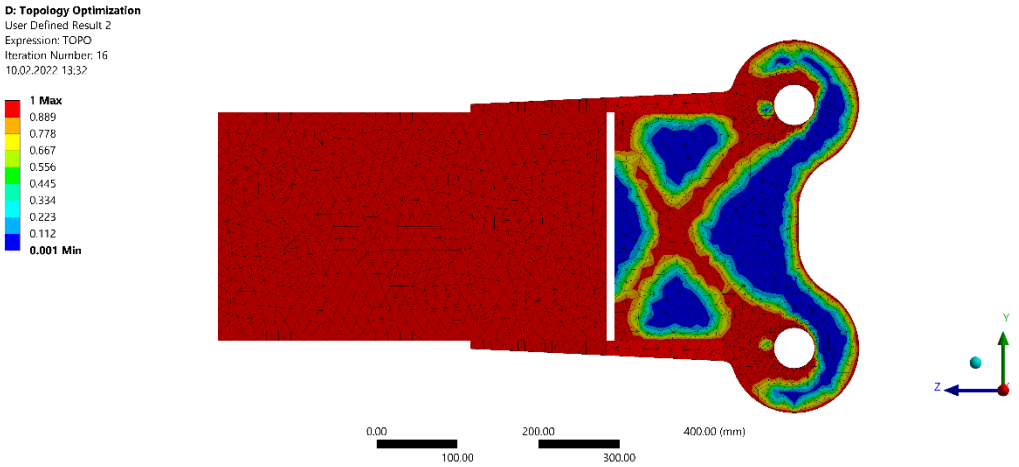

Figure 5.11 TOPO results of the riveted case.

For the riveted model of the wing fuselage bracket with rivets, it is easy to understand that there are not too many elements middle point of the structure that is carrying a load on them. Figure 5.12 it is more understandable results according to mesh density for the welding model.

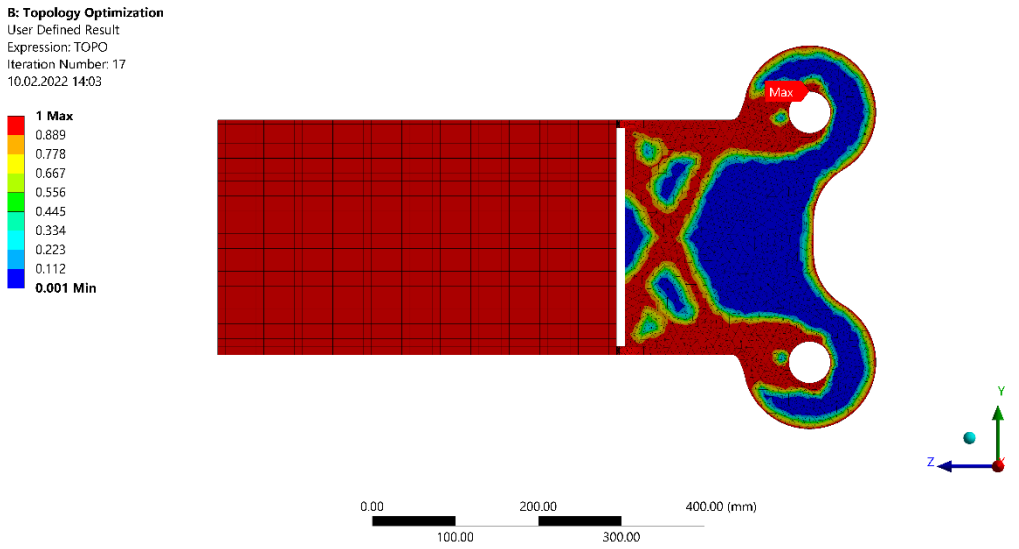

Figure 5.12 TOPO results of the welding case.

According to these results, especially in Figure 5.11 and Figure 5.12, it is easy to create a structure in mind. Predesign sight can be done by examining these results. In the second case, numerous materials could be eliminated, as previously mentioned, similar to the riveted model. It cannot be safe when we remove these kinds of material from

boundary conditions. So, new designs were done as regards this situation. Not only topology optimization but also shape and size optimizations were done on the models. Topology optimization is paraphrased as the addition of size and shape optimization together. Actually, these designs were mentioned in Figure 4.12 and Figure 4.14. Also, there were lots of figures which showed boundary conditions or any other things about them. To see them more clearly, Figure 5.13 might be examined.

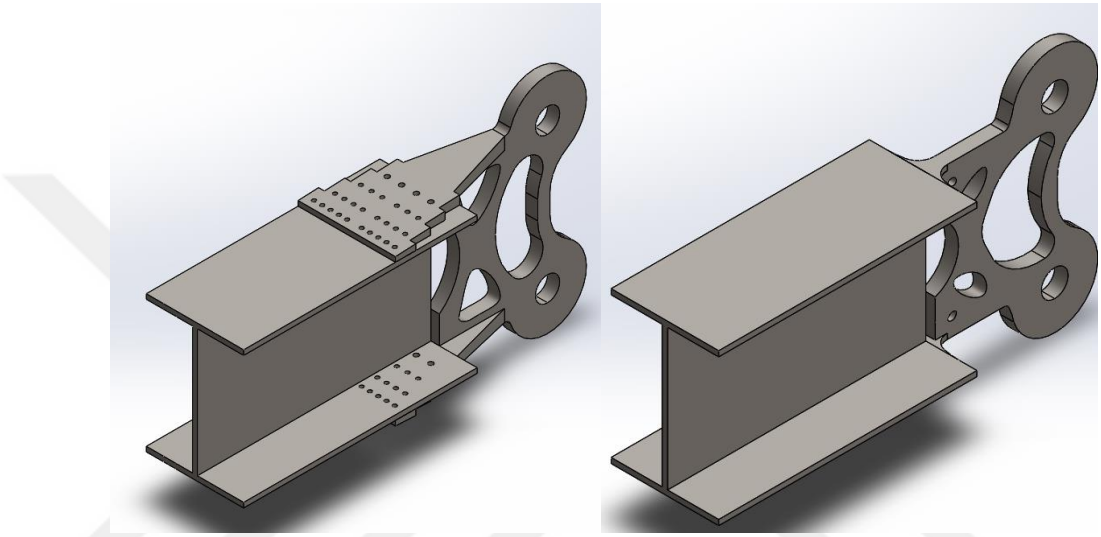

Figure 5.13 New designs of two cases.

5.4 Verification Results for New Designs

The initial step involves the execution of static verification for the two cases at hand. Prior to this section, precise boundary conditions and mesh details had been established. The load was the same, and this analysis will be a validation operation for this result statically. The identical meshing procedure was consistently employed across all operations to ensure convergence. Figure 5.14 illustrates the outcome of the static analysis conducted on the new riveted model, which represents a lighter version compared to the previously depicted Figure 4.1. The static analysis aims to assess the structural behavior and performance of the revised riveted model under various loading conditions.

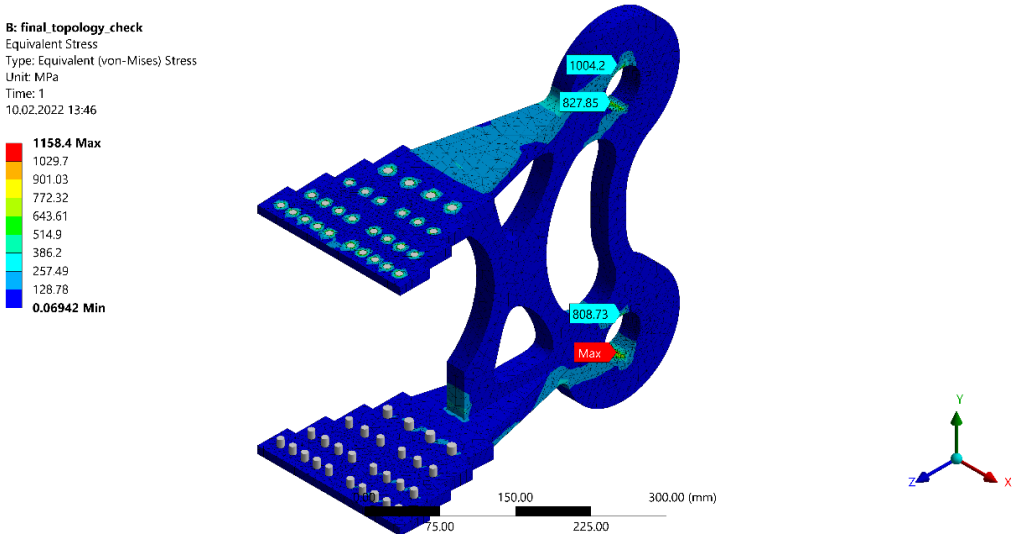

Figure 5.14 Topology optimized analysis result for riveted case.

As same as Figure 5.3, the maximum stress region appeared on the connection region. It was an envisaged result because there was no chance of the connection region. What is more, there was no problem with the topology optimized region. The optimized region was safe according to loading conditions.

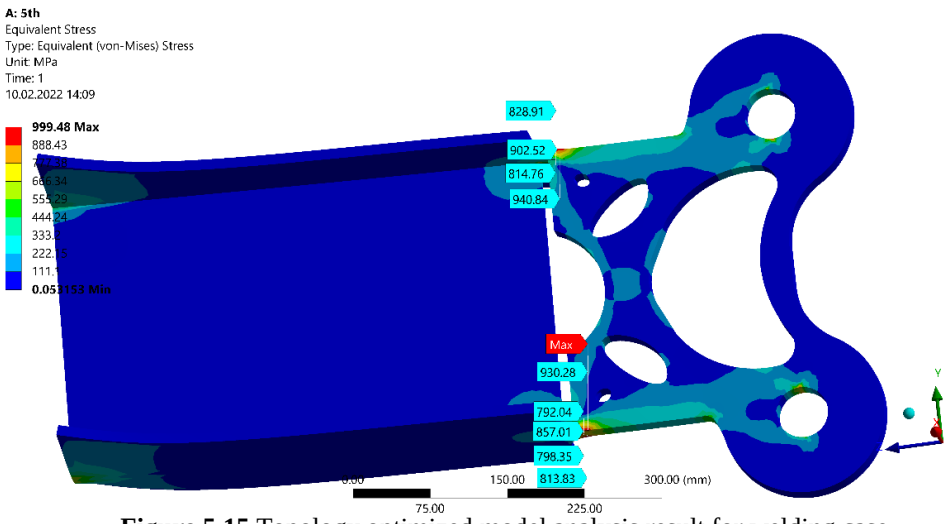

Figure 5.15 Topology optimized model analysis result for welding case.

In the first one, which is Figure 5.14, there was stress distribution around the fixed supports, which were close to the 1150 MPa level. Figure 5.15, which illustrates the topology optimized model of the welding case, shows maximum stress again similar region to the non-optimized one. This value was approximately 1000 MPa, and both

were safe as material properties. These regions will be important points for future works which were related to cracks. The stress intensity factor in this region should be considered as dangerous. Various crack sizes should be checked for structure safety.

Transient Verification

Until this section, all these results were shown statically for new designs. These models can be analyzed dynamically too. Table 4.7 gives information about transient loading conditions. According to this table, transient loading was applied to the structure, and these models were dynamically verified, too, by comparing static results. Figure 4.18 and Figure 4.19 give information about loading conditions and boundary conditions. After loading the application, the analysis was started. Figure 5.16 shows the analysis results according to time.

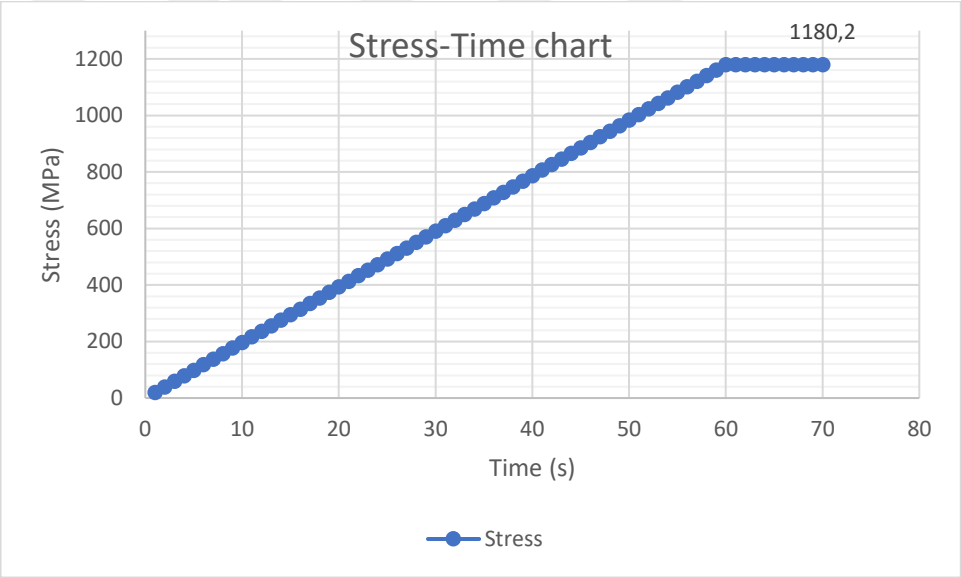

Figure 5.16 Chart for topology optimized model of riveted model.

As Figure 5.16, this chart shows stress results according to time. Starting from the 0-loading condition, in Figure 4.6, it can be seen more clearly that loads change according to time, and at the end of 60 seconds 6g load is applied to the structure. Results say that an average of 1200 MPa stress was obtained close to fixed support again. The stress distribution was similar to that observed in the static analysis.

Transient control processes were also applied to the welding case. This loading information is given in Figure 4.19. Figure 5.17 shows the transient verification of the welding case.

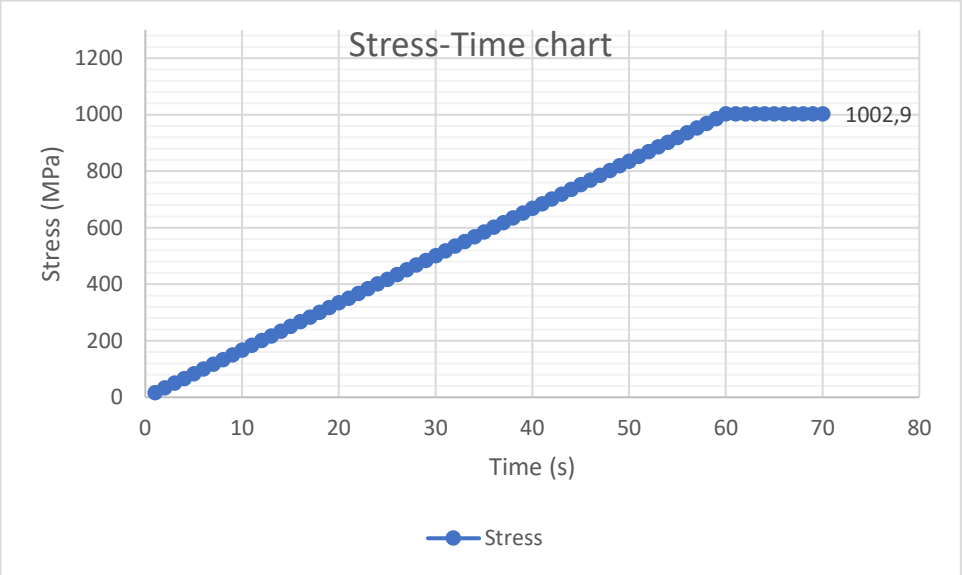

Figure 5.17 Chart for topology optimized model of welding state.

Based on the results, it was observed that the stress level on the structure reached approximately 1000 MPa. The distribution of stress throughout the structure was found to be like the anticipated pattern.

5.5 Lack of Bonding and Porosity

During the welding operation, it is a case it might be a concern. In the welding area, there can be a lack of penetration. As mentioned before, it simulated as 90% bond and 10% lack of penetration. It is a case where both sides of the root when fail to fuse to the weld. Statical analysis results show that this is a dangerous case, as seen in Figure 5.18. Over 1800MPa stress has been seen on the structure where the penetration is a problem. This area has many stress values regardless of the design parameters because of welding parameters and attention to welding technique.

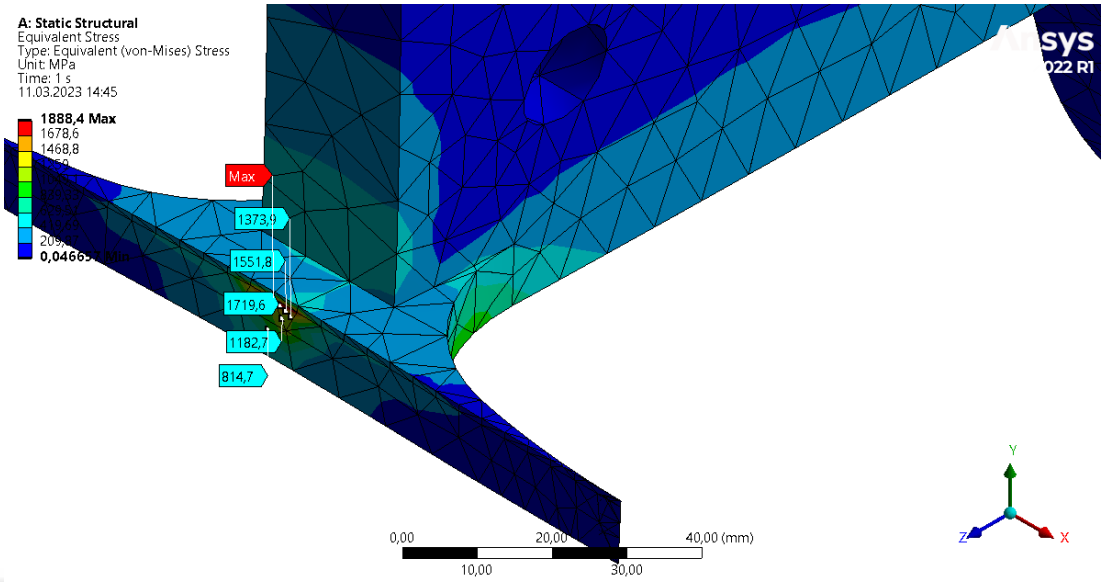

Figure 5.18 Lack of penetration of the welding state.

The stress of 1888 MPa has already exceeded the mechanical limit of the material. Therefore, stress intensity factor analysis will not be conducted in this region. If there is a case of lack of penetration due to welding, this structure will directly fail. Table 5.1 presents the results for the 10% and 5% lack of bonding in the structure. Both of them experience failure, and this means that welding case a problematic approach for the application. It should be noted that if there is an obligation to use this method, an inspection of the welding must be done, and the lack of penetration must be checked.

Table 5.1 Lack of bonding results.

%	Stress
10%	1888 MPa
5%	1606 MPa

Another notable aspect of this application pertains to the outcomes of the porosity analysis, which, as anticipated, present problematic results. The initial expectation was that stress levels in regions exhibiting porosity would be elevated. This is attributed to the compromised structural integrity arising from the existence of voids or discontinuities within these regions.

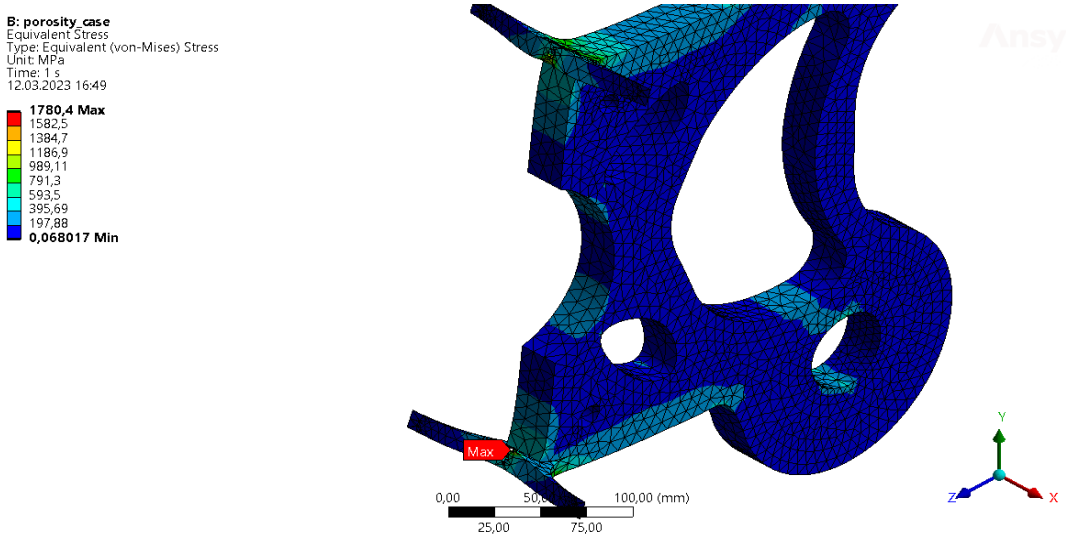

Figure 5.19 Porosity case stress results.

Higher than 1750 MPa stress has occurred on the welding section close to the porosity. This kind of porosity can be named subsurface or distributed porosity, and it can be hidden below the floor of the bead. In this sense, porosity creates unstable scenarios as it causes local wall thinning and causes irregularities in the internal structure. It can cause stress transfers on the I beam and wing fuselage bracket because this defect also affects both the I beam and wing fuselage bracket. Lack of bonding and porosity can be classified as the most dangerous defect approach during the study because of the interaction between both structures. This porosity is more difficult to detect than lack of bonding. But there are some methods to avoid these kinds of failures.

Table 5.2 Porosity results.

Porosity size	Stress
5 mm (2c)	1780 MPa
4 mm (2c)	1253 MPa

After welding application, if the correct procedure is applied to the structure, it is a failure case that can be avoided. X-ray or a grinder is properly equipped to find out this shape of porosity. This case is a risk for the wing fuselage bracket, but there is a way to prevent this situation. It has been revealed after the analysis that welding methods require extra inspection steps.

5.6 Stress Intensity Factor (SIF)

As mentioned in the previous chapter, stress intensity factors were calculated for the models. Initially, the approach of maintaining the contacts between the I beam, and wing fuselage bracket was used to calculate the stress intensity factors. The stress values were examined using the program, and Figure 5.20 illustrates the results of the critical stress points on the body. It was observed that the stress values converged even when the connection approach was changed.

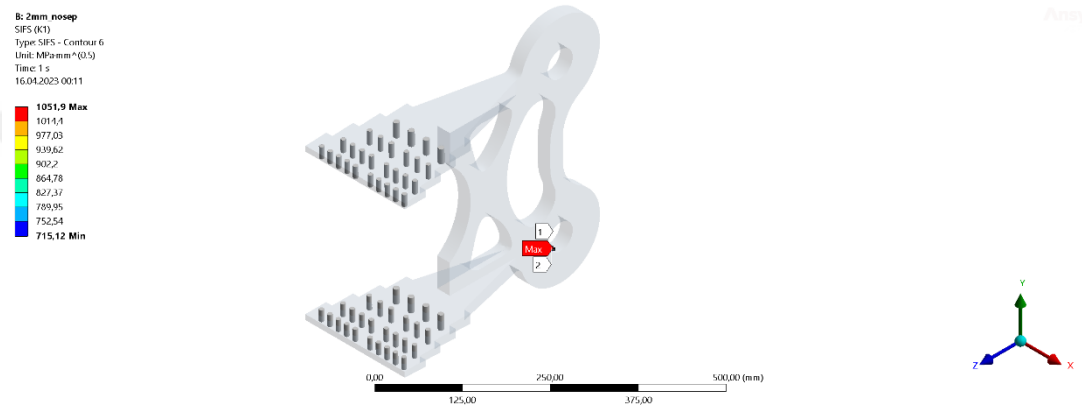

Figure 5.20 Stress intensity factor on the wing fuselage bracket crack tip.

According to this result, connection modification may be done. This K value for 2 mm major and minor radii crack must be converged with the same analysis conditions. Normalized SIF(K_I/K_o) 1051.9/1581,138 is equal to 0,665, which is converged with Figure 5.22. It was expected that stress concentration should be close to the crack tip. It is a defect in the body, and it should be close to the region. They can be due to vibration, overloading, internal stresses, defective assembly, or fatigue close to the stress-loading regions. K value helps to examine the stress state close to the crack tip. Chapter three gives detailed information about the stress intensity factor. This value will change according to crack size and tip. Loading conditions and specimen width can also affect the results. The subsequent analysis will focus on examining the effects of crack size on the body and its implications for damage tolerance. The chart which is given in Figure 5.21 shows the stress intensity factor change along the crack tip. Major and minor radius was chosen as 2 mm, and it gives a 6.283 mm crack arc length.

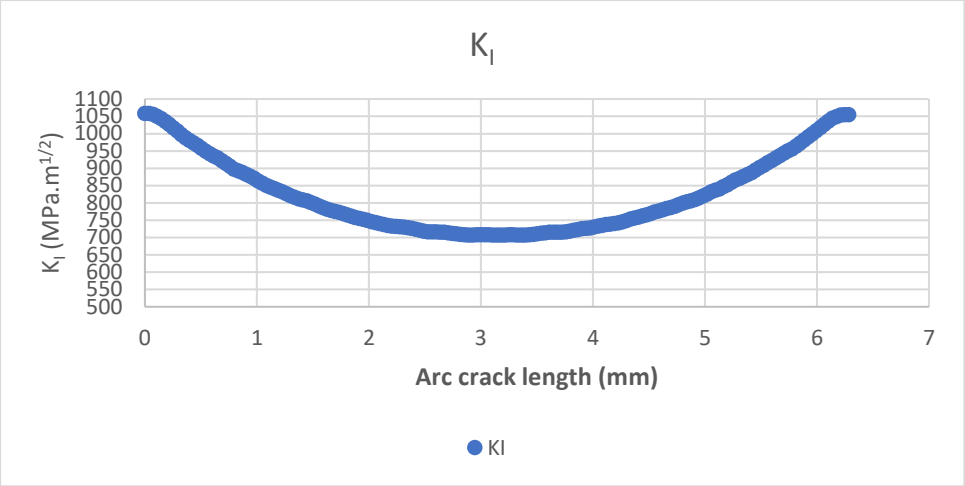

Figure 5.21 Stress Intensity Factor along the crack tip.

Two sets of data were utilized to obtain the results, and it was observed that these results were consistent with those obtained from a larger set of 100 simulations. Time-dependent solvers will be used for further applications. These contours were drawn on the chart. Here is the K_I dominant result, which is the opening mode and simulates tensile mode. K_{II} and K_{III} were so minor when we compared them with K_I. The strain energy release rate, which is G, can be calculated by using K values. But it is optional for these applications. The connection between the I beam, and wing fuselage bracket must be removed to see crack growth parameters. According to loading conditions, it is easy to catch that the bending moment is a dominant force on the bracket through the fixed holes. To simplify the idea, Figure 5.22 can be examined.

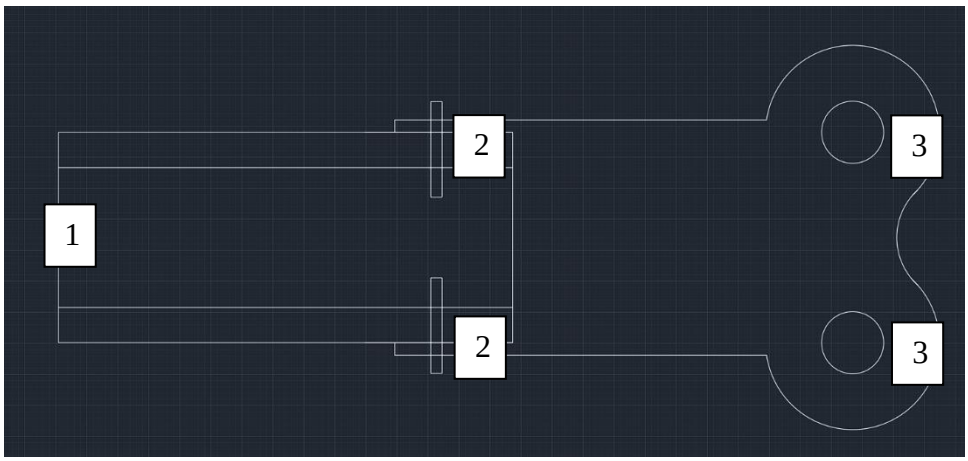

Figure 5.22 Connection simplification.

The diagram presented illustrates several key points of interest. Firstly, point 1 represents the loading area, where an upward force is applied. This force induces bending in the structure, particularly at point 3, which serves as a support for the wing fuselage bracket. Point 2 signifies the connection points, which can be either rivets or welding areas, depending on the specific model. These connections aim to integrate the I beam and wing fuselage bracket into a single body. This integration allows for a more unified analysis of the structure and facilitates future studies.

SMART crack growth application of the ANSYS does not support contacts or other mode applications of the crack. Only bonded structures may be analyzed by using the SMART application. To apply it, all the bodies were contacted by using a design modeler application of ANSYS as one body, and bending forces became dominant on the structure. As seen in the figure, the most dangerous points will be connection points and supports points on the structure. For this situation, old analyses were used to understand stress intensity points, and application of the cracks were applied to these areas.

SIF values and crack growth were calculated on the structure by using the ANSYS workbench and SMART crack growth tool. Lcr values, as mentioned before, were taken differently during the analysis 1.2-1.5 and 1.8 were applied to the body. It specifies the fracture-affected zone on the crack. Different Lcr values give close SIF results during the analysis. As mentioned before, it only changes the affected zone of the crack. It is an expectation that crack growth will be high when the lcr value increases. As seen in Figure 5.23, all SIF calculations converged during the different values of lcr, but crack growth values changed during the increase of lcr values.

Here is the important point there is no change where the crack growth starts during the analysis because SIF values converged each other, and when the SIF < 1, there would be no crack growth as statically [26]. When it is bigger than 1, there will be crack growth according to your lcr values which define the affected zone on the body. This finding highlights the influence of these critical factors on the structural response and crack propagation behavior.

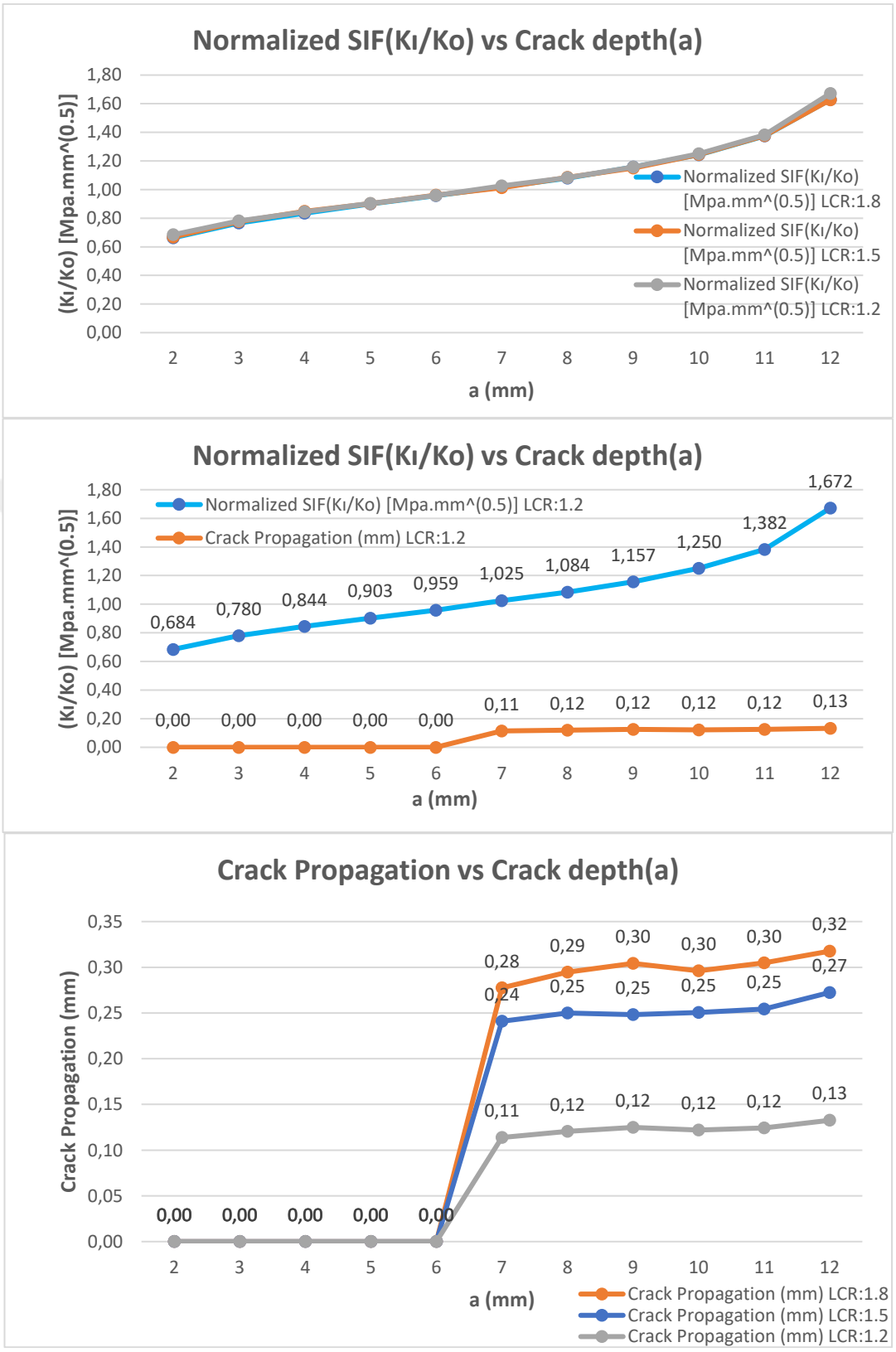

Figure 5.23 Results for the riveted case.

Another point of view was related to the crack shape. It was a case to understand the crack shape's effect on the body. Topology optimized model's analysis which has rivets, was employed with different crack sizes, as in Table 4.13. According to different major and minor radii of semi-elliptical cracks, short and long cracks were applied on the body.

A value gives the ratio of the major and minor radii. According to the a/c value, cracks were classified as short and long cracks. When the value of 'a/c' is 0.5, it is referred to as a 'long crack,' while in the case of a 'short crack,' the 'a/c' value is 2 for this study. Normalized SIF values and crack growth values were also calculated for the short and long cracks. Figure 5.24 shows the result of them.

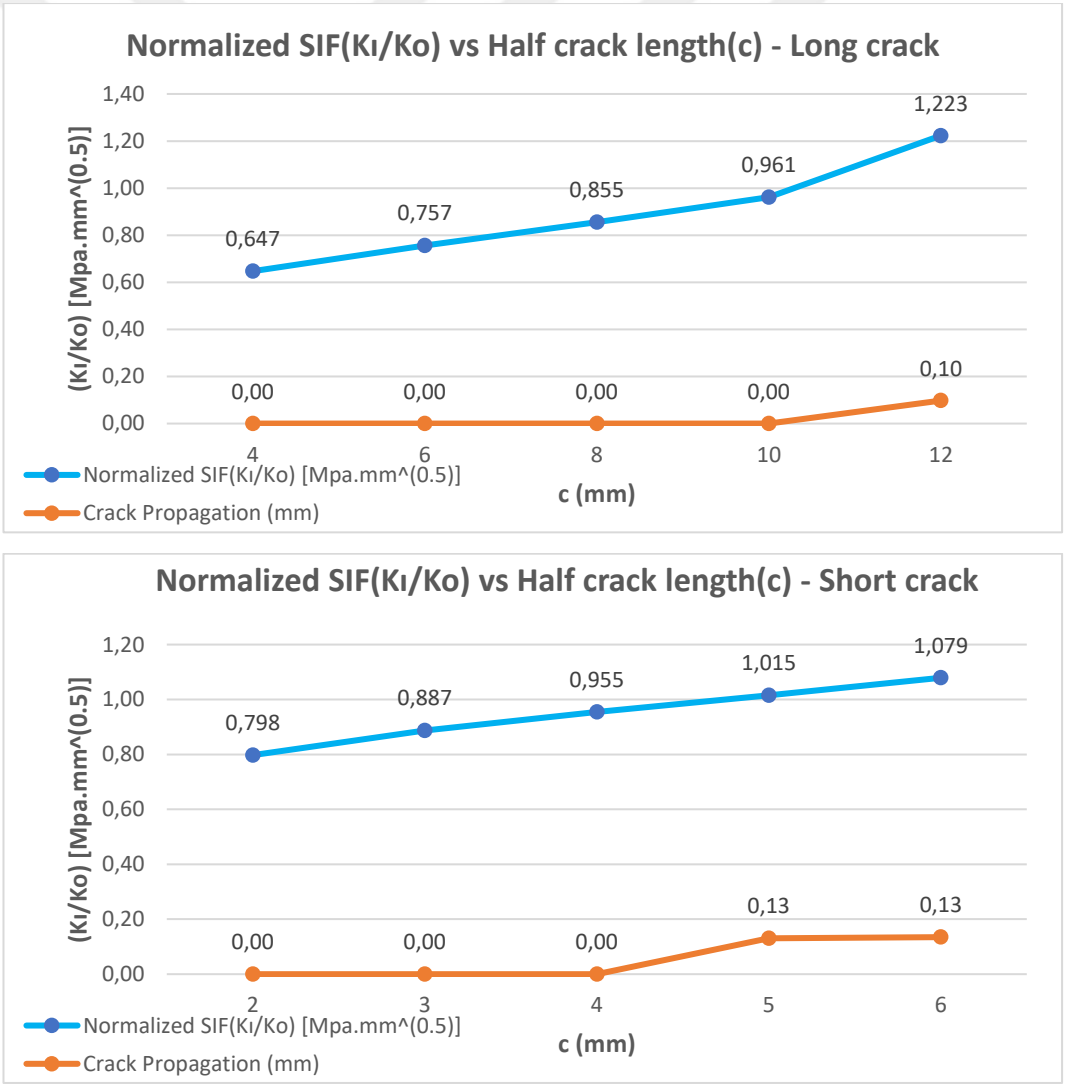

Figure 5.24 a/c=0.5(long crack) and a/c=2(short crack) results.

In accordance with Figure 5.24, it was observed that long cracks are safer than short cracks. It may be simplified, as seen in Figure 5.26, and it is interpreted as short and long cracks in the body.

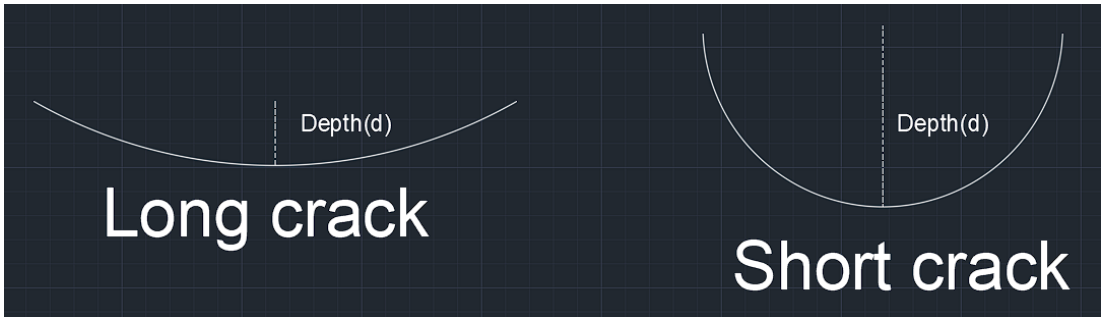

Figure 5.25 Long and short crack comparison.

As seen in Figure 5.25 long crack's depth value is smaller than its diameter, and the depth of it is also smaller than when we compare it to short cracks generally. It can be investigated that the depth of the crack affects crack growth in the body with a negative effect. It also had been seen that long cracks are also safe when it approaches 10 mm half crack length, but it is not safe for short cracks. As expected, in old analyses, the normalized stress intensity factor is smaller than one where there is no crack growth situation on the wing fuselage bracket.

The same approach was applied to the welding case, considering it as a single-body structure. The bonded connection was used to simulate the welding, following the same approach as the one-part body. The crack area was chosen near the critical stress concentration point on the structure. Stress intensity factors (SIF) of the body in the welding case were also compared using different largest contour values of 1, 1.5, and 2. The results can be observed in Figure 5.26. It was observed from previous analyses that as the largest contour values of the crack increased, the crack growth value also increased. It is important to note that the normalized SIF values of the crack should converge with each other, regardless of the lcr values of the crack. Moreover, the normalized SIF values must be greater than 1 for crack growth to occur on the structure.

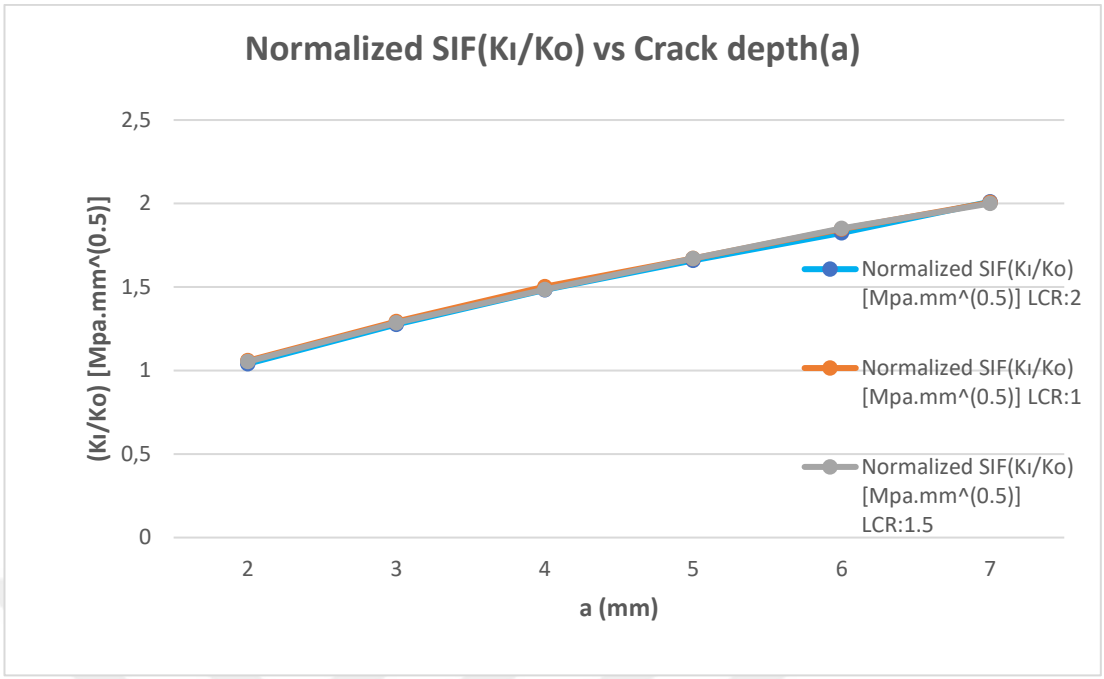

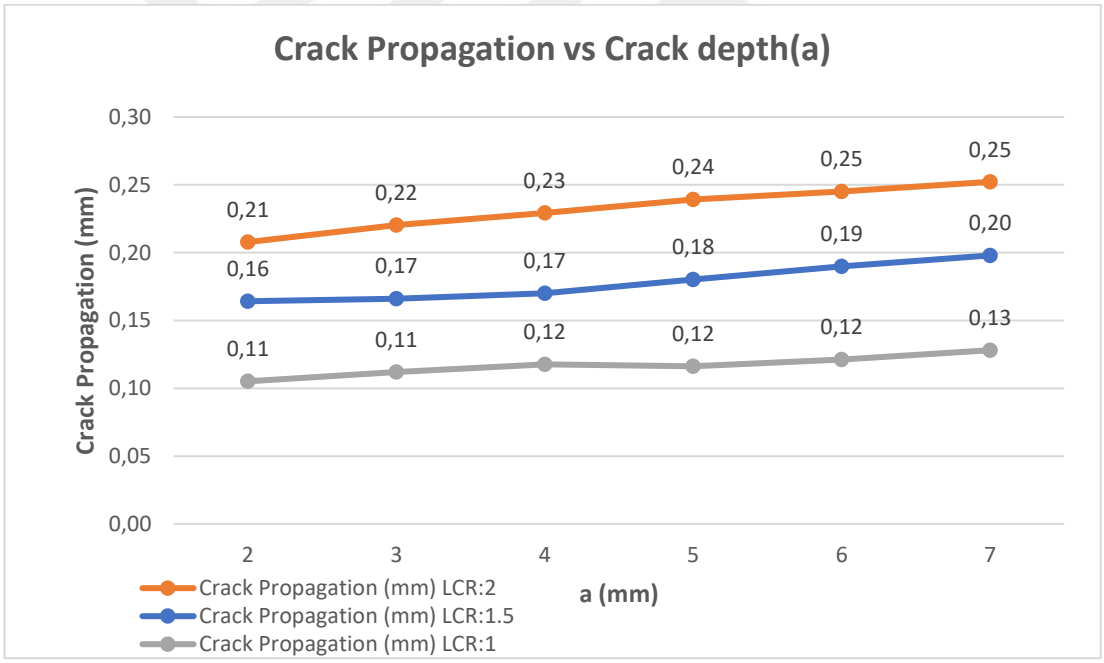

Figure 5.26 Welding case results.

CHAPTER 6

CONCLUSION

6.1 Outcomes

In aerospace applications, mass reduction is always a major problem in designing structures. Based on the studies outlined in this thesis, there is great potential to decrease the mass of structures by using topology optimization applications of finite element software while maintaining the same loading conditions and stress levels.

This thesis has reviewed recent topology optimization applications and methods, including the density-based method and the optimality criteria. These methods have been used to achieve mass reduction results. In the topology optimization studies, the wing fuselage bracket demonstrated a mass reduction of approximately 6.15 kg (22.98%). For the welded model, the bracket analyzed has been approximately lightened by 5.43 kilograms, and its mass has been reduced by 29.85%. This reduction is beneficial in terms of the energy consumption (fuel) of the aircraft and its environmental impact. It can be concluded that topology optimization is a helpful and efficient tool for designers under certain circumstances. Following the optimization procedure, a significant reduction in mass was achieved, and the resulting stress distribution and stress concentration fields were analyzed. The obtained results align well with the yield properties of AISI 4340, as the values remained below the yield strength. Table 6.1 provides details on the mass reduction for two different cases.

Table 6.1 Mass reduction of the brackets.

Model	Weight before optimization	Weight after optimization	Gained weight	Percent decrease in mass
Wing fuselage bracket	26.745 kg	20.598 kg	6.147 kg (only lug)	22.98%
Welded model	18.172 kg	12.747 kg	5.425 kg (only lug)	29.85%

Although greater mass reductions can be attainable through additional optimization procedures, it's crucial to account for operational criteria to meet elevated expectations

in the aerospace industry. For critical locations where the stress level is tremendous for the structure, stress intensity factors were calculated, and representative cracks of expected types were included in the body to analyze failure modes in detail. Based on literature reviews and considering the dominance of bending load in the structure, primarily mode I failure modes were analyzed. To simulate this situation, mode I dominant cracks were applied to the body, including both symmetrical and asymmetrical cracks. Different crack depth-to-length ratios were analyzed, considering both long and short cracks.

The study of semi-elliptical cracks plays a vital role in understanding the fracture behavior and structural integrity of materials. Through the application of fracture mechanics principles, engineers and scientists can predict crack growth, estimate remaining life, and design robust structures. By unraveling the mechanics of semi-elliptical cracks, we gain insights into the complex interplay of stresses, material properties, and geometric factors that influence fracture behavior. This knowledge fuels advancements in materials science and engineering practices and ensures the safety and reliability of critical components in numerous industries.

Some of the values indicated no crack growth during the analysis. According to this, it can be inferred that a limit may be specified when considering the stress applicable limit for fluorescent penetration inspection. Generally, linear indications are not allowed in aerospace applications according to specifications. Indications of 2 mm on the structure might be accepted by the analyses, but there is a safe region due to safety factors.

The normalized SIF factor for 2 mm cracks is specified to be around 0.684. As a result, 1/0.684 is below the safety factor of 1.5. Therefore, an additional analysis was conducted. Symmetrically, 1.5 mm indications were applied to the body, and the normalized SIF factor was observed to be 0.609 while a/c=1. It provides a safety factor higher than 1.5. A factor of safety increases the safety of structure and reduces the risk of failure of a product. Figure 6.1 shows the updated version of the normalized SIF factors.

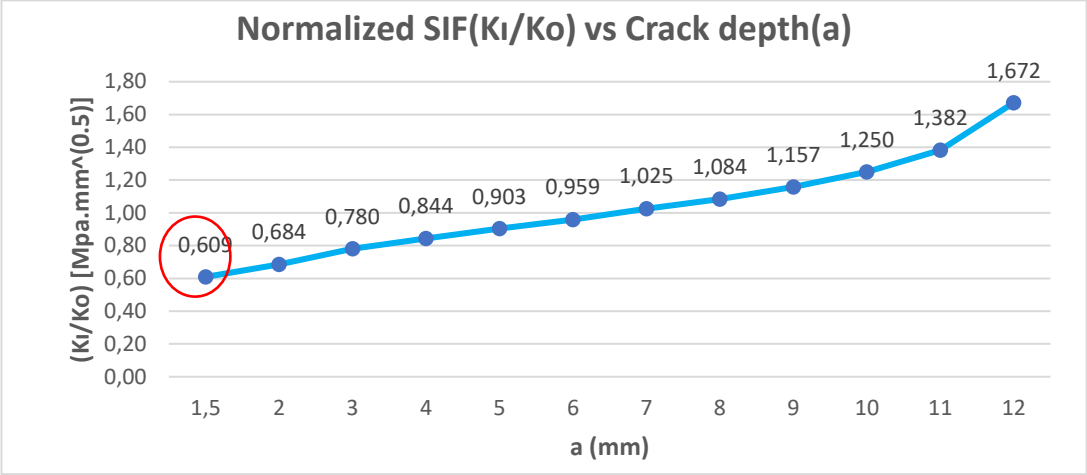

Figure 6.1 SIF factors of the optimized wing fuselage bracket with the riveted joint.

The 1.5 mm indications provide a higher safety factor than 1.5. This figure also answers which type of crack might be less dangerous on the structure, indicated by the red marking. As seen in Figure 6.2, the graph below represents the case-1 riveted and the case-2 welded models. When we consider the reference line passing through 1, there will be no crack propagation in the regions below the line. However, crack propagation is inevitable in the areas above the line.

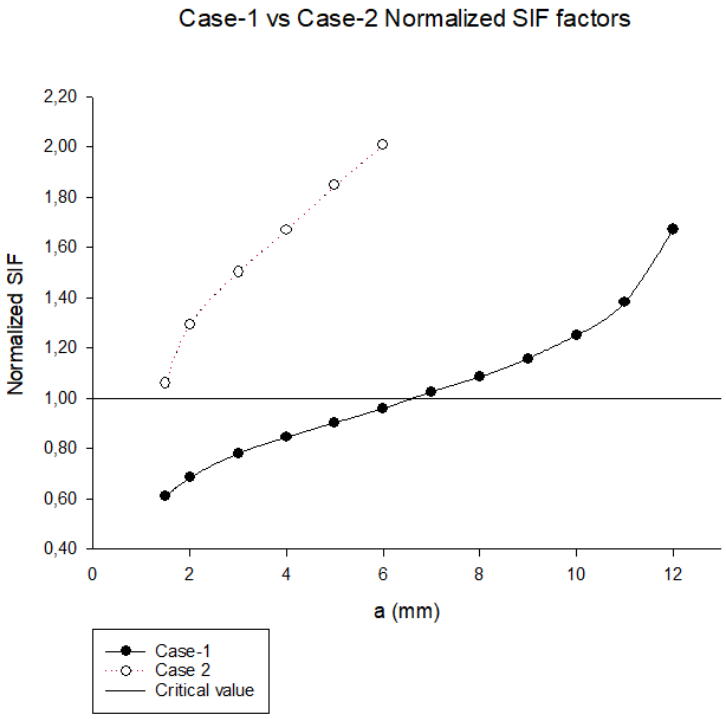

Figure 6.2 Case-1 vs Case-2.

This result was also verified by solving the analysis using 100 sets. It converged with the normalized SIF factor marked in red in Figure 6.1. Additionally, during numerous analyses, it was observed that the crack growth values provided by the program were not reliable. When different largest contour radii were applied to the body, different crack size values were obtained from the program. This highlights the fact that if K_I/K_{theo} is greater than 1, crack growth will occur, but it is not possible to determine its magnitude. During the analyses, it was observed that the riveted and optimized models yielded better results compared to the welded model, as seen in Figure 6.2.

Another point is that long cracks are safer than shorter ones according to employed loading conditions. Short and long cracks are important considerations for structural integrity assessment in aerospace applications. However, the trustability of each type of crack depends on the specific circumstances and the purpose of the analysis. As the 'a/c' value decreases, cracks become safer.

Short cracks typically refer to cracks that are relatively small in length compared to the dimensions of the structure, but their depth is greater than that of long cracks. Detecting and analyzing short cracks can be more challenging compared to long cracks. Short cracks may initiate and propagate under certain conditions, such as high-stress concentrations or fatigue loading. The detection and monitoring of short cracks require advanced inspection techniques, such as non-destructive testing methods like ultrasonic or eddy current inspection. While short cracks can be critical and lead to sudden failure, they are generally less predictable and require more sophisticated analysis techniques.

On the other hand, long cracks are cracks that extend over a significant portion of the structure's dimensions. Long cracks are typically easier to detect and monitor visually or with conventional inspection methods. They can be assessed using established fracture mechanics principles and analysis techniques, such as calculating stress intensity factors and fatigue crack growth rates. Long cracks tend to follow more predictable growth behavior and can be reliably evaluated using standardized methods.

In summary, while both short cracks and long cracks are important in aerospace applications, long cracks, which are not deep, are generally more reliable and easier to

analyze using established fracture mechanics principles. However, it is crucial to consider both types of cracks and employ appropriate inspection and analysis techniques to ensure the structural integrity of aerospace components. As the length of the crack increases, and the crack depth decreases, the cracks become safer compared to their previous versions. Additionally, when the crack depth-length ratio (a/c value) decreases, the probability of failure also decreases.

It is also observed that regardless of the stress level in the structure, early failure in the attachments that use welding methods may occur during crack analysis. Different stress concentration points, regardless of the stress level, exhibit varying levels of failure. Additionally, in the case of welded connections, crack initiation directly fails at the stress distribution point near the connection point. Consequently, the stress intensity factor (K), which is assessed as a function of crack geometry, structural geometry, and stress distribution on the part, plays a significant role. Furthermore, it has been found that the localization of approaches is crucial for crack propagation, but the notion that a structure with lower stress levels is always safe is false. The issue of crack propagation should be evaluated independently in areas with potential risk.

It should not be overlooked that in all the analyses, it is assumed that the internal structure of the body is flawless. However, if there is an internal defect in the structure that starts to propagate in the opposite direction to the analyzed crack, the two cracks may merge with each other. As a result, it will lead to a reduction in the fracture life. In these cases, robust risks may occur, and it is impossible to perform analyses using ANSYS smart simulation. Multiple-site cracking and other environmental effects, such as corrosive effects, accelerate crack growth. However, it may be observed that instead of monobloc connections like welding, riveted connections, classified as lattice sheets, are safer and exhibit slower crack propagation.

In addition to the crack application, welding simulations were conducted for cases such as lack of penetration and porosity in the bending area. During the analyses, lack of penetration and porosity led to failure in the wing fuselage bracket seen in Figure 6.3. The figure shows that all stress levels have already exceeded the material yield stress. This is because rivet connections are safer compared to welding connections.

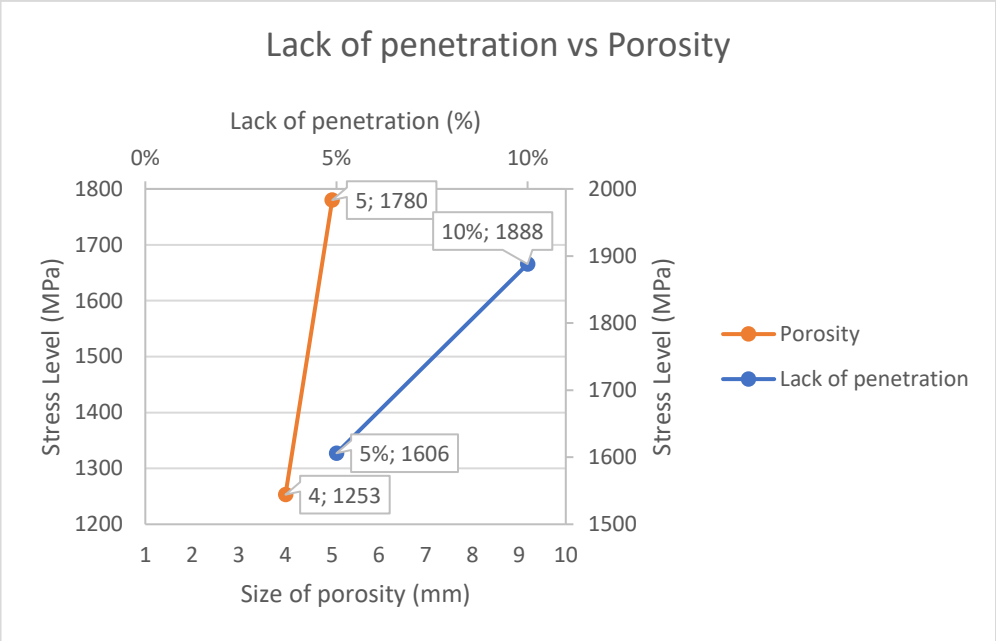

Figure 6.3 Lack of penetration and porosity stress level.

Based on assessments from various perspectives, the topology-optimized wing fuselage bracket with a riveted joint emerges as the best-optimized model in this study. The findings of this study make it suitable for applying different aerospace applications with bending load-dominant scenarios, aiding in the selection of the appropriate method of attachment.

In the chosen scenario, the regions eliminated from the mass, apart from topology optimization, were also re-designed with consideration for manufacturability. This process led to a design not only suitable for additive manufacturing but also for machining. The designs were optimized with parameters for cutting tools' performance, accessibility, and machining processes, resulting in a cost-reduction approach considering the parts that would enter the manufacturing process. By considering factors such as cutting tool performance, ease of accessibility during machining, and overall machining processes, the research aimed to optimize manufacturing efficiency and reduce production costs. This approach ensures that the proposed design is not only structurally optimized but also economically viable, aligning with cost-conscious considerations that are crucial in the aerospace industry.

REFERENCES

[1] Jaw L, Mattingly J. Aircraft engine controls: American Institute of Aeronautics and Astronautics Virgin. 2009.

[2] Witek LJEFA. Failure analysis of the wing-fuselage connector of an agricultural aircraft.13:572-581. 2006.

[3] E.R.M H, Patel SJIJoIRiS, Engineering, Technology. Stress Analysis for Wing Attachment Bracketof a six seater Transport Airframe Structure.2:3170-3177. 2013.

[4] Zhu J-H, Zhang W-H, Xia LJAoCMiE. Topology optimization in aircraft and aerospace structures design.23:595-622. 2016.

[5] Bendsoe MP, Sigmund O. Topology optimization: theory, methods, and applications: Springer Science & Business Media. 2003.

[6] Seabra M, Azevedo J, Araújo A, Reis L, Pinto E, Alves N, et al. Selective laser melting (SLM) and topology optimization for lighter aerospace componentes.1:289-296. 2016.

[7] Tomlin M, Meyer J. Topology optimization of an additive layer manufactured (ALM) aerospace part. Proceeding of the 7th Altair CAE technology conference. p. 1-9. 2011.

[8] Berrocal L, Fernández R, González S, Periñán A, Tudela S, Vilanova J, et al. Topology optimization and additive manufacturing for aerospace components.4:83-95. 2019.

[9] Balamurugan KJMTP. Fracture analysis of fuselage wing joint developed by aerodynamic structural materials.38:2555-2562. 2021.

[10] Ferro CG, Mazza A, Belmonte D, Seclì C, Maggiore PJPC. A comparison between 3D Printing and Milling process for a Spar Cap Fitting (wing-fuselage) of UAV Aircraft.62:487-493. 2017.

[11] Rao NB, Rao KSJI-IJfSR, Development. Dynamic Analysis and Fatigue Life Estimation of Wing Fuselage Attachment Bracket of an Airframe Structure.4. 2017.

[12] Reddy S, Komalarao D, Ramesh MJIRJoE, Technology. Static and fracture analysis for aircraft fuselage and wing joint with composite material.6:2169-2175. 2019.

[13] Sriranga B, Kumar RJIJoRiE, Technology. Stress analysis and fatigue life prediction of wing-fuselage lug joint attachment bracket of a transport aircraft.3:818-822. 2014.

[14] Ganesh SCNN. Design and Analysis of Wing fuselage attachment bracket for fighter aircraft. IJERGS;4. 2016.

[15] Rigby R, Aliabadi MJEFA. Stress intensity factors for cracks at attachment lugs.4:133-146. 1997.

[16] Venkatesha B, Prashanth K, Deepak Kumar TJGJoRIE. Investigation of fatigue crack growth rate in fuselage of large transport aircraft using FEA approach. 2014.

[17] Mikheevskiy S, Glinka G, Algera DJIJoF. Analysis of fatigue crack growth in an attachment lug based on the weight function technique and the UniGrow fatigue crack growth model.42:88-94. 2012.

[18] Yang R, Chahande AJSo. Automotive applications of topology optimization.9:245-249. 1995.

[19] Sigmund O, Maute KJS, Optimization M. Topology optimization approaches.48:1031-1055. 2013.

[20] Guanghui S, Chengqi G, Dongliang Q, Dongtao W, Lei T, Tong GJCJoA. An aerospace bracket designed by thermo-elastic topology optimization and manufactured by additive manufacturing.33:1252-1259. 2020.

[21] Munk DJ, Auld DJ, Steven GP, Vio GAJS, Optimization M. On the benefits of applying topology optimization to structural design of aircraft components.60:1245-1266. 2019.

[22] Munk DJ, Miller JDJAJ. Topology Optimization of Aircraft Components for Increased Sustainability.1-16. 2021.

[23] Newman J. Stress-intensity factor equations for cracks in three-dimensional finite bodies subjected to tension and bending loads: Langley Research Center, National Aeronautics and Space Administration. 1984.

[24] Newman Jr J, Raju I. Stress-intensity factor equations for cracks in three-dimensional finite bodies. ASTM Natl Symp on Fracture Mech. 1981.

[25] Meneghetti G, Campagnolo A, Avalle M, Castagnetti D, Colussi M, Corigliano P, et al. Rapid evaluation of notch stress intensity factors using the peak stress method: Comparison of commercial finite element codes for a range of mesh patterns.41:1044-1063. 2018.

[26] Qian J, Fatemi AJEfm. Mixed mode fatigue crack growth: a literature survey.55:969-990. 1996.

[27] Moreira P, De Matos P, Camanho P, Pastrama SD, De Castro PJM, design. Stress intensity factor and load transfer analysis of a cracked riveted lap joint.28:1263-1270. 2007.

[28] Olason A, Tidman D. Methodology for topology and shpe optimization in the design process. 2010.

[29] Spillers WR, MacBain KM. Structural optimization: Springer Science & Business Media. 2009.

[30] Christensen PW, Klarbring A. An introduction to structural optimization: Springer Science & Business Media. 2008.

[31] Gebisa AW, Lemu HG. A case study on topology optimized design for additive manufacturing. IOP conference series: materials science and engineering: IOP Publishing. p. 012026. 2017.

[32] Rozvany GIJS, optimization M. Aims, scope, methods, history and unified terminology of computer-aided topology optimization in structural mechanics.21:90-108. 2001.

[33] Liu S, Li Q, Liu J, Chen W, Zhang YJE. A realization method for transforming a topology optimization design into additive manufacturing structures.4:277-285. 2018.

[34] Li X-p, Zhao L-y, Liu Z-z. Topological optimization of continuum structure based on ANSYS. MATEC Web of Conferences: EDP Sciences. p. 07020. 2017.

[35] Bendsøe MPJSo. Optimal shape design as a material distribution problem.1:193-202. 1989.

[36] Querin OM, Victoria M, Alonso C, Loyola RA, Montrull PM. Topology design methods for structural optimization: Butterworth-Heinemann. 2017.

[37] Kim G-W, Park Y-I, Park KJIJoAT. Topology Optimization and Additive Manufacturing of Automotive Component by Coupling Kinetic and Structural Analyses.21:1455-1463. 2020.

[38] Liu J, Gaynor AT, Chen S, Kang Z, Suresh K, Takezawa A, et al. Current and future trends in topology optimization for additive manufacturing.57:2457-2483. 2018.

[39] Perez N. Linear Elastic Fracture Mechanics: Springer. 2004.

[40] Rolfe ST, Barsom JM. Fracture and fatigue control in structures: Applications of fracture mechanics: ASTM International. 1977.

[41] Bui HD, Leblond J, Stalin-Muller N. Background on Fracture Mechanics. Academic Press. 2001.

[42] Ugural AC, Fenster SK. Advanced mechanics of materials and applied elasticity: Pearson Education. 2011.

[43] Kastratović G, Vidanović N, Grbović A, Rašuo BJFt. Approximate determination of stress intensity factor for multiple surface cracks.46:39-45. 2018.

[44] Newman Jr J, Raju IJEfm. An empirical stress-intensity factor equation for the surface crack.15:185-192. 1981.

[45] Kastratović G, Grbović A, Vidanović NJAmm. Approximate method for stress intensity factors determination in case of multiple site damage.39:6050-6059. 2015.

[46] Murakami Y, Keer L. Stress intensity factors handbook, vol. 3. 1993.

[47] Poe Jr C. Stress intensity factor for a cracked sheet with riveted and uniformly spaced stringers. 1971.

[48] Chin PLJFR. Stress Analysis, Crack Propagation and Stress Intensity Factor Computation of a Ti-6Al-4V Aerospace Bracket using ANSYS and FRANC3D. 2011.

[49] Pan J, Lin S-HJFT, Analysis. Fracture mechanics and fatigue crack propagation.237. 2005.

[50] Han Q, Wang Y, Yin Y, Wang DJEFM. Determination of stress intensity factor for mode I fatigue crack based on finite element analysis.138:118-126. 2015.

[51] Nor KM, Ibrahim MN, Choiron MAJME. An overview of fracture mechanics with ANSYS.10:59-67. 2018.

[52] Zhu N, Oterkus EJJoM. Calculation of stress intensity factor using displacement extrapolation method in peridynamic framework.36:235-243. 2020.

[53] Kurowski PM. Finite element analysis for design engineers: SAE International. 2022.

[54] Ansys IJv. ANSYS meshing user's guide.15317:724-746. 2013.

[55] Guide AMUsJAIC, PA, USA. Release 2021 R1. 2021.

[56] Kohnke P. Ansys. Springer. 1982.

[57] Stolarski T, Nakasone Y, Yoshimoto S. Engineering analysis with ANSYS software: Butterworth-Heinemann. 2018.

[58] Madenci E, Guven I. The finite element method and applications in engineering using ANSYS®: Springer. 2015.

[59] Ahangar RG, Verreman YJJoFA, Prevention. Assessment of mode I and mode II stress intensity factors obtained by displacement extrapolation and interaction integral methods.19:85-97. 2019.

[60] Banks-Sills L. Application of the finite element method to linear elastic fracture mechanics. 1991.

[61] Krueger RJAMR. Virtual crack closure technique: History, approach, and applications.57:109-143. 2004.

[62] Ritchie RO, Francis B, Server WLJMTA. Evaluation of toughness in AISI 4340 alloy steel austenitized at low and high temperatures.7:831-838. 1976.

[63] Lee W-S, Su T-TJJompt. Mechanical properties and microstructural features of AISI 4340 high-strength alloy steel under quenched and tempered conditions.87:198-206. 1999.

[64] Nakai M, Eto TJMS, A E. New aspect of development of high strength aluminum alloys for aerospace applications.285:62-68. 2000.

[65] Huda Z, Taib NI, Zaharinie TJMC, Physics. Characterization of 2024-T3: An aerospace aluminum alloy.113:515-517. 2009.

[66] Petrašinović N, Petrašinović D, Rašuo B, Milković DJFT. Aircraft duraluminum wing spar fatigue testing.45:531-536. 2017.

[67] Dagdag O, Hsissou R, Berisha A, Erramli H, Hamed O, Jodeh S, et al. Polymeric-based epoxy cured with a polyaminoamide as an anticorrosive coating for aluminum

2024-T3 surface: experimental studies supported by computational modeling.5:1-13. 2019.

[68] Murr LJJoME, Performance. A review of FSW research on dissimilar metal and alloy systems.19:1071-1089. 2010.

[69] Sumanth M, Ayyappa TJIJTRE. Comparative analysis of aircraft wing fuselage lug attachment bracket.5:4422-4429. 2018.

[70] Berzins MJEwC. Mesh quality: a function of geometry, error estimates or both? ;15:236-247. 1999.

[71] Fatchurrohman N, Chia S. Performance of hybrid nano-micro reinforced mg metal matrix composites brake calliper: simulation approach. IOP Conference Series: Materials Science and Engineering: IOP Publishing. p. 012060. 2017.

[72] Zhu Y. Best Practices for Contact Modeling using ANSYS. 2017.

[73] Thompson MK, Thompson JM. ANSYS mechanical APDL for finite element analysis: Butterworth-Heinemann. 2017.

[74] Wu J-Y, Lee RJIToA, Propagation. The advantages of triangular and tetrahedral edge elements for electromagnetic modeling with the finite-element method.45:1431-1437. 1997.

[75] Marzuki MAB, Abd Halim MH, Mohamed ARNJAJoE, Sciences A. Determination of natural frequencies through modal and harmonic analysis of space frame race car chassis based on ANSYS.8:538-548. 2015.

[76] Bedri R, Al-Nais M. Prestressed modal analysis using finite element package ANSYS. Numerical Analysis and Its Applications: Third International Conference, NAA 2004, Rousse, Bulgaria, June 29-July 3, 2004, Revised Selected Papers 3: Springer. p. 171-178. 2005.

[77] Jasthi BK, Curtis T, Widener CA, West M, Carriker M, Dasgupta A, et al. Friction Stir Processing of Direct-Metal-Deposited 4340 Steel. *Friction Stir Welding and Processing VIII*: Springer. p. 191-198. 2015.

[78] Pei X, Dong PJS, Welding To, Joining. Shear localisation modelling of friction stir weld formation process.19:416-426. 2014.

[79] Ozen M, Fellow A. Meshing workshop. MESHING WORKSHOP. 2014.

[80] Singh AK, Dey V, Rai RNJMTP. Techniques to improveweld penetration in TIG welding (A review).4:1252-1259. 2017.

[81] Kah P, Rajan R, Martikainen J, Suoranta RJIJoM, Engineering M. Investigation of weld defects in friction-stir welding and fusion welding of aluminium alloys.10:1-10. 2015.

[82] Özcan R. Fatigue and fracture analysis of helicopter fuselage structures: Middle East Technical University. 2013.

[83] John R, Jata K, Sadananda KJIJof. Residual stress effects on near-threshold fatigue crack growth in friction stir welds in aerospace alloys.25:939-948. 2003.

[84] Testing ASf, Fatigue MCEo, Fracture. Standard test method for measurement of fatigue crack growth rates. American Society of Testing Materials. 2008.

[85] E-03 A. Standard Test Method for Determining Threshold Stress Intensity Factor for Environment-Assisted Cracking of Metallic Materials. ASTM International West Conshohocken, PA. 2013.

[86] Şen G. Determination of fracture and fatigue behaviours of 4340 steel: Middle East Technical University. 2015.

[87] Wang X, Lambert SJEFM. Stress intensity factors for low aspect ratio semi-elliptical surface cracks in finite-thickness plates subjected to nonuniform stresses.51:517-532. 1995.

APPENDICES

Appendix -A: Workflow Chart for Section 4.2.1

Appendix -B: Workflow Chart for Section 4.2.2

Appendix -C: Workflow Chart for Section 4.2.3

Appendix -D: Workflow Chart for Section 4.2.4

Appendix -E: Workflow Chart for Section 4.3

Appendix -A: Workflow Chart for Section 4.2.1

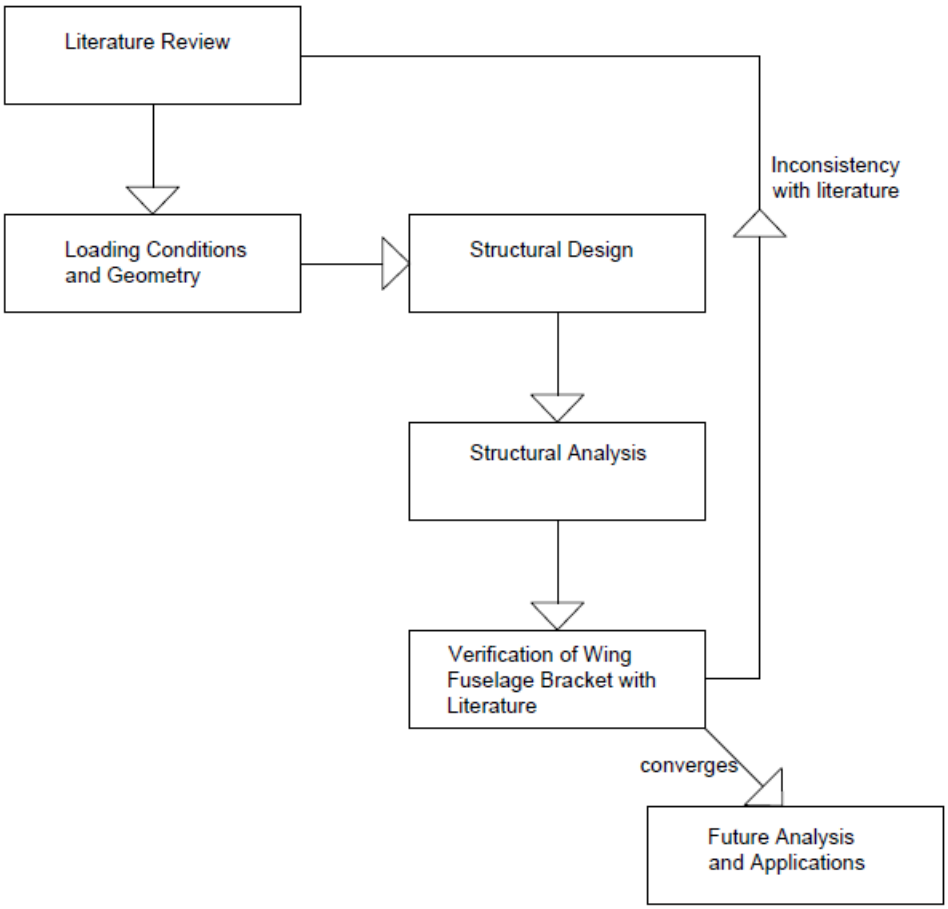

Appendix -B: Workflow Chart for Section 4.2.2

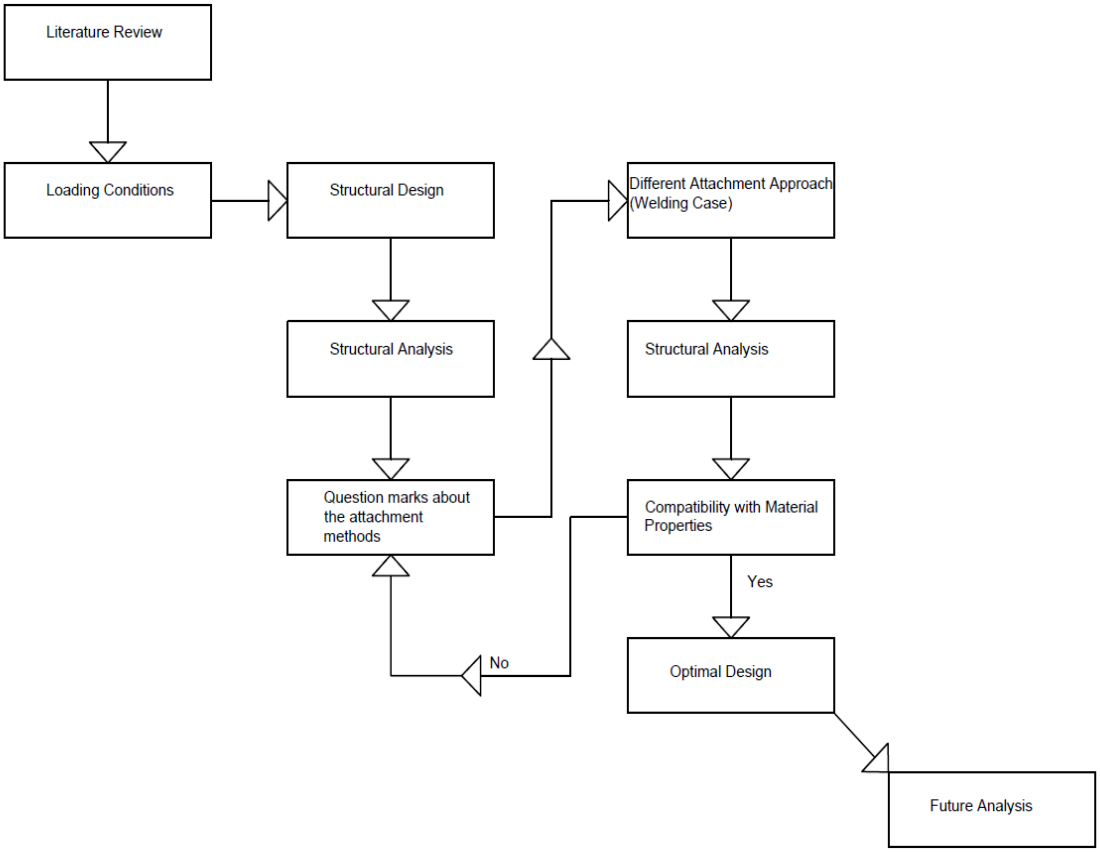

Appendix -C: Workflow Chart for Section 4.2.3

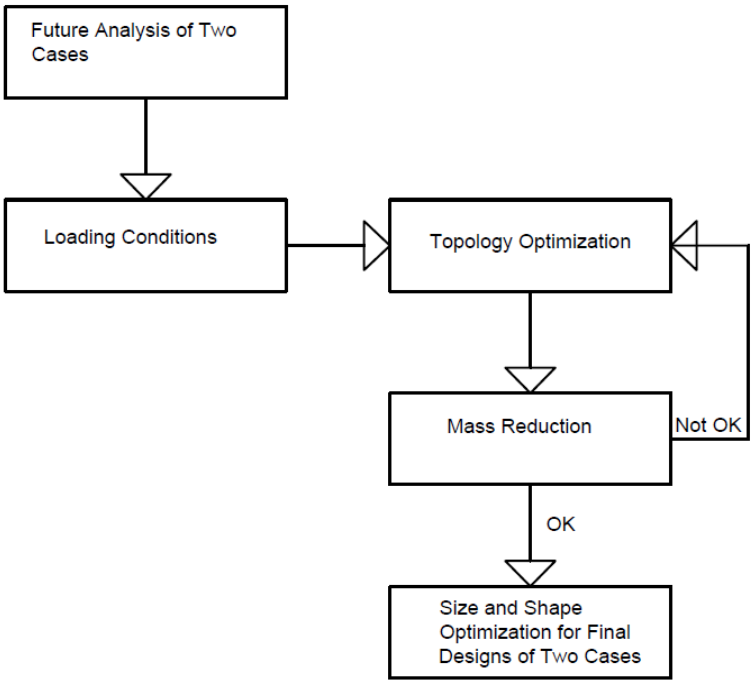

Appendix -D: Workflow Chart for Section 4.2.4

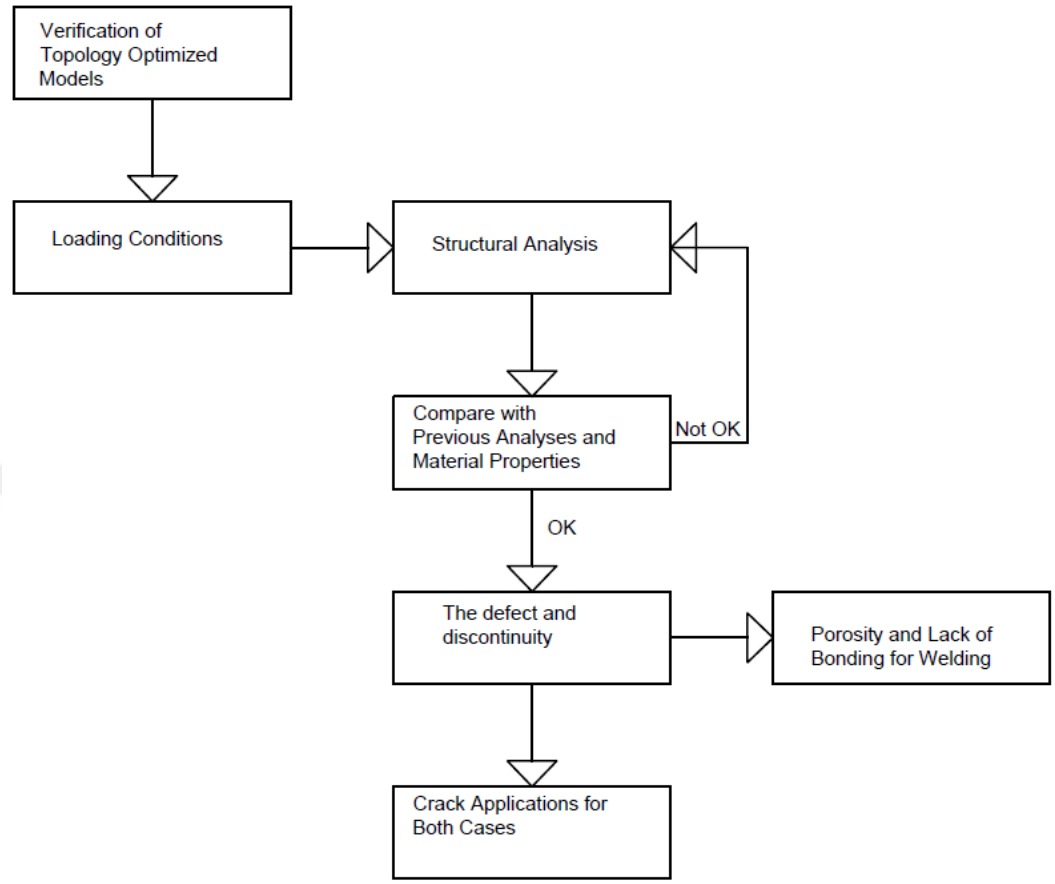

Appendix -E: Workflow Chart for Section 4.3